

The
GEOLOGICAL BULLETIN
of the
PUNJAB UNIVERSITY

Number 29

December, 1994

CONTENTS

	Page
Source of Sulfur in the Base Metal Deposits of Khuzdar District Balochistan, Pakistan.	1
Genesis of Gunga Barite Deposits near Khuzdar Sulfur Isotopic Evidence	5
Sedimentology of Datta Formation at Kalapani, Abbottabad, Northwest Himalayas, Pakistan.	11
Origin of Elongated Gypsum Crystal in the Salt Range Formation, Nilawahan Gorge, Central Salt Range.	29
Urban Geology of the Dera Ghazi Khan Area, South Punjab Pakistan.	35
A Turbidimetric Technique for Measuring the Soil Structural Stability	43
Aggregate Stability of a Saline Sodic Soil Under Irrigated Kallar Grass Faisalabad, Pakistan.	53
Clays, A Source of Environmental Degradations and A Remedy for Environmental Pollution	65
Geology and Structure of the Main Mantle Thrust (Raikot-Naran Segment), South Eastern Kohistan Northern Pakistan	71

SOURCE OF SULFUR IN THE BASE METAL DEPOSITS OF KHUZDAR DISTRICT, BALOCHISTAN, PAKISTAN.

BY

SHAMIM AHMED SIDDIQUI

Department of Geology, University of Balochistan, Quetta, Pakistan.

Abstract : *Base metal deposits of Khuzdar District are hosted by the Jurassic Zidi Formation in its upper stratigraphic horizon at Gunga, while at other locations it is the Middle Member which carries the mineralization. Sulfur isotopic compositions of the minerals such as galena, sphalerite and pyrite were studied as part of the efforts to gain some knowledge about their origin. For this purpose, six samples were collected in such a way as to represent all the available sites. The $\delta^{34}\text{S}$ values of all the sulfide phases vary between -1.9 and $+4.5$ permil, with an average value of 0.44 permil, and a total range of 6.4 permil. Three possible mechanisms which could furnish sulfur needed for the formation of sulfide ore minerals, were considered in the light of the isotopic data. The mechanisms include : sulfur derived from primary magma, sulfur generated during the reduction of seawater sulfate by the bacteria, and sulfur produced as a result of the reduction of seawater sulfate by other means (nonmicrobial), such as organic matter. Out of the three mechanisms, the last one seems to be supported by our isotopic data. Thus, it was the H_2S which evolved as a result of nonmicrobial reduction of seawater sulfate, most probably, brought about by organic matter, which reacted chemically with the base metal in the ore bearing solutions to precipitate sulfide minerals.*

INTRODUCTION

The reddish brown beds underlying the well known barite deposits of Gunga (Fig. 1, p. 10) were originally considered simply represent iron mineralization. However they became the focus of attention once it was realized that these were possible lead and zinc deposits. The lead-zinc mineralization in this area crops out in the form of a large gossan extending in a N-S direction for about 600 meters along the strike. Similar gossans also occur at a few more nearby localities : Surmai, Malkhor, Ranjlaki, and Sekran within a distance of about 8 to 24 km from the Gunga deposits but none of them is associated with barite. These gossans are siliceous and chiefly

contain oxidized iron minerals and minor amount of scattered sphalerite and galena on the surfaces. These gossans are composed of leached and silicified calcareous siltstone and red to yellow iron oxide at Gunga. However, at other locations it is the limestone belonging to the Middle Member of the host Zidi Formation which turned into gossan. They are the oxidized outcropping cellular masses of limonite (goethite) and some other oxidized minerals overlying sulfide deposits. They point to the presence of unaltered sulfide minerals underneath. The drilling carried out by the Geological Survey of Pakistan around 1983 actually revealed the occurrence of sulfide ore minerals (sphalerite, galena,

marcasite, pyrite) in sufficient amount at depth.

The sediment hosted lead-zinc-barite deposits at Gunga vary in thickness from about 100 to 200 feet (Jankovic, 1986). The mineralization can be differentiated into an upper barite zone and a lower sulfide zone. The upper barite zone which is a few meters to about 80 meters thick consist of massive barite. The lower part of this barite bed also carries mineralization of galena, sphalerite, and pyrite in the form of streaks, patches and lenses. Underlying this zone is the lower sulfide mineralization zone which consists of 30 to 70 meter thick interbedded siliceous sediments, mainly siltstone and shale, and lesser amount of limestone (Jankovic, 1986). No sulfate zone overlying sulfide mineralization developed on locations other than Gunga.

In order to investigate the origin of these sulfide mineral deposits, their sulfur isotopic compositions were studied.

GEOLOGIC SETTING

The collision between the Indian and Eurasian Plates gave rise to a vast fault and fold zone known as the Pakistan Fold Belt which extends E-W on the northern side, makes certain bends and then runs almost N-S in the western part of the country. These N-S trending mountains in the west comprise two major ranges; the Sulaiman Range in the north and the Kirthar Range in the south.

The district of Khuzdar lies within the Kirthar Range which runs north-south for about 600 km. The strike of the ranges in the Khuzdar area changes abruptly and repeatedly from N-S to E-W and back again to N-S. This is why the area had been termed as "Khuzdar Knot" (Jones, 1960). The term refers to its knot-like appearance on geologic maps and connotes no genetic implications. The Khuzdar-Bela Metallogenic Province which extends southward from Khuzdar for about 350 km to the Arabian Sea is bounded by the Kirthar Fault on the east and by the Ornach-Nal and Gazan Fault Sys-

tems on the west and north respectively. The Kirthar Fault runs for about 150 miles to the south and is a zone of thrusting (Jones, 1960). It is believed that this block which is located on the western margin of the Indo-Pakistan Subcontinent has not only dragged along Ornach-Nal Fault, considered to be a sinistral transform boundary between the Indian and Eurasian Plates, but also may have rotated counter-clockwise as an independent tectonic unit (Sarwar and DeJong, 1979).

The area is mainly composed of Jurassic and Cretaceous sequences of marine sediments deposited in a shelf environment under fluctuating conditions (Fatmi, 1986). The Pb-Zn-barite mineralization in the area is found associated with interbedded Jurassic limestone and shale sequence in the upper part of the Zidi Formation. The Zidi Formation is a massive assemblage, about 1000 feet thick (Fatmi, 1986), deposited in a shallow sedimentary basin. This formation is widely exposed in the study area, west of Khuzdar and is often repeated by folding and faulting. It is overlain unconformably by calcareous shale and argillaceous limestone of Cretaceous age.

SULFUR ISOTOPES

For the sulfur isotope studies, specimens were collected from three deposits at Gunga, Surmai, and Malkhor. Samples included those collected from the surface of the deposit as well as ones obtained from the drill core from the Gunga and Surmai locations. Since the surface expression of sulfide mineralization in the area is only in the form of gossan which consists of leached oxidized material, it was difficult to collect good samples of the sulfide minerals from the surface. However, some galena crystals could be gathered from within the gossan as well as from within the barite. Because of limited access, only a small number of samples could be obtained from the drill core. Six sulfide samples collected from Khuzdar District were selected in such a way as to represent all of the available sites.

SAMPLE ANALYSIS

Most of the samples were crushed in a simple mortar to a coarse grain sized material and then individual mineral grains were painstakingly separated from the associated shaly or calcareous matrix by hand under a binocular microscope. All samples were then kept submerged in 10% HCl and rinsed with distilled water to remove any unwanted material sticking to the mineral surface.

Sulfur isotopes were determined following the method of Thode et al. (1961). In this method the sulfur in the sulfide specimens is burned in a stream of purified oxygen inside a fused quartz tube placed in an electric furnace, at a temperature of 1200°C to obtain SO₂. After the removal of the impurities from the SO₂ thus produced, it is collected and stored in a sealed pyrex tube for analysis on mass spectrometer.

DISCUSSION

There were perhaps three possible mechanisms which could furnish sulfur for sulfide mineralization: 1) it can come from a primary magmatic source with a $\delta^{34}\text{S}$ equal to 0 permil; 2) when sulfate reducing bacteria reduce seawater sulfates in a closed system, the resulting H₂S becomes depleted in S due to isotopic fractionation because of the kinetic effects. The remaining sulfates in the sea thus becomes enriched in $\delta^{34}\text{S}$ as compared to sulfide minerals which are formed in that reservoir; 3) it can be generated by nonmicrobial reduction of seawater sulfate.

Since these deposits have no observable connection to any magmatic activity (Sillitoe, 1980, p. 382), there seems to be little chance that magmatic sulfur could be the source. If it is considered that sulfide minerals formed due to the precipitation effected by reduced sulfur from the seawater sulfates at low temperatures, these should have a broad range of randomly distributed $\delta^{34}\text{S}$ values. In addition, if the closed system conditions prevailed, greater isotopic fractionation could take place be-

tween the sulfate source and the resulting H₂S (Jensen, 1967, p. 147). So a sulfide ore formed by bacteriogenic sulfur should exhibit the following characteristics; its $\delta^{34}\text{S}$ values should vary over a comparatively broad range, and it should be depleted in $\delta^{34}\text{S}$ relative to the SO₄ from which the sulfur for the formation of sulfide was derived. As compared to this, the deposits formed at high temperatures like those of magmatic origin do not show much variation or a large range in their values, because kinetic isotopic reactions are not very effective at elevated temperatures. Moreover, those formed at high temperature using S from magmatic source have their $\delta^{34}\text{S}$ values near zero permil.

In this context when we examine data of the Pb-Zn deposits of Khuzdar District (see Table), we see that $\delta^{34}\text{S}$ values vary over a narrow range, between -1, 9 and +4.5‰. These values seem to suggest that the sulfur was not bacteriogenic. This view is also supported by what Orr (1974) has stated. According to him, only a low concentration of H₂S is generated by this process of microbial sulfate reduction and this is inhibited at temperatures higher than 50-60°C. Since the temperatures in our case are slightly on a higher side, this second mechanism of H₂S generation is more plausible.

CONCLUSION

The isotopic compositions of our samples ($\delta^{34}\text{S}$ values) vary between -1.9 permil to +4.9 permil with a total range of 6.4 permil. Since the data neither have a zero permil value, nor do they have a broad range in the values (a range of merely 6.4 permil is only a narrow range), it is concluded that the sulfur in these deposits was not magmatic, nor was it obtained from the H₂S produced by bacterial reduction of seawater sulfate. The only possibility is that the required H₂S for the precipitation of sulfide minerals was produced during the reduction of seawater sulfate by some other means, most probably, reaction with organic matter. This idea is further supported by the temperatures of the formation of these deposits, which have been estimated to be on a little higher side, i.e., above 60°C.

REFERENCES

- Fatmi, A.N., 1986. Zidi Formation (Ferözabad Group) and Parh Group (Monajhal Group) Khuzdar District, Baluchistan, Pakistan. *Rec. Geol. Surv. Pakistan*, 75, 32 p.
- Faure, G., Principles of Isotope Geology, 2nd Ed., John Wiley and Sons, 589 p.
- Jankovic, S., 1986. The mineral association and genesis of the lead-zinc-barite deposits of Gunga, Khuzdar District, Baluchistan, Pakistan *Rec. Geol. Surv. Pakistan*, 71, 22 p.
- Jensen, M.L., 1967. Sulfur isotopes and mineral genesis : Chapter 5, In, Barnes, H.L. (Ed.) *Geochemistry of hydrothermal deposits*, Holt, Rinehart, and Winston Inc., New York, 143-165.
- Jones, A.G., 1960. Reconnaissance geology of part of West Pakistan : A Colombo Plan Cooperative Project : Govt. of Canada, Toronto, 550 p.
- Ohmoto, H., 1972. Systematics of sulfur and carbon isotopes in hydrothermal ore deposits *Econ. Geol.* 67, 551-578.
- Ohmoto, H., and Rye, R.O., 1979. Systematics of sulfur and carbon isotopes, In, Barnes, H.L., (Ed), *Geochemistry of hydrothermal ore deposits*, 2nd Ed., Wiley Interscience, New York, 509-561.
- Orr, W.L., 1974. Changes in sulfur content and isotopic ratios of sulfur during petroleum maturation-study of Big Horn Basin Paleozoic oils : *Bull. Amer. Assoc. Petrol. Geol.* 58, (11), 2295-2318.
- Rye, R.O., and Ohmoto, H., 1974. Sulfur and carbon isotopes and ore genesis : A review : *Econ. Geol.* 69, 826-842.
- Sarwar, G., and DeJong, K.A., 1979. Arcs, Oroclines, Syntaxes : The curvature of mountain belts in Pakistan : Farah and DeJong (Eds.) *Geodynamics of Pakistan*, 341-349.
- Sillitoe, R.H., 1978. Metallogenic evolution of collisional mountain belt in Pakistan : A preliminary analysis : *Jour. Geol. Soc. London* 135, 377-387.
- Thode, H.G., Monster, G.H., Dunford, H.B., 1961. Sulfur isotope geochemistry *Acta Geochem. Cosmochem.* 25, 159-174.

TABLE

Sulfur isotopic composition in sulfide minerals from Khuzdar District.

Sr.	Sample	Location	Mineral	$\delta^{34}\text{S}$
1.	SS-SD-18	Malkhor	Galena	-1.9
2.	SS-SD-7	Surmai	Sphalerite	-0.9
3.	SS-SD-5	Surmai	Galena	-0.5
4.	SS-SD-11	Surmai	Galena	-0.5
5.	SS-SD-6	Gunga	Galena	0.1
6.	SS-SD-21	Surmai	Sphalerite	0.3
7.	SS-SD-19	Gunga	Galena	1.5
8.	SS-SD-3	Gunga	Pyrite	3.3
9.	SS-SD-13	Surmai	Sphalerite	4.5

GENESIS OF GUNGA BARITE DEPOSITS NEAR KHUZDAR SULFUR ISOTOPIC EVIDENCE

BY

SHAMIM AHMED SIDDIQUI

Department of Geology, University of Balochistan, Quetta, Pakistan.

Abstract : The large stratabound lead-zinc-barite deposits of Gunga occur on the western margin of the Indian Plate. They are hosted by the Jurassic Zidi Formation in its upper stratigraphic horizon. In order to investigate their origin, 6 barite samples were analyzed for their sulfur isotopic composition. The $\delta^{34}\text{S}$ values of our samples range from +26.8‰ (permil) to +33.0‰ (permil) with an average of 28.7‰. These values are much higher than the isotopic values of the sulfates in the Jurassic oceans, in which the host Zidi Formation was deposited. These higher values match with the values of the source of sulfur in the Gunga barite deposits. It is suggested that the sulfur in the barite was derived from the Cambrian or Precambrian evaporites, supposed to be underlying the Pakistan fold belt above the Indian continental basement. The sulfur from the underlying evaporites was extracted by the basinal brines circulating through the rocks due to the ensuing tectonic compression caused by intercontinental collision. Barium, like several other metals, e.g., Fe, Zn, Pb may have been leached from the surrounding rocks by the same brines. Barite would have precipitated as a result of chemical reaction between the barium and sulfate ions under favourable physico-chemical conditions at the site of the present deposits.

INTRODUCTION

The massive barite deposits of Gunga near Khuzdar in the Balochistan Province (Fig. 1) were initially described by the geologists of the Geological Survey of Pakistan (Ahmed, 1950), and later by the Hunting Survey Corporation (1960). They were also studied by Schmidt et al. (1961), and by Klinger and Ahmed (1967) who also estimated tonnage of the deposits. These deposits have been actively exploited for commercial purposes by a mining company for about two decades. The beds which lie under these huge barite deposits represent lead and zinc mineralization in the form of large siliceous gossan extending in a N-S direction. Similar gos-

sans occur at Surmai, Malkhor, Ranjlaki, and Sekran to the south and north west of the Gunga deposit within a distance of 8 to 24 kilometers but none of them is associated with any barite. These gossans are composed of leached and silicified calcareous siltstone and red to yellow iron oxide. They are the oxidized outcropping cellular masses of limonite (goethite) and some other oxidized minerals overlying sulfide deposits. They are indicative of the presence of unaffected sulfide minerals underneath. The drill-core obtained by the Geological Survey of Pakistan around 1983 actually revealed sufficient sulfide mineralization (sphalerite, galena, pyrite, and marcasite) at depth.

Thus, at Gunga there are two distinct zones of mineralization: the upper barite (sulfate) zone and the lower sulfide zone. The upper barite zone consists of a massive barite bed ranging in thickness from a few meters to 80 meters. Its lower part carries also sphalerite and galena in the form of streaks, patches and lenses. These tabular ore bodies, along with iron sulfides form a zone which varies in thickness from 10 to 40 meters (Jankovic, 1986).

To gain some insight into the genesis of these ore deposits a study about the sulfur isotopes in the barite was undertaken.

GEOLOGIC SETTING

The geology of Pakistan carries evidence of one of the most important diastrophic events in geological history—an intercontinental collision. The collision occurred in Early Eocene culminating in Miocene and Pliocene, but the movement still continues, though, at a slow rate. The vast fold and thrust zones represented by the Great Himalayan mountain ranges are spectacular manifestation of this geological phenomenon. This fault and fold zone which extends roughly E-W in the northern part of Pakistan, while forming some syntaxial bends becomes oriented in a N-S direction in the western region. These north-south trending mountains in the west comprise two major ranges; the Sulaiman Range in the north and the Kirthar Range in the south.

The district of Khuzdar lies within the Kirthar Range which runs north-south for about 600 km. The strike of the ranges in the Khuzdar area changes abruptly and repeatedly from N-S to E-W and back again to N-S. This is why the area had been termed as "Khuzdar Knot" (Jones, 1960). The term refers to its knot-like appearance on geologic maps and connotes no genetic implications. The Khuzdar-Bela Metalogenic Province which extends southward from Khuzdar for about 350 km to the Arabian Sea is bounded by the Kirthar Fault on the

east and by the Ornach-Nal and Gazan fault systems on the west and north respectively. The Kirthar fault runs for about 150 miles to the south and is a zone of thrusting (Jones, 1960). It is believed that this block which is located on the western margin of the Indo-Pakistan subcontinent has not only dragged along Ornach-Nal fault, considered to be a sinistral transform boundary between the Indian and Eurasian plates, but also may have rotated counter-clockwise as an independent tectonic unit (Sarwar and DeJong, 1979).

The area is mainly composed of Jurassic and Cretaceous sequences of marine sediments deposited in a shelf environment under fluctuating conditions (Fatmi, 1986). The Pb-Zn-Barite mineralization in the area is found associated with interbedded Jurassic limestone and shale sequence in the upper part of the Zidi Formation.

SULFUR ISOTOPES

In order to make a study of the sulfur isotopes in sulfates, all of the 6 samples were collected from the Gunga deposit, as none of the other gossans have any associated barite. However, the samples were selected in such a way as to represent all varieties of barite, i.e., massive, crystalline, second generation barite, barite from within the gossan, and barite from the north body.

Analytical method

These barite samples were then analyzed by Krueger Geochron Laboratories (Massachusetts) for sulfur isotopes, following the method of Thode, et. al. (1961). In this method the sulfur in the sulfide specimens is burned in a stream of purified oxygen inside a fused quartz tube, placed in an electric furnace, at a temperature of 1200°C to obtain SO₂. After the removal of the impurities from the SO₂ thus produced, it is collected and stored in a sealed Pyrex tube for analysis on mass spectrometer.

For sulfate samples, barite is reduced first to sulfide by boiling them in a mixture of HI, H₃PO₃,

and HCl. The H_2S thus obtained is then absorbed in a solution of cadmium acetate, acetic acid, and distilled water to form CdS . This is then converted to Ag_2S by reacting with $AgNO_3$ for easy filtration. Afterwards, the Ag_2S is burned in a simple combustion tube at high temperature as described above. The final analysis for the isotopic values of the sulfur is carried out with mass spectrometer under standard conditions.

DISCUSSION

Source of Sulfur

A $\delta^{34}S$ value of about 20‰ (permil) represents the isotopic composition of S in the modern marine sulfates (Faure, 1979, p. 531). The $\delta^{34}S$ value has varied through different periods of geological history and a large number of $\delta^{34}S$ values of marine sulfate minerals suggest (Claypool et al., 1980) that they varied from 30‰ in Cambrian period through about 10‰ at the end of Permian to 20‰ at present (Fig. 2). The $\delta^{34}S$ values of the sulfur in the Jurassic oceans was about 17‰. The isotopic composition of our barite samples range from +26.8‰ to +33‰ (see Table), with an average value of +28.7‰ when we omit the anomalous +63‰ value of one of the samples because it is not certain if this is real transposition of digits, or an analytical error. This average value is much higher than what would normally be expected for Jurassic marine sulfates. These high values can be explained in three ways: 1) the sulfur needed to deposit barite ($BaSO_4$) did not come from sea water, instead, it came sulfur enriched brines which brought other elements like Ba, Fe, Zn, Pb, etc., and formed the deposit. This S had higher concentration of heavy isotopes than that of the Jurassic sea water sulfate because of its source, which could be perhaps in some Cambrian or Precambrian evaporites; 2) at the time of deposit formation, fractionation of isotopes took place as a result of some chemical isotopic exchange reaction such as reduction; 3) the increase in the values of $\delta^{34}S$ brought about by the diagenesis of the sediments.

(1) Transported Sulfur

These sulfide and sulfate deposits are strata-bound, contained in the limestone, mudstone and shale. No igneous rocks except tectonically emplaced ophiolites to which no direct relation has been known to exist (Sillitoe, 1978, p. 382), are found in or immediately around the study area. So there seems to be little chance that the source of sulfur lies in direct magmatic fluids. The other possibility of sulfur being derived from some external source may be that the ore bearing solutions migrated through rocks containing evaporites before reaching the site for precipitation. Except for a few pieces of gypsum that were found near the gossan at Gunga, no concrete evidence of any evaporite bed is present in or around the area. However, a possibility can be considered: it has been suggested (Sarwar & DeJong, 1979, p. 346; Klootwijk et al., 1981) that very peculiar structural features of the Pakistan fold belt, e.g., oroclines, hairpin bends, lobe or garland structure of Sulaiman Range etc. were formed due to the southward tectonic transport in a thin-skin fashion as a result of the compression caused by intercontinental collision (Fig. 3). The movement on such a mammoth scale was facilitated by the plastic flow of evaporite formations present underneath the fold belt. Salt mines at Khewra in northern Pakistan may be considered as an evidence of the presence of salt in the region. This salt unit, known as the Salt Range Formation contains also gypsum and anhydrite beds, in addition to the salt. Some exposures of salt have also been reported in the Sulaiman Range which lie a few hundred kilometers north of Khuzdar. If the mineralizing solutions traveled deep so as to pass through evaporite formation (considered Cambrian or Precambrian in age), then they might derive sulfur from the anhydrite and gypsum as sulfate. Or, if the hydrologic regime was favorable, groundwater could have dissolved sulfates from these evaporites and be mixed with connate brines. This sulfur would be isotopically

heavy as it originally came from the Precambrian sea water sulfate. This could have reacted with barium being transported, probably as chloride complex, in solution to form barite. The change of pH due to the mixing of the two types of fluids may have facilitated precipitation.

(2) Chemically fractionated sulfur

Since the $\delta^{34}\text{S}$ values are very different from those of the sulfide minerals which may suggest that biogenic reduction was brought about by the sulfate reducing anaerobic bacteria in a restricted or lagoonal Jurassic environment closed to sulfates. As a result of kinetic isotopic effect, evolving H_2S would become depleted in ^{34}S while SO_4 would be enriched in ^{34}S (Jensen, 1967, p. 146-147; Ohmoto & Rye, 1979, p. 539-544). This sulfate water may have been stored in the pore spaces of the rocks, and when SO_4 came in contact with barium, barite was formed with a relatively high content of $\delta^{34}\text{S}$ as observed today.

(3) Diagenetically fractionated sulfur

Isotopic data obtained by Goldhaber & Kaplan (1980) from the sediments of the Gulf of California shows variation in the $\delta^{34}\text{S}$ values with change of depth. Significant increase in $\delta^{34}\text{S}$ values with increasing depth is observed. This reflects the effect of diagenesis of sediments on the sulfur isotopic

values. So the $\delta^{34}\text{S}$ values in case of Khuzdar barite may be due to the nature and state of diagenesis of the Zidi Formation.

However, sulfur being derived from the connate brines contained in the Cambrian evaporitic rocks, seems to offer a relatively easy and simpler explanation for the high isotopic values encountered in the barite of Khuzdar deposits.

CONCLUSION

The sulfur isotopic values of the barite samples from Gunga do not match with those of the sulfates present in the Jurassic oceans in which, the host rocks of these deposits were deposited. This discrepancy in the ages of the host rock and the hosted, is explained by the suggestion that the sulfur used in the formation of these deposits was not extracted from the Jurassic seawater sulfates. Instead it was derived from the deeply underlying Cambrian or Precambrian evaporitic formations by the circulating basinal fluids. These fluids were kept in motion by the constant compression of the rocks caused by the collision between the Indian and Eurasian plates. This presents a simple and a reasonable solution to the problem, particularly, in view of the evidence for tectonic transport of the Pakistan fold belt over the evaporitic decollement surface in a thin-skin fashion.

REFERENCES

- Ahmad, W., 1950. Summary of field notes on the area between Khuzdar and Nal, Kalat Division : *Geol. Surv. Pakistan File* 173.
- Banks, C.J., and Warburton, J., 1986. "Passive—roof" duplex geometry in the frontal structure of the Kirthar and Sulaiman mountain belts, Pakistan : *Jour. Struct. Geol.*, **8**, 229-237.
- Claypool, G.E., Holster, W.T., Kaplan, I.R., Sakai, H., and Zak, I., 1980. The age curves of sulfur and oxygen isotopes in marine sulfate and their mutual interpretation : *Chem. Geol.*, **28**, 199-260.
- Fatmi, A.N., 1986. Zidi Formation (Ferozabad Group) and Parh Group (Monajhal Group) Khuzdar district, Baluchistan, Pakistan, *Rec. Geol. Surv. Pakistan*, **75**, 32 p.
- Faure, G., 1986. Principles of isotope geology, 2nd Ed., John Wiley and Sons, 589 p.
- Goldhaber, M.B., and Kaplan, I.R., 1980. Mechanism of sulfur incorporation and isotope fractionation during early diagenesis in sediments of the Gulf of California. *Marine Chem.* **9**, 95-143.
- Hunting Survey Corporation, 1960. Reconnaissance geology of part of West Pakistan : Report published for the Govt. of Pakistan by the Govt. of Canada, Toronto, 550.
- Jankovic, S., 1986. The mineral association and genesis of the lead-zinc-barite deposits at Gunga, Khuzdar district, Baluchistan, Pakistan : *Rec. Geol. Surv. Pakistan*, **71**, 22 p.
- Jensen, M.L., 1967. Sulfur isotopes and mineral genesis : Chapter 5, In, Barnes, H.L. (Ed), *Geochemistry of hydrothermal deposits*, Holt, Rinehart, and Winston Inc., New York, 143-165.
- Jones, A.G., 1960. Reconnaissance geology of part of West Pakistan : A Colombo Plan Cooperative Project : Govt. of Canada, Toronto, 550 p.
- Klinger, F., Ahmad, M.I., 1967. Barite deposits near Khuzdar, Kalat Division, West Pakistan : *Rec. Geol. Surv. Pakistan*.
- Klootwijk, C.T., Russel, N., DeJong, K.A., and Ahmed, H., 1981. A paleomagnetic reconnaissance of northern Balochistan, Pakistan : *Jour. Geoph. Res.* **86**, No. B1, 289-306.
- Ohmoto, H., 1972. Systematics of sulfur and carbon isotopes in hydrothermal ore deposits : *Econ. Geol.* **67**, 551-578.
- Ohmoto, H., and Rye, R.O., 1979. Systematics of sulfur and carbon isotopes, In, Barnes, H.L., (Ed), *Geochemistry of hydrothermal ore deposits*, 2nd Ed., Wiley Interscience, New York, 509-561.
- Rye, R.O., and Ohmoto, H., 1974. Sulfur and carbon isotopes and ore genesis : A review : *Econ. Geol.* **69**, 826-842.
- Sarwar, G., and DeJong, K.A., 1979. Arcs, oroclinal, syntaxes : The curvature of mountain belts in Pakistan : In, Farah and DeJong, *Geodynamics of Pakistan*, 341-349.
- Schmidt, R.G., Ahmad, M.I., Asad, S.A., 1961. Mineral commodity, *Geol. Surv. Pakistan File*.
- Sillitoe, R.H., 1978. Metallogenic evolution of collisional mountain belt in Pakistan : A preliminary analysis : *Jour. Geol. Soc. London*, **135**, 377-387.
- Thode, H.G., Monster, G.H., Dunford, H.B., 1961. Sulfur isotope geochemistry : *Acta Geochem. Cosmochem* **25**, 159-174.

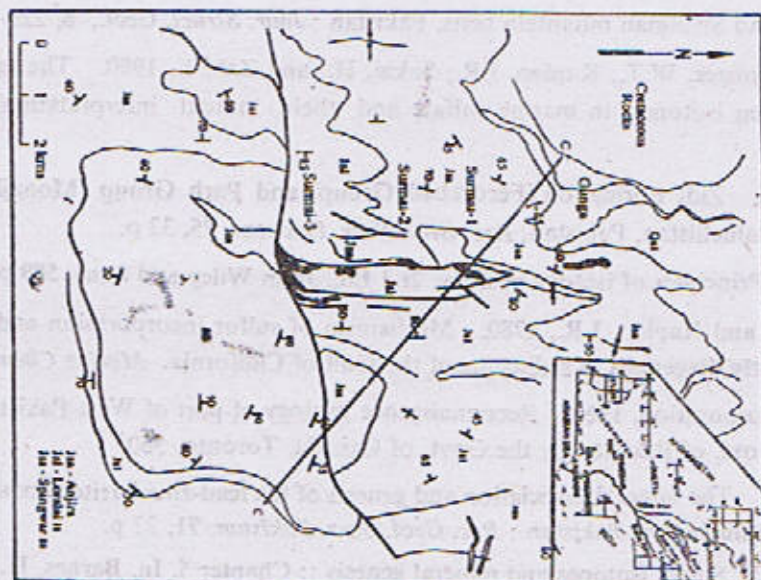


Fig. 1. Geological map of the Ganga-Sutlej area, Khushkar District, Balochistan.

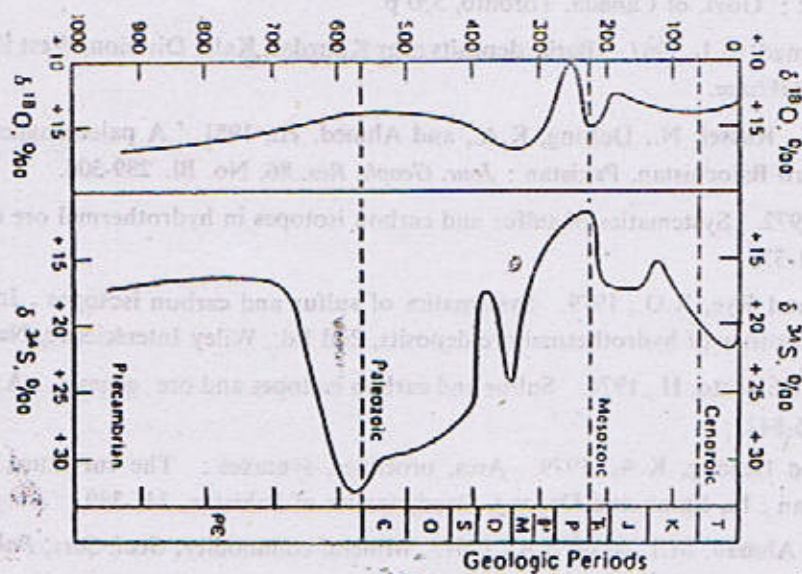


Fig. 2. Variation of $\delta^{18}\text{O}$ and $\delta^{34}\text{S}$ of marine sulfate minerals from Late Precambrian to the present (cf. Faure, 1986).

SEDIMENTOLOGY OF DATTA FORMATION AT KALAPANI, ABBOTT- ABAD, NORTHWEST HIMALAYAS, PAKISTAN

By

M. NAWAZ CHAUDHRY, ADIL MANZOOR,* MUNIR GHAZANFAR

Institute of Geology, Punjab, University Lahore-54590, Pakistan

*University of Oslo, Norway

AND

NAVEED AHSAN

Building Research Station, Q. A. Campus, Lahore-54590, Pakistan

Abstract : *Datta Formation of Early Jurassic age from Kalapani, District Abbottabad has been studied for the microfacies, petrographic characteristics, diagenesis, environment of deposition, provenance and burial and uplift history. This Formation was supposed to be absent at Kalapani (Shah, 1977). However, according to our studies it is 17.96 m thick at Kalapani. It is composed predominantly of fine grained quartz arenites with one horizon of quartz wacks, two horizons of arenaceous limestone and a lateritic band. Overall carbonate is the predominant cement. Clays, quartz and iron oxides are minor to subordinate cements. The heavy mineral suite includes iron, oxides tourmaline, epidote, sphene and biotite. This assemblage indicates an ultimate igneous metamorphic sialic source with minor basifemetabasic component. The overall composition of the sandstone, its textural and compositional maturity, the restricted suite of heavy minerals, their amounts and shapes indicate a recycled origin for the sandstones of Datta Formation. The granitoid component was of S-type. Lack of kyanite, sillimanite and garnet suggest that high grade gneisses were not exposed in the source area. This fact is further supported by the presence of blue tourmaline which indicates autochthonous granitoid intrusions in the epizone with thermal aureoles.*

The cement stratigraphy in addition to submarine and very early calcite cementation indicates the following sequence; early quartz cement → Kaolinite cement → early calcite cement → dolimitic cement → ferroan calcite cement and finally late deep burial quartz cement.

The environment of deposition varies from lower to upper shore face, lagoonal and subareal. Datta Formation was deposited during an over all transgression during the Early Jurassic. Within an overall transgression two minor phases of regression and three phases of transgression have been identified. The maximum depth of burial is estimated at about 4550 m at which oil and gas maturation and reduction of primary porosity took place.

INTRODUCTION

Datta Formation is a persistent and widely exposed unit of Upper Indus Basin. It is very well exposed at a number of places in Kohat,

Potwar and Hazara area. Overall, it shows wide variation in thickness, lithology and environment of deposition. It was deposited in continental, supratial, intertidal as well as lacustrine

environments.

It contains large quantities of silica sand, fire clay and high alumina clays. It is also an important hydrocarbon reservoir.

Gee (1954) and earlier workers named this unit as variegated stage. However Danilchik (1961) and Danilchik and Shah (1967) renamed it as Datta Formation. This name which has now been approved by the Stratigraphic Committee of Pakistan has also been applied to the lower parts of Samana Bed of Davies (1930) in parts of Kohat, Kala-Chitta and Hazara, Red Beds and part of Kioto Limestone of Middlemiss (1896) and lower part of Maira Formation of Davies and Gardezi (1965).

In Hazara area this unit is mainly composed of very fine to medium grained quartz arenites with subordinate beds and layers of limestone, arenaceous limestone, siltstone, microconglomerates lithic arenites and occasional hardground.

In Salt Range and Kala Chitta this unit comprises of variegated sandstone, silt stone, shale, mudstone, fire clay, high alumina refractory clays, silica sand, calcareous, dolomitic and carbonaceous horizons. For details the reader is referred to Shah (1977), Hussain et al. (1967), Cheema (1974), Ashraf et al. (1973), Baloch (1986) and Chaudhry et al. (1994).

The type section is located in Datta Nala (lat. $30^{\circ} 00'N$; long $71^{\circ} 19'E$) in the Surghar Range. The thickness at the type locality is 212m. Maximum reported thickness of Datta Formation is 400m in Shaikh Budin Hill in Surghar Range.

According to Shah, (1977) the Datta Formation varies in thickness, in Hazara area, from 0- 10 m and is absent at Kalapani. However our work shows that this Formation ranges in thickness from 0.6m near Thai to as much as 17.96m at Kalapani.

In this area it is an overall transgressive facies and lies unconformably over Hazara Formation of Upper Proterozoic age.

Its age has generally been considered as Pre-Toarcian (Shah, 1977).

Contrary to the descriptions of Shah (1977) Shinawari Formation can hardly be identified as a distinct lithostratigraphic unit in Galiat area of Hazara.

GEOLOGY OF BAGNOTAR-KALAPANI AREA

The overall stratigraphic sequence of the Hazara area of Attock Hazara Fold and Thrust Belt is given in Table 1. But in the area of Kalapani this Formation overlies Upper Proterozoic Hazara Formation with an unconformity. In this section the Abbottabad Formation of Upper Proterozoic and Hazira and Galdanian Formations of Early Cambrian age are missing. The location map of the area is given as Fig. 1.

The measured section is 17.96m thick. At Kalapani this formation is composed predominantly of quartz arenite with one horizon of quartz wacke, two horizons of arenaceous limestone and a laterite band. Its microfacies and lithological features are given in Table 2.

For regional geology, palaeontology and stratigraphy the reader is referred to benchmark papers of Latif (1970b, 1970c, 1972 and 1973) and Butt (1986).

PETROGRAPHY OF DATTA FORMATION AT KALAPANI

In the following are discussed salient petrographic features of the microfacies of Datta Formation from Kalapani (Table 2). The mineral composition of the microfacies studied is given in Table 3. The textural parameters and porosity types are listed in Table 4.

The various carbonate minerals in thin sections were distinguished using staining techniques of

Dickson (1965). Clay minerals were identified by employing X-ray diffraction techniques.

DKP-1 : Carbonate Cemented Quartz Arenite

This microfacies (Plate A-1) is very fine grained, texturally and compositionally mature and well sorted. The grains are subrounded. Slate clasts are 1.0%. The grains are almost entirely of quartz. There are a few polycrystalline quartz fragments. The accessory to trace minerals are limonite, haematite, sphene, tourmaline, plagioclase, zircon, epidote and carbonaceous matter. Carbonate is the predominant cement with 9% ferroan calcite, 20% non ferroan calcite and 10% non ferroan dolomite. Some dolomite has been dedolomitized to non ferroan calcite. Non ferroan calcite appears to be mainly an earlier cement which is replaced by ferroan calcite. Textural evidence suggests that dolomite replaces both non ferroan calcite as well as ferroan calcite. Dedolomitization appears to be the last replacement.

Quartz grains are in contact with one another at a few places, here they show point contacts. Quartz cement is trace to minor. Quartz grains are moderately corroded and replaced by carbonate. Quartz overgrowths over quartz are rarely seen under the petrographic microscope. The carbonate cement shows low amplitude stylolites and pressure seams.

DKP-2 : Carbonate and Quartz Cemented Quartz Arenite

It (Plate A-2) is fine grained subangular to subrounded moderately well sorted quartz arenite. It is texturally and compositionally mature. It is composed predominantly of quartz grains with accessory to trace minerals like limonite, haematite, zircon, sphene, muscovite, tourmaline, biotite, epidote, chert and carbonaceous matter. Inclusions of rutile needles and tiny tourmaline grains occur in some quartz grains.

Both, carbonates as well as quartz serve as a cement. The carbonate cement is composed of 3% non ferroan calcite, 20% ferroan calcite and 10% non ferroan dolomite. Quartz is also an important cement. Quartz overgrowths over quartz, concavoconvex contacts and a few long contacts are present. At places, quartz grains are slightly corroded and marginally replaced by carbonate.

Rare low amplitude stylolites in carbonate part may be present.

DKP-3 : Pelletoidal Packstone

The pellets (51%) are fine to medium grained (plate A-3), grey to dark grey in colour, moderately well sorted and generally oval to rounded but, some what elongated in shape.

The pellets lack nuclei. However central part of some pellets may be composed of spar indicating the presence of an early spar cement. This spar is mainly non ferroan calcite. But, at places, it may be replaced by ferroan calcite.

Haematite and limonite is 3.5% and quartz grains are 3%. Bioclasts are 5%. Some bioclasts have strongly micritized shells with spar in the middle indicating algal boring.

The pellets are embedded in carbonate cement which is mainly micritic. The carbonate cement is composed of 15% non ferroan calcite, 10% ferroan calcite and 8% non ferroan dolomite.

DKP-4 : Hard Ground/Laterite

Iron oxides (both haematite and limonite) constitute 55% of the rock (Plate A-4). The clastic part of this hard ground is composed of medium grained, subrounded moderately well sorted and strongly fractured quartz grains (36%). Chert fragments are 2%. A few quartz grains contain inclusions of rutile and tourmaline. A few complete to incomplete rims and coats of kaolinite occur around clasts of quartz and chert.

Clay (7%) also occurs as a pore filling cement. The predominant cementing material is haematite. Quartz overgrowths over quartz are seen at some places. Haematite corrodes quartz grains marginally.

DKP-5 : Clay and Haematite Cemented Quartz Wacke

This microfacies (Plate A-5) is fine grained, subangular to subrounded well sorted and texturally and compositionally mature. The grains are almost entirely of quartz. Most of the clay (17%) and haematite (14%) has been transported to the site of deposition. The accessory to trace minerals are muscovite, chert, tourmaline, plagioclase, microcline, zircon and carbonaceous matter. Inclusions of tourmaline, rutile and zircon are present in some quartz grains. Quartz is 61%.

The cement is predominantly an intimate admixture of clay and haematite with bent and distorted thin books and flakes of muscovite serving as reinforcement. The cement is however unevenly distributed. At places it occurs as patches with quartz grains floating in it. At other places it forms thin films to thick coats around the clasts (Plate B-1).

A few grains show overgrowths. In clays a few pressure seams are seen. Mica flakes are bent and distorted.

DKP-6 : Carbonate and Clay Cemented Quartz Arenite

The clastic part of this microfacies (Plate A-6) is fine grained, subangular to subrounded and moderately well sorted. It is texturally submature but compositionally mature. Quartz is the predominant constituent of the clastic part. The accessory to trace amounts of haematite, limonite, biotite, chert, muscovite, epidote, tourmaline, plagioclase, microcline, sphene, zircon and carbonaceous matter is present. There are a few polycrystalline quartz grains. Bioclasts are

replaced by non ferroan calcite.

Cementing material is mainly carbonate having 25% non ferroan calcite and 8% ferroan calcite. Clay (7%) is a subordinate cement. Non ferroan calcite appears to be earlier cement which was replaced by dolomite which in turn has been replaced by non ferroan calcite as well as ferroan calcite. Dedolomitization appears to be the last replacement. Now there is no dolomite or ferrom dolomite left. At a few places quartz grain are in contact with one another. Here they show minor point contacts. Quartz cement is trace to minor.

Quartz grains are moderately corroded by carbonate cement. A few quartz grains show quartz overgrowths over quartz. The carbonate cement shows the development of a few stylolites.

DKP-7 : Carbonate, Clay and Haematite / Limonite Cemented Quartz Arenite

This microfacies (Plate A-7) has fine grained, subrounded and moderately well sorted clastic part. It is texturally submature and compositionally mature. The accessory to trace minerals are biotite, chert, muscovite, plagioclase, microcline, tourmaline, zircon, sphene, epidote and carbonaceous matter. Inclusions of rutile needles and tiny tourmaline grains may be present in the quartz grains.

Cement is predominantly an intimate admixture of carbonate, clays and iron oxides with some bent mica flakes serving as reinforcement. The haematite and limonite are however unevenly distributed while clays and carbonate cement is more or less uniformly distributed. Non ferroan calcite appears to be the earlier cement which is replaced by ferroan calcite.

Contacts amongst the quartz grains are generally long. A few point contacts having thin films of clays and carbonate are also exhibited by quartz. Moderate corrosion of quartz grains by

the cement is observed. At places quartz grains show overgrowths.

DKP-8 : Carbonate Cemented Quartz Arenite

This microfacies (Plate A-8) is fine grained, subrounded and moderately well sorted. It is compositionally mature and texturally submature. The grains are predominantly of quartz (50%). Accessory to trace minerals of this facies are clays (kaolinite/illite), iron oxides (haematite/limonite), chert, sphene, carbonaceous matter, muscovite, biotite, microcline, plagioclase, epidote, zircon and carbonaceous matter. A few quartz grains have inclusions of tourmaline.

Bioclasts have been replaced by non ferroan calcite. Clays occur either as pore fillings or thin films along contacts amongst quartz grains.

Carbonate is the predominant cement with 20% non ferroan calcite and 18% ferroan calcite. At a few places dolomite is completely replaced by non ferroan calcite. Non ferroan calcite seems to be the earlier cement and is replaced by the ferroan calcite.

A few quartz grains show heavy overgrowths. At places stylites are observed. Rarely point contacts are observed with thin films of clays. At places quartz grains are moderately corroded by carbonate cement.

DKP-9 : Arenaceous Wackestone

It is fine grained, subrounded and moderately sorted (Plate A-9). It is texturally submature and compositionally mature. The accessory to trace minerals/constituents are pellets, olites, Iron oxides (haematite, limonite), clays (kaolinite/illite), biotite, muscovite, sphene, chert, tourmaline, plagioclase and carbonaceous matter. Inclusions of rutile are rarely seen. At places a few polycrystalline quartz grains are present. Bioclasts (11%) are also present. They are replaced by the non ferroan calcite. Predominant cement of this facies is carbonate with 49%

ferroan calcite and 10% non ferroan calcite. Stylolites also occur. Quartz overgrowth over quartz grains are rarely observed. At places significant corrosion of quartz grains by carbonate cement is observed.

DKP-10 : Carbonate, Iron Oxides (and Clay) Cemented Quartz Arenite

This microfacies (Plate A-10) is fine to medium grained, bimodal, subrounded and poorly sorted. It is texturally submature and compositionally mature. The grains are predominantly of quartz (40%). There are a few polycrystalline quartz grains. The accessories are muscovite, tourmaline, chert, sphene, biotite, plagioclase, microcline, epidote, zircon, bioclasts (algal) and carbonaceous matter. Inclusions of rutile are rarely observed in quartz grains.

Cement is predominantly an intimate admixture of carbonate, iron oxides and clays. The clays and iron oxides are unevenly distributed while the carbonate cement is evenly distributed. It appears that primary cement was non ferroan calcite which has been partially replaced by ferroan calcite.

Very rare point contacts are present. Overgrowths of tourmaline over tourmaline are seen at places. Heavy quartz overgrowths over quartz grains are observed. Stylolites are frequently seen. Quartz grains are moderately corroded by cement.

DKP-11 : Carbonate, Quartz, Clay and Iron Oxide Cemented Quartz Arenite

In this microfacies (Plate A-11) the clastic part is almost entirely fine grained, moderately sorted, bimodal, subangular to subrounded. Quartz is 66%. It is texturally submature and compositionally mature. The accessory to trace constituents are chert, plagioclase, muscovite, tourmaline, zircon, microcline, bioclasts (algal) and carbonaceous matter. Inclusions of tourmaline in quartz grains are present.

Cement is predominantly carbonate i.e. ferroan calcite and non ferroan dolomite with a mixture of clay and iron oxides (limonite/haematite) which are unevenly distributed. Textural evidence suggests that non ferroan dolomite has been completely replaced by ferroan calcite. Quartz is also a subordinate cement.

The contacts amongst the quartz are concavo-convex and long. Stylolites are also present in the cement. Overgrowths of tourmaline over tourmaline grains and overgrowths of quartz over quartz grains are observed. Corrosion of quartz grains by cement is also seen (Plate B-2).

DKP-12 : Carbonate, Quartz and Clay Cemented Quartz Arenite

The microfacies (Plate A-12) is fine grained, subangular to subrounded texturally submature, compositionally mature and moderately well sorted. The clastic part of this microfacies is mainly quartz (61%). The accessories are iron oxides (limonite and haematite), chert, tourmaline and carbonaceous matter. At places quartz grains have inclusions of tourmaline. Rare polycrystalline quartz grains are also present.

Cement is predominantly carbonate with 6% non ferroan dolomite, 8% ferroan calcite and 6% non ferroan calcite. Ferroan dolomite appears to have been the earlier cement which is partially replaced by ferroan calcite. At the end ferroan calcite and non ferroan dolomite is partially replaced by non ferroan calcite.

Clays are deposited in the pore spaces and also occur as thin films around quartz grain. Quartz cement is also present.

Contacts amongst the quartz grains are point and concavoconvex. At places quartz overgrowths over quartz are observed. Moderate corrosion of quartz grains by cement and clay is seen.

FACIES OF DATTA FORMATION AND THEIR TENTATIVE INTERPRETATION

In the following 12 microfacies of the Datta Formation at Kalapani are grouped in 6 facies based on environment of deposition (Table 2, Fig. 3). This section of the formation represents a mixed clastic-carbonate microtidal shore line of a generally transgressive origin (with lagoons) formed in Lower Jurassic.

In detail three transgressive and two regressive episodes within the framework of a general transgression are recognised (Fig. 3).

Facies A

It (DKP-1 and 2) marks beginning of a transgression at the base of Datta Formation at Kalapani. This facies is fine to very fine grained subangular to subrounded, texturally and compositionally mature and well sorted carbonate and quartz cemented quartz arenite with few slate clasts and grit streaks. It is reworked and deposited on upper shore face in high energy conditions.

Facies B

This facies (DKP-3) marks an onset of a regression. Pellets are fine to medium grained, moderately well sorted and oval to rounded. It was deposited in a lagoon in low energy conditions.

Facies C

It marks a subareal exposure due to regression (iron oxides 55% and quartz 36%) with a few bauxitic/kaolinite pellets at bottom and clay (17%) and haematite (14%) rich quartz (61%) wacke.

Facies D

It marks a second phase of transgression. It contains three microfacies (DKP-6, 7 and 8). It is fine grained, mainly subrounded, modera-

rately well sorted, texturally submature and compositionally mature quartz arenite with a few bioclasts. It was deposited in low energy conditions on lower shoreface.

Facies E

It was deposited during regression. It (DKP-9) is an arenaceous wackestone. Its elastic part is fine grained, subrounded and moderately sorted quartz grains in sparry cement. It was deposited in low energy conditions in a lagoon.

Facies F

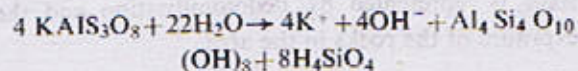
It is a transgressive facies. It comprises of three microfacies (DKP-10, 11 and 12). It is fine to medium grained bimodal (lag) subangular to subrounded poorly sorted clay cemented quartz arenite. It is texturally submature and compositionally mature. It was deposited during high energy conditions on upper shoreface.

The facies above contain marine fossils like brachiopods, belemnites, marine algae, gastropods and lamellibranchs (Except Facies C).

DIAGENESIS

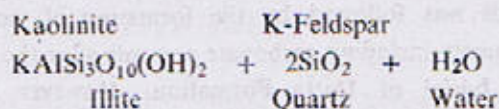
Clay Cement

The kaolinite cement is considered as mainly secondary and formed due to the attack of CO_2 bearing acidic waters of meteoritic origin on the K-feldspar, at shallow depth in the early stages of burial according to the following equation.



This however is an over simplified reaction which has not yet been duplicated in laboratory at low temperatures (Krauskopf, 1982).

This early diagenetic kaolinite cement was partially transformed to illite with increasing depth of burial according to the following equation



Various depths of burial (3.5-4.0 Km) have been proposed for this transformation by Chuhan et. al. (1992) and Chaudhry et al. (1994) (1000m) for this transformation.

Bjorlykke and Aagaard (1992) suggest a depth of burial of 3.5-4 km for this transformation.

In the case of Datta Formation such transformation is partial. After maximum depth of burial the area was uplifted and subjected to the circulation of CO_2 bearing meteoric waters. Small amounts of kaolinite were probably also formed during this late diagenetic stage by partial transformation of surviving K-Feldspar.

Quartz Cement

Early films of quartz cement, if formed, were subsequently replaced by deep burial quartz cement. The main quartz cementation probably took place during pressure solutioning at depths of burial greater than 2.5 km. Suturing of quartz grains and development of stylolites attest to widespread pressure solutioning of quartz of Datta Formation.

Carbonate Cement

The Datta Formation was deposited along a mixed elastic-carbonate shoreline. This is shown by the fact that the Datta sandstones almost everywhere in Hazara are interbedded with bioclastic, oolitic and pelletoidal limestone. Algal limestone beds also occur in Datta Formation near Jaster Gali (Chuhan et al. 1992).

The carbonate horizons are of course subordinate to the siliciclastic component of Datta Formation.

It is therefore quite likely that part of the carbonate cement in siliciclastic horizons submarine or very early diagenetic in origin.

This was followed by the formation of various cements including carbonate cements after the start of burial of Datta Formation. However it is not possible to estimate the proportion of submarine or very early diagenetic carbonate cement.

This was followed by the formation of early pore filling kaolinite cement at shallow depth, most probably in the presence of waters of meteoric origin (Selly, 1985).

After the formation of early kaolinite cement, on further burial, non ferroan calcite was deposited as slightly acidic circulating meteoritic waters changed their PH. It, at places replaces early kaolinite cement. This was followed on still deeper burial by reduction in the activity of oxygen and onset of reducing conditions due to the transformations taking place in organic matter. This coupled with the presence of iron oxides resulted in the formation of ferroan calcite and ferroan dolomite. During final uplift dedolomitisation and formation of some calcite occurred.

BURIAL AND UPLIFT HISTORY

In the case of Datta Formation of Kalapani the total thickness of stratigraphic column from Datta to Hangu Formation (Table 1) is estimated at about 680m. To this may be added another 110m on the top of Kawagarh Formation which has been leached to give rise to a laterite band of about 1m thick with approximately 30% total iron oxides (Chaudhry et al. 1994). In this way the total depth of burial in the first stage upto the beginning of Danian is estimated at 790m. At this depth of burial the rock was subjected to a temperature of about 40°C and pressure of 0.19Kb. Temperatures and pressures are discussed after Pettijohn et. al., (1986). During this burial Kaolinite was followed by the onset of precipitation of non ferroan calcite. During further burial reducing conditions prevailed due to the transformation in the organic matter. And in the presence of iron oxides, calcite was converted

to ferroan calcite and dolomite changed to ferroan dolomite. During this subsidence the decrease in primary intergranular porosity was not significant. Such conditions were much above the oil window.

In second stage after Danian the total depth of burial was 1515m. The temperature was approximately 53°C and pressure was about 0.3Kb. Lockhart, Patala, Margalla Hill, Chorgali and Kuldana formations were deposited at that time and stylolites were developed in limestones. Probably during this stage kaolinite started partially transforming into illite. This transformation continued to the next stage of burial.

In the third stage the total depth of burial reached upto 4550m in which Murree Formation was deposited on top of the Kuldana Formation. A 3035m thick column of Murree Formation is estimated. Towards the last stages of this burial the temperature was about 185°C and pressure was approximately 1.12Kb. Significant porosity reduction and oil formation could therefore have occurred at the end of Miocene. Most microstylolites in quartz arenites could therefore have developed during the last stages of this burial with maximum precipitation of quartz cement.

During uplift of the basin small amounts of late diagenetic kaolinite precipitated as pore filling. At places it has replaced a few sutured quartz contacts. Deposition of this Kaolinite is caused by the flux of acidic meteoric waters. The last stage is represented by dedolomitisation and the exposure of the rocks in the area.

ACKNOWLEDGEMENTS

We acknowledge with thanks the financial assistance of the University of the Punjab, Lahore under the Project "Lithostructural Mapping and Sedimentological Study of Murree-Abbottabad Section, North West Himalaya".

We also thank Dr. K. Rass Masood for his help in microphotography.

REFERENCES

- Ashraf, M., Ahmad, M., and Faruqi, F. A., 1973. Jurassic bauxite and kaolinite deposits of Chhoi area, Kala Chitta Range, Punjab, Pakistan, *Geol. Bull. Punjab Univ.*, **12**, 41-53.
- Baloch, I.H., 1986. A mineralogical study of the industrial utilization of bauxitic clays of Nawa area, Kala Chitta range, Attock District, Pakistan. *Acta Mineralogica Pakistanica*, **2**, 144-152.
- Bjoreyke, K., and Aagaard, P., 1992. Clay minerals in North Sea sandstones. In: Houseknecht, D.W. and Pittman, E.D. (Eds.), Origin, diagenesis and petrophysics of clay minerals in sandstones *Soc. Econ. Pal. Min. Spec. Publ.* **47**, 65-80.
- Butt, A. A., Plate tectonic and the Upper Cretaceous biostratigraphic synthesis of Pakistan. *Acta mineralogica Pakistanica*, **2**, 60-64.
- Chaudhry, M. N., Chuhan, F. A., and Ghazanfar, M., 1994. Microfacies, Diagenesis, Environment of Deposition and Burial History of Datta Formation from Bara Oter, Distt. Abbottabad. *Kashmir Jour. Geol.* **11-12**, 43-58.
- Chaudhry, M.N., Ghazanfar, M. and Ahsan, N., 1994. Rates of sedimentation of Kawagarh Formation at Glah, Abbottabad-Nathia Gali Road and timing of uplift at K-T boundary in Pakistan. *Pak. Jour. Geol.* **2 and 3**, (1,) 29-32.
- Cheema, M.R., 1974. Geology of Chhoi-Jabbi-Wala Kas area with emphasis on early Jurassic high alumina clay and bauxite deposits, Northern Kala Chitta, Campbellpur District, Punjab Province Pakistan. *Geol. Surv. Pakistan. Technical Report*, **129**, 19-3.
- Chuhan, F.A., Chaudhry, M.N., and Ghazanfar, M., 1992. Microfacies, Diagenesis and Environment of Deposition of Datta Formation from Jaster Gali, District Abbottabad, Hazara, Pakistan, *Geol. Bull. Punjab Univ.*, **27**, 47-62.
- Danilchik, W., 1961. The Iron formation of the Surghar and western Salt Range, Mianwali District, West Pakistan, *U.S. Geol. Surv. Prof. Paper*, **424-D**, 228-231.
- Danilchik, W., and Shah, S. M. I., 1967. Stratigraphic nomenclature of formations in Trans-indus Mountains, Mianwali District, West Pakistan. *U. S., Geol. Surv. Proj. Paper*. **424-D**, 228-231.
- Danilchik, W., and Shah, S. M. I., 1967. Stratigraphic nomenclature of formations in Trans-Indus Mountains, Mianwali District, West Pakistan, *U.S., Geol. Surv. Proj. Report*, (IR) PR-33, 445
- Davies, R.G., and Gardezi, A.H., 1965. The presence of Bouleiceras in Hazara and its geological implications. *Geol. Bull. Punjab Univ.* **26**, 23-30.
- Davies, R. G., 1930a. The fossil fauna of Samana Range and some neighbouring areas; Part I, An Introductory Note; *Mem., Geol. Surv. India Palaeont. Indica, New Series*, **15**, 1-15.
- Dickson, J. A. D., 1966. Carbonate identification and genesis as revealed by staining. *our Sed. Pet.*, **36**(2), 491-505.

- Gee, E.R., 1945. The age of the Saline Series of the Punjab and of Kohat. *Proc. India Natl. Acad. Sci., Sec. B*, 14, Pt. 6, 269-310.
- Hussain, T and Khan, A.L., 1967. Fire clay deposits of Kala Chitta Range, District Campbellpur, West Pakistan, *Geol. Survey, Pakistan Report*, 1-89.
- Krauskopf, K.B., 1982. Introduction to Geochemistry, McGraw Hill Book Company, London, 617 p.
- Latif, M.A., 1970a. Micropalaeontology of the Chanali Limestones, Upper Crétaceous of Hazara, West Pakistan *Geol. Jahrb. Bundesanst.*, 15, 25-61.
- Latif, M.A., 1970b. Micropalaeontology of the Galis Group. Hazara, West Pakistan; *Geo. Jahrb. Bundesanst.* 15, 63-66.
- Latif, M.A., 1972. Lower Palaeozoic (? Cambrian) Hyolithids from the Hazara Slate, Pakistan; *Nature, Phys. Sci.* 240, 100, 1-92.
- Latif, M.A., 1973. Partial extension of the evaporite faciès of the Salt Range to Hazara, Pakistan; *Nature Phys. Sci.* 244, 138, 124-125.
- Middlemiss, C. S., 1896. The geology of Hazara and the Black Mountains. *Mem., Geol. Surv., India*, 26, 302 p.
- Pettijohn, F.J., Potter, P.E., Siever, R., 1986. Sand and Sandstone. Second Edition, Springer-Verlage New York, 552 p.
- Selley, R.C., 1985. Elements of Petroleum Geology, W.H. Freeman and Company New York., 449 p.
- Shah, S.M.I., 1977. Stratigraphy of Pakistan, *Mem. Geol. Surv. Pakistan*, 12, 34-43.

Table 1. Stratigraphic Table of the Area.

Age	Formation	Lithology
Early Miocene	Murree	Grey and reddish sandstone and shales
Early to Early Middle Eocene	Kuldana	Maroon to varicolour shales and marls
Early Eocene	Chorgali	Thinly bedded limestone and marls
Early Eocene	Margala Hill Limestone	Nodular foraminiferal limestone
Eocene to Early Palaeocene	Patala	Greenish grey/khaki shales with limestone
Middle Palaeocene	Lockhart Limestone	Nodular foraminiferal limestone
Early Palaeocene	Hangu	Sandstone, claystone, laterite.
.....Disconformity.....		
Late Cretaceous	Kawagarh	Fine grained, light grey limestone/marl
Early Cretaceous	Lumshiwal	Grey to brownish, coarse sandstone
Late Jurassic to Early Cretaceous	Chichali	Dark grey shales with sandstone beds, medium grained
.....Disconformity.....		
Middle Jurassic	Samanasuk	Limestone with dolomitic patches
Early Jurassic	Datta	Calcareous Sandstones/ limestones
.....Disconformity.....		
Precambrian	Abbottabad	Dolomites with sandstone, shale and boulder bed at base
.....Unconformity.....		
Late Precambrian	Hazara	Slates, sandstones and quartzites

Facies Microfacies Sample Position (m)	Description of Microfacies,	Environment
DKP-12	Carbonate, Quartz and Clay Cemented Quartz Arenite : Fine grained, subangular to subrounded, and moderately well sorted. Light grey to light brown on fresh surface, medium rusty brown to grey rusty brown on weathered surface.	
DKP-11	Carbonate, Quartz, Clay and Iron Oxides Cemented Quartz Arenite. Fine grained, subangular to subrounded and moderately sorted. Light grey to light brown on fresh surface medium rusty brown to grey rusty brown on weathered surface.	
F DKP-10	Carbonate, Iron Oxides (and clay) Cemented Quartz Arenite. Fine grained, bimodal, subrounded but poorly sorted. Light grey to light brown on fresh surface and medium rusty brown to grey rusty brown on weathered surface.	Upper shore face, high energy
TRANS GRESS ION		
E DKP-9	Arenaceous Wackestone : The elastic part is fine grained, subrounded, moderately sorted quartz grains in abundant sparry cement. Light grey to light yellowish on fresh surface, light greyish brown to light rusty yellow on weathered surface.	Lagoonal low energy
REGRESSION		
DKP-8	Carbonate Cemented Quartz Arenite : Fine grained, subrounded, moderately well sorted and fossiliferous quartz arenite. Medium grey on fresh surface and light rusty grey on weathered surface.	
DKP-7	Carbonate, Clay and Haematite/Limonite Cemented Quartz Arenite : Fine grained subrounded and moderately well sorted. On fresh surface medium grey to white, light rusty grey on weathered surface.	
D DKP-6	Carbonate and Clay Cemented Quartz Arenite: Fine grained, subangular to subrounded and moderately well sorted quartz grains. Medium grey on fresh surface and light rusty grey on weathering surface.	Lower shore face low energy
TRANS GRESS ION		
DKP-5	Clay and Haematite Cemented Quartz Wacke : Fine grained, subangular to subrounded moderately well sorted clay and haematite cemented quartz wacke. Medium grey on fresh surface and yellowish grey on weathered surface.	
C DKP-4	Hard Ground/Laterite : Limonite/Haematite with subordinate medium grained subrounded and moderately well sorted quartz grains, fresh surface dull red to grayish red, weathering surface deep rusty brown.	Subareal residual deposit
B DKP-3	Pelletoidal Packstone : Pellets are fine to medium grained and moderately well sorted. Very dark grey on fresh surface, medium rusty brown to grey on weathered surface.	Lagoonal low energy
REGRESSION		
DKP-2	Carbonate and Quartz Cemented Quartz Arenite : Fine grained subangular to subrounded, moderately well-sorted carbonate and quartz cemented quartz arenite. Medium to dark grey on fresh surface having thin carbonate layers.	
A DKP-1	Carbonate Cemented Quartz Arenite : Very fine grained, sub-rounded and well sorted. Medium grey on fresh surface, light rusty on weathered surface with few slate clasts.	Upper shore face, reworked
TRANS GRESS ION		

Table No. 2. Facies and Microfacies Description of Measured Section of Datta Formation at Kalapani from Bottom to Top.

Table No. 2. Facies and Microfacies Description of Measured Section of Datta Formation at Kalapani from Bottom to Top.

TABLE No. 3. Mineral Composition of Datta Formation at Kalapani

Microfacies	DKP-12	DKP-11	DKP-10	DKP-9	DKP-8	DKP-7	DKP-6	DKP-5	DKP-4	DKP-3	DKP-2	DKP-1
Quartz	65.0	66.0	40.0	23.0	50.0	65.0	45.0	61.0	36.0	3.0	55.0	45.0
Non-Ferroan Calcite	6.0	—	19.0	10.0	20.0	7.0	25.0	—	—	15.0	3.0	20.0
Ferroan Calcite	8.0	3.0	24.0	49.0	18.0	10.0	8.0	—	—	10.0	20.0	16.0
Non-Ferroan Calcite	6.0	11.0	—	—	—	—	—	—	—	8.0	8.0	10.0
Ferroan Dolomite	—	—	—	—	—	—	—	—	—	—	—	—
Kaolinite	3.4	3.0	2.8	0.4	3.0	3.0	4.0	7.0	3.0	—	—	—
Illite	2.6	3.3	2.5	0.3	1.0	4.0	3.0	10.0	4.0	—	—	—
Bioclats	—	Tr	0.2	11.0	2.5	—	4.0	—	—	5	—	—
Plagioclase/Albite	—	0.5	0.1	Tr	0.2	0.4	Tr	0.5	—	—	—	Tr
Microcline	Tr	1.5	Tr	—	0.3	0.1	Tr	Tr	—	—	—	—
Biotite	—	—	0.2	0.6	0.3	2.0	2.0	—	—	—	Tr	—
Clasts/Slate	—	—	—	—	—	—	—	—	—	—	2.0	3.0
Iron Oxides	4.0	6.4	6.0	2.0	2.0	5.0	4.3	14.0	55.0	3.5	5.0	3.0
Tourmaline	Tr	0.7	0.7	Tr	Tr	0.2	Tr	0.5	—	—	1.0	Tr
Sphene	Tr	0.3	0.3	0.1	0.5	0.1	Tr	Tr	—	—	1.5	1.0
Muscovite	—	Tr	1.5	0.5	0.5	0.7	0.2	1.5	—	—	1.0	—
Zircon	—	1.3	Tr	—	Tr	0.1	Tr	Tr	—	—	1.5	Tr
Epidote	—	—	Tr	—	Tr	Tr	Tr	Tr	—	—	Tr	Tr
Chert	Tr	Tr	0.7	0.1	0.7	1.4	0.5	0.3	2.0	—	Tr	—
Carbonaceous Matter	Tr	Tr	Tr	1.0	0.5	Tr	Tr	0.2	Tr	0.5	Tr	Tr
Pellets	—	—	—	Tr	—	—	—	—	—	51	—	—
Porosity	5.0	3.0	2.0	2.0	0.5	1.0	4.0	5.0	—	4.0	2.0	1.0

PLATE-A

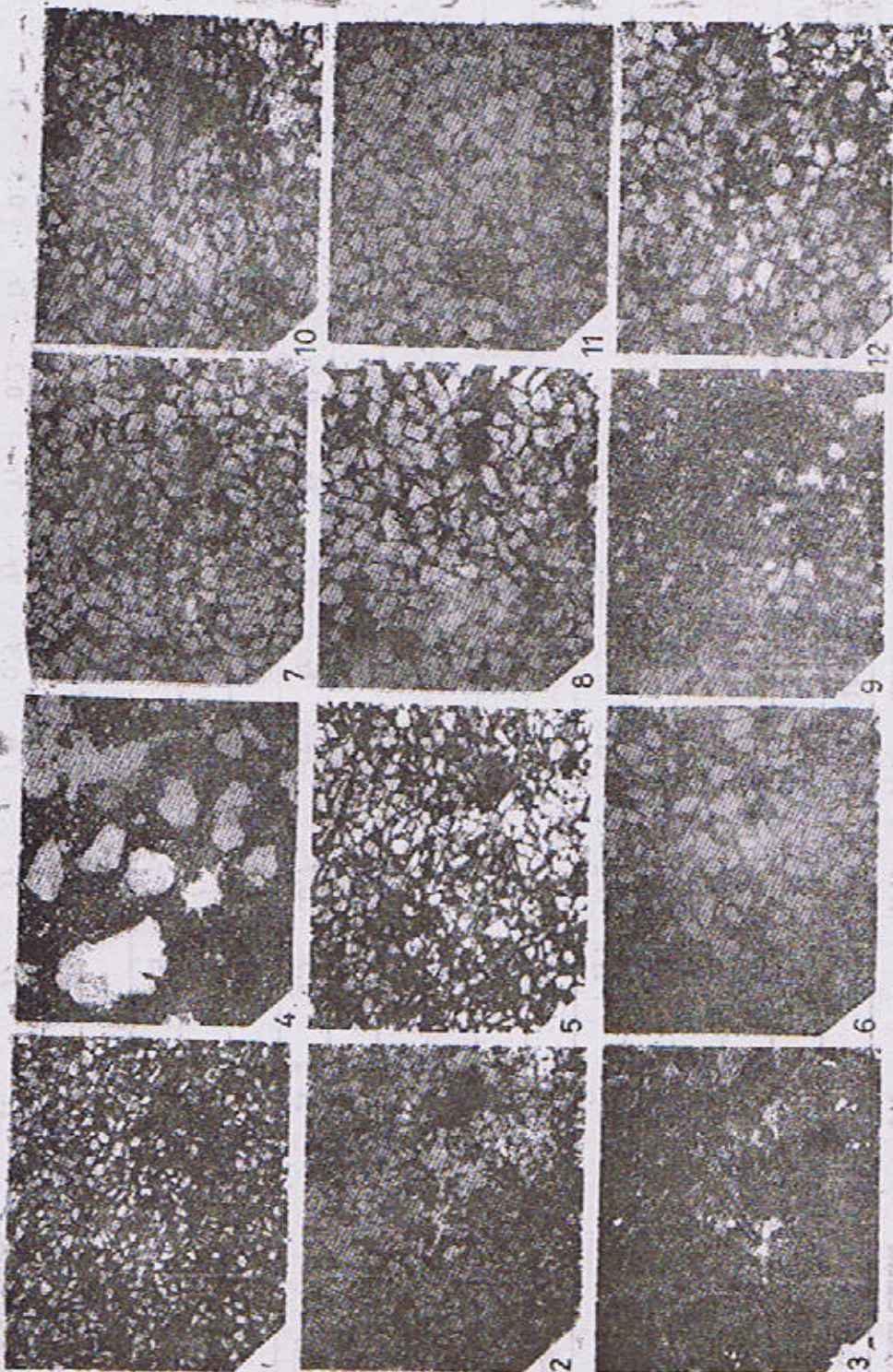


Image	Image	Image	Image	Image	Image	Image	Image	Image	Image	Image	Image
1	2	3	4	5	6	7	8	9	10	11	12
Compos	Compos	Compos	Compos	Compos	Compos	Compos	Compos	Compos	Compos	Compos	Compos
SEI	SEI	SEI	SEI	SEI	SEI	SEI	SEI	SEI	SEI	SEI	SEI
BEI-TOPO	BEI-TOPO	BEI-TOPO	BEI-TOPO	BEI-TOPO	BEI-TOPO	BEI-TOPO	BEI-TOPO	BEI-TOPO	BEI-TOPO	BEI-TOPO	BEI-TOPO
BEI-CL	BEI-CL	BEI-CL	BEI-CL	BEI-CL	BEI-CL	BEI-CL	BEI-CL	BEI-CL	BEI-CL	BEI-CL	BEI-CL

Figure 1. Scanning Electron Micrographs of Dental Composites at 1000x Magnification

PLATE B



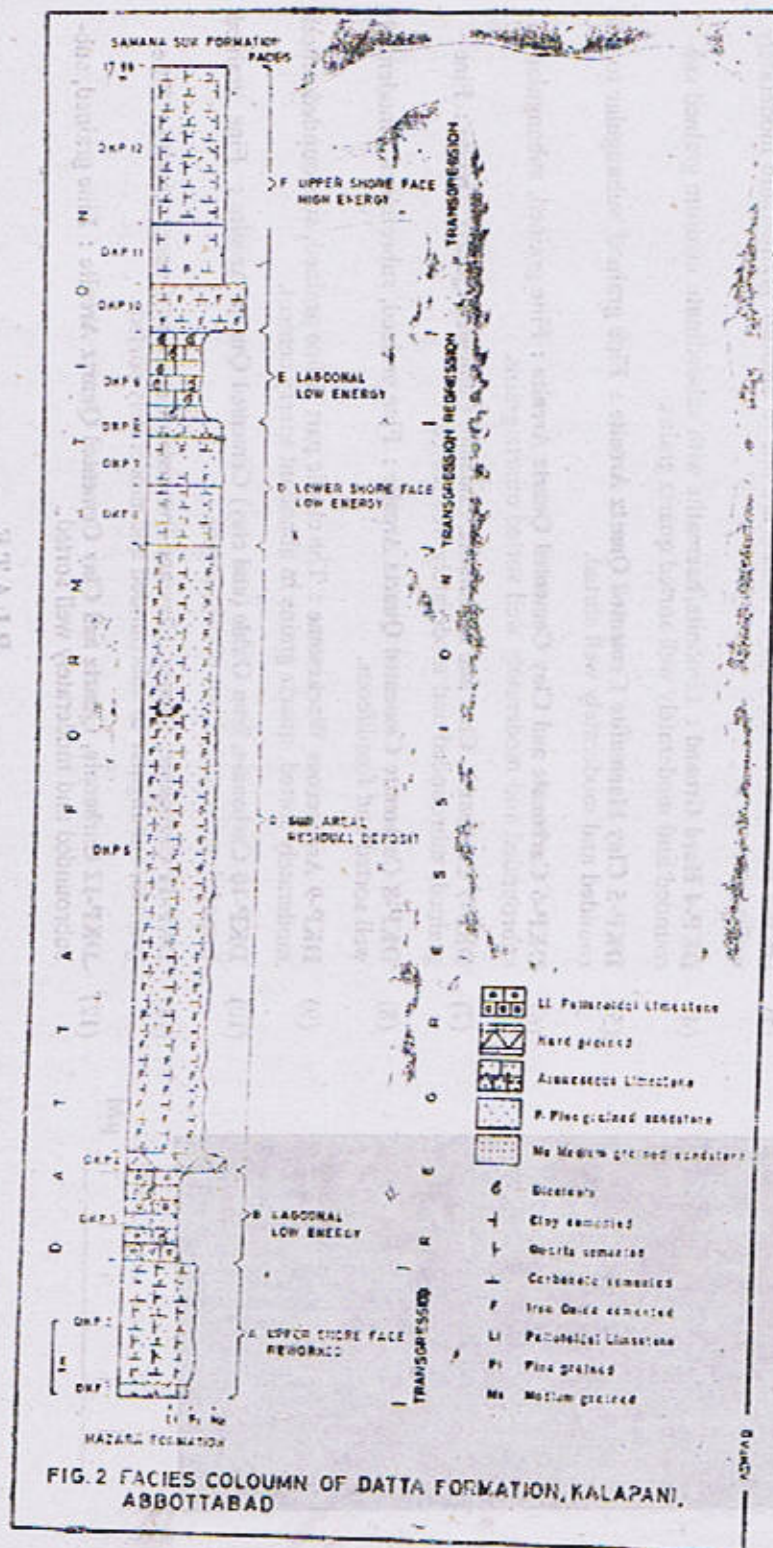
0 500
µm

PLATE A

- (1) DKP-1 Carbonate Cemented Quartz Arenite : Very fine grained, subrounded and well sorted.
- (2) DKP-2 Carbonate and Quartz Cemented Quartz Arenite : Fine grained subangular to subrounded and moderately well sorted.
- (3) DKP-3 Pelletoidal Packstone : Pellets are fine to medium grained and moderately well sorted.
- (4) DKP-4 Hard Ground : Limonite/haematite with subordinate medium grained subrounded and moderately well sorted quartz grains.
- (5) DKP-5 Clay Haematite Cemented Quartz Arenite : Fine grained, subangular to subrounded and moderately well sorted.
- (6) DKP-6 Carbonate and Clay Cemented Quartz Arenite : Fine grained, subangular to subrounded and moderately well sorted quartz grains.
- (7) DKP-7 Carbonate, Clay and Haematite/Limonite Cemented Quartz Arenite : Fine grained, subrounded and moderately well sorted.
- (8) DKP-8 Carbonate Cemented Quartz Arenite : Fine grained, subrounded, moderately well sorted and fossiliferous.
- (9) DKP-9 Arenaceous Wackestone : The clastic part is fine grained, subrounded, moderately sorted, quartz grains in abundant sparry cement.
- (10) DKP-10 Carbonate, Iron Oxide (and clay) Cemented Quartz Arenite : Fine grained, bimodal, subrounded but poorly sorted.
- (11) DKP-11 Carbonate, Quartz, Clay and Iron oxide Cemented Quartz Arenite : Fine grained, subangular to subrounded and moderately sorted.
- (12) DKP-12 Carbonate, Quartz and Clay Cemented Quartz Arenite : Fine grained, subrounded and moderately well sorted.

PLATE

- (1) High alumina clay rims over Quartz Grains.
- (2) Carbonate Corrosion of Quartz Grains.



Facies	Microfacies DKP	Sorting	Textural Maturity	Grain Shape	Grain Size	Porosity Type
	12	M. Well	Sub-mature	S. angular-S. rounded	Fine	Enlarged intergranular, oversized fabric selective.
	11	Moderate	Sub-mature	S. angular-S. rounded	Fine	Oversized fabric selective, enlarged intergranular.
F	10	Poor	Sub-mature	S. angular-S. rounded	Fine	Intracement, vug, oversized fabric selective.
E	9	Moderate	Sub-mature	S. rounded	Fine	Oversized fabric selective, intracement.
	8	M. Well	Sub-mature	S. rounded	Fine	Intracement.
	7	M. Well	Sub-mature	S. rounded	Fine	Intergranular, oversized fabric selective.
D	6	M. Well	Sub-mature	S. angular-S. rounded	Fine	Intracement, vug, fracture.
	5	Well	Sub-mature	S. angular-S. rounded	Fine	Regular intergranular, oversized fabric selective.
	4	M. Well	Mature	S. rounder-S. rounded	Medium	Fracture, vug and intracement.
B	3	Well	Mature	S. rounder-S. rounded	Fine/Medium	Vug, intracement.
	2	Well	Mature	S. angular-S. rounded	Fine	Regular intergranular, oversized fabric selective.
	A	Well	Mature	S. rounded	V-Fine	Intracement.

Table No. 4 Textural parameters and porosity types of Data Formation from bottom to top at Kalapani.

ORIGIN OF ELONGATED GYPSUM CRYSTALS IN THE SALT RANGE FORMATION, NILAWAHAN GORGE, CENTRAL SALT RANGE

BY

RIAZ AHMAD SHEIKH AND SHAFEEQ AHMAD

Institute of Geology, Punjab University, Lahore-54590, Pakistan.

Abstract : *Elongated crystals of gypsum found in a marly matrix at a number of places below the bright red marl beds in the Salt Range are formed by the evaporation of reconstructed brine produced with percolation of groundwater or rainwater through rocks containing soluble calcium sulfate minerals. The Gypsum-Anhydrite beds interbedded with dolomite, marl etc. have been deposited from seawater evaporation.*

INTRODUCTION

During a visit to the Nilawahan Gorge in the Salt Range near Nurpur (Fig. 1), irregular mesh of elongated gypsum crystals were found in a marly matrix, below the bright red marl beds (Sahwal Marl Member of the Salt Range Formation). Bright red marl beds of the Salt Range Formation also contain lenticular gypsum, rock salt and dolomite (Ahmad and Siddiqui, 1992). The sequence of rocks exposed in the Nilawahan Gorge is illustrated (Fig. 2). The present paper deals with the gypsum mineralisation in the Salt Range Formation.

GYPSUM MINERALIZATION

Kerr and Thompson (1963), attributed bladed gypsum crystals, rosettes and thin layers of gypsum between contrasting rock type to be precipitated by highly charged groundwater derived from the overlying flat.

Blatt et al., (1980), described Gypsum/Anhydrite are deposited from the brine generated either by seawater or reconstructed brine. The reconstructed brine is produced with percolation of

groundwater or rainwater through rocks containing soluble calcium sulfate minerals or salt. Evaporation of this brine increases the concentration of the brine to the point at which gypsum precipitates out.

With the evaporation of seawater, it has been observed that evaporation to dryness of a column of normal seawater 1000 m thick produces only 0.75 m of gypsum and about 13.7 m of halite. The precipitation of gypsum begins when seawater concentrates to slightly more than one third of this original volume. The deposition of relatively thick sections of gypsum or anhydrite with relatively little halite indicates the availability of a new seawater source or brine for evaporation and that the brine was not allowed to concentrate to the point at which halite separates. If, however, seawater is allowed to evaporate and new seawater is constantly being added to maintain the original volume, the brine will become concentrated to a point at which halite separates out. In case concentrated brine is removed and at the same time new seawater is added, it is possible that under equilibrium conditions of concentration, gypsum will precipitate out (Bhandar Kas Gypsum Member of the Salt Range Formation) which is not exposed in the Nilawahan Gorge).

It has been suggested by many workers such as Possiak (1940), Bundy (1958), Conley and Bundy (1958), Murray (1964) and Zen (1965), that most, if not all, calcium sulfate of natural evaporites was originally deposited as gypsum. The reasons being (1) petrographic observations that much anhydrite is pseudomorphous after twinned gypsum, (2) the scarcity of anhydrite in modern evaporites deposits, and (3) experimental evidence that anhydrite cannot be synthesized under pressure temperature conditions consistent with natural evaporite environments.

The secondary nature of the present relationship between gypsum and anhydrite in the pre-Recent marine evaporites of the world is due to effects of post depositional burial. Gypsum at the surface may be traced downward into anhydrite and that at depths of about 2000-3000 feet, gypsum is practically absent. Anhydrite pseudomorphous after twinned gypsum has been reported by Schaller and Henderson (1932), Stewart (1953) and Borchert and Baier (1953). At shallower depths gypsum has been shown to have replaced anhydrite (Stewart, 1953; Goldman, 1952; Ogniben, 1955; Sund, 1959 and Murray, 1964). This indicates that both gypsum and anhydrite in sedimentary deposits may be metamorphic, but this does not prove that the replaced gypsum, or anhydrite, was primary in origin (Zen, 1965).

Bramkamp and Powers, (1955), Morris and Dickey (1951), Masson (1955), Phleger and Ewing (1962), Wells (1962), reported primary gypsum in recent marine and nonmarine evaporites.

The scarcity of anhydrite in modern evaporite deposits is predicted by the experimental work carried out by Hardie (1967). The Gypsum-Anhydrite equilibrium values of Hardie (1967) are more compatible with the field observations that gypsum is the common phase and anhydrite rare in unmetamorphosed evaporite deposits.

Brine temperatures range from 24° to 39° and

anhydrite is found in carbonate muds of the Sabkha or supertidal salt flat where ground water chlorinities exceed about 24 percent salinity in the Persian Gulf deposits (Hardie, 1967). He also observed that in a sea water brine saturated with halite ($a_{H_2O} < 0.75$), gypsum should dehydrate to anhydrite at temperature above about 18°C.

Due to inefficiency of anhydrite nucleation, it is not found in recent saline deposits of either continental or marine environments. King (1971) described, in basin concept of deposition, from a brine-filled basin with restricted circulation.

According to Faure (1992), $CaSO_4$ does not actually precipitate from a supersaturated solution of its ions. Instead, Gypsum, $CaSO_4 \cdot 2H_2O$ forms, which subsequently crystallizes to anhydrite due to its irreversible nature of reaction. Gypsum continues precipitating till the activities of the ions are so reduced that ion activity product (IAP) becomes equal to solubility product (K_{sp}) and solid gypsum is in equilibrium with its ions.



The precipitation of a salt from a supersaturated solution not only reduces the concentrations of the ions but actually changes the chemical composition of the remaining solution.

The enrichment or depletion of Ca^{2+} , SO_4^{2-} in the residual solution with precipitation of gypsum depends upon the initial molar Ca^{2+}/SO_4^{2-} ratio. If this ratio is greater than 1.0, the activity of SO_4^{2-} approaches zero and the $[Ca^{2+}]/[SO_4^{2-}]$ rises towards infinity (Fig. 3).

In case the initial molar $Ca^{2+}/SO_4^{2-} < 1.0$, the precipitation of gypsum causes depletion in Ca^{2+} and enrichment in sulfate.

CONCLUSION

In the existing geological conditions of the Nilawan Gorge, the gypsum crystals appear to have formed from reconstructed brine, produced with

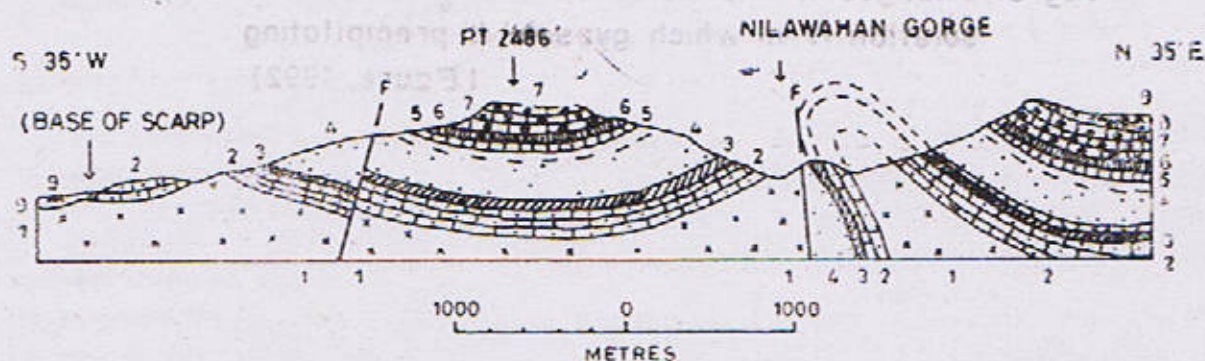
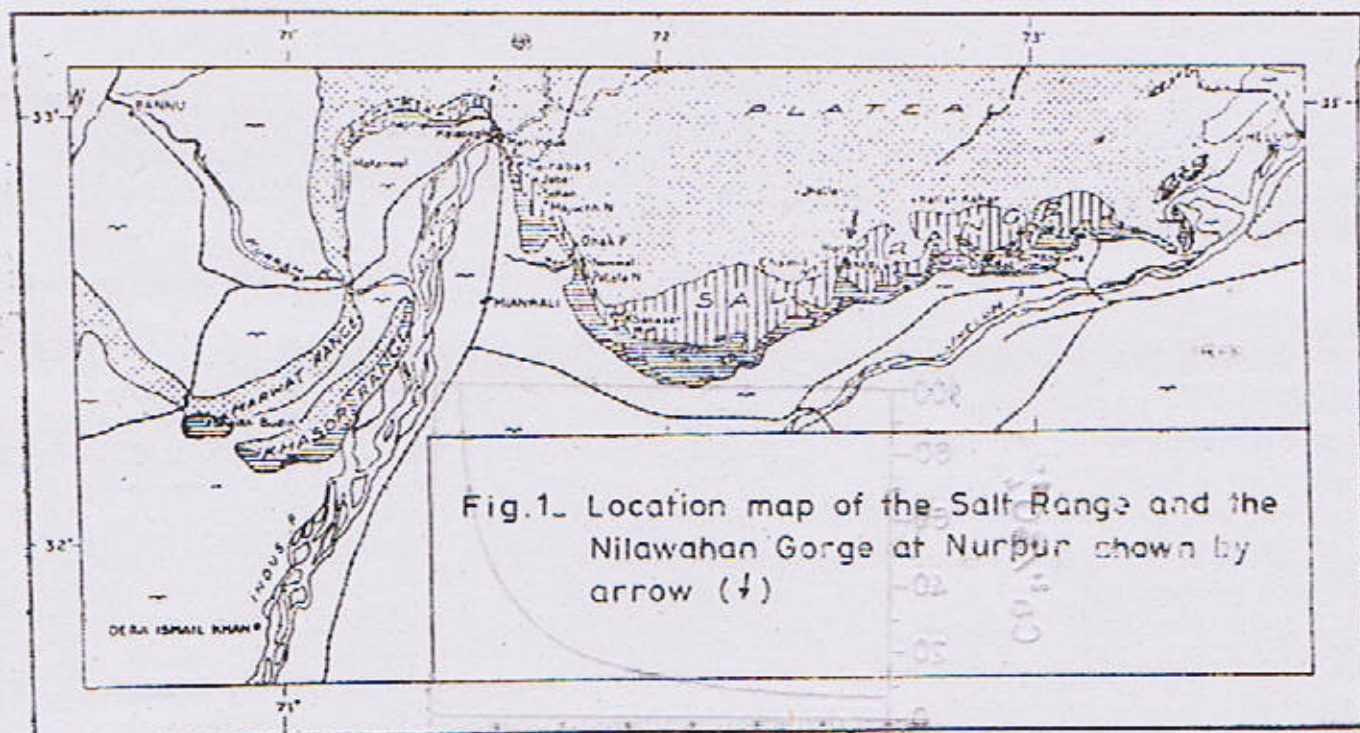
percolation of groundwater or rainwater through rocks containing soluble calcium sulfate minerals. Evaporation of this increased the concentration to a point at which gypsum precipitated and due to soft sediments, which can be easily pushed aside, gypsum crystals grew by displacement. The force of crystallization pushed aside the surrounding host sediments and crystals formed relatively free of in-

clusions of the host sediment.

The gypsum in the Nilawahen Gorge thus appears to have been formed from a solution having initial molar $\text{Ca}^{2+}/\text{SO}_4^{2-} > 1.0$. As a result of precipitation of gypsum, the depletion of SO_4^{2-} ions, increased the availability of Ca^{2+} ions in the residual solution that reacted with other ions to form carbonates, clays.

REFERENCES

- Ahmad, Z. and Siddiqui, R. A., 1992. Minerals and rocks for Industry. *Geol. Surv. Pakistan*, 1, 298-311.
- Blatt, H., Middleton, G. and Murray, R., 1980. Origin of Sedimentary Rocks, Prentice-Hall, Inc., Englewood Cliffs, New Jersey, 541-557.
- Bundy, W.M., 1956. Petrology of gypsum-anhydrite deposits in southwestern Indiana. *Jour. Sed. Pet.*, 26, 240-252.
- Borchert, H. and Baier, E., 1953. Zur Metamorphose Ozeaner Gipsablagerungen. *Neues Jahrb. Min. Abh.*, 103-154.
- Bramkamp, R.A. and Powers, R.W., 1955. Two Persian Gulf lagoons *Jour. Sed. Pet.*, 139-140.
- Conley, R.F. and Bundy, W.M., 1958. Mechanism of gypsification. *Acta Geochim et Cosmochim*, 57-72.
- Faure, G., 1992. Principles and Applications of Inorganic Geochemistry. Macmillan Publishing Company, New York, 205-210.
- Goldman, M.I., 1952. Deformation, metamorphism, and mineralization in gypsum-anhydrite caprock, sulfur salt dome, Louisiana. *Mem. Geol. Surv. Amer.*, 1698.
- Hardie, L.A., 1967. The gypsum-anhydrite equilibrium at one atmosphere pressure *Amer. Min.*, 171-200.
- Kerr, S.D. and Thompson, A., 1963. Origin of nodular and bedded anhydrite in Permian shelf sediments, Texas and New Mexico. *Bull. Amer. Assoc. Petrol. Geol.*, 47, 1726-1732.
- King, R.H., 1971. Sedimentation in Permian Castile area, in Origin of Evaporites. *Bull. Amer. Assoc. Petrol. Geol.* 47, 1726-1732.
- Masson, P.H., 1955. An occurrence of gypsum in Southwest Texas. *Jour. Sed. Pet.*, 72-79.
- Morris, R.C. and Dickey, P.A., 1951. Modern evaporite deposits in Peru, *Bull. Amer. Assoc. Petrol. Geol.*, 2467-2474.
- Murray, R.C., 1964. Origin and diagenesis of gypsum and anhydrite. *Jour. Sed. Pet.*, 512-523.
- Ogniben, L., 1955. Inverse graded bedding in primary gypsum of chemical deposition. *Jour. Sed. Pet.*, 273-281.
- Plieger, F.B. and Ewing, G.C.E., 1962. Sedimentology and Oceanography of coastal lagoons in Baja California, Mexico *Geol. Soc. Amer. Bull.* 145-182.
- Possia, E., 1940. Deposition of calcium sulfate from sea water. *Amer. Jour., Sci.*, 559-568.
- Schaller, W.T. and Henderson, E.P., 1932. Mineralogy of drill cores from the potash field of New Mexico and Texas. *U. S. Geol. Surv. Bull.*, 124.
- Stewart, F.H., 1953. Early gypsum in the Permian evaporites of northeastern England. *Proc. Eng. Geol. Assoc.*, 33-39.
- Sund, J.O., 1959. Origin of the New Brunswick gypsum deposits. *Bull. Canad. Min. Metal.* 707-712.
- Wells, A.J., 1962. Recent dolomite in the Persian Gulf. *Nature*.
- Zen, E. An, 1965. Solubility measurements in the System CaSO_4 - NaCl - H_2O at 35° 50° and 70° and one atmosphere pressure. *Jour. Pet.*, 124-164.



1. Salt Range Formation, 2. Khewra Sandstone, 3. Kussak, Jutana & Tobra Formation, 4. Lower Permian (Generally clastics), 5. Amb Formation, 6 & 7. Lower Tertiary, 8. Kamli Formation, 9. Alluvium and F = Fault.

Fig. 2. SECTION N.E - S W ACROSS NILAWAHAN AT U-BEND 3.2 km FROM EXIT.

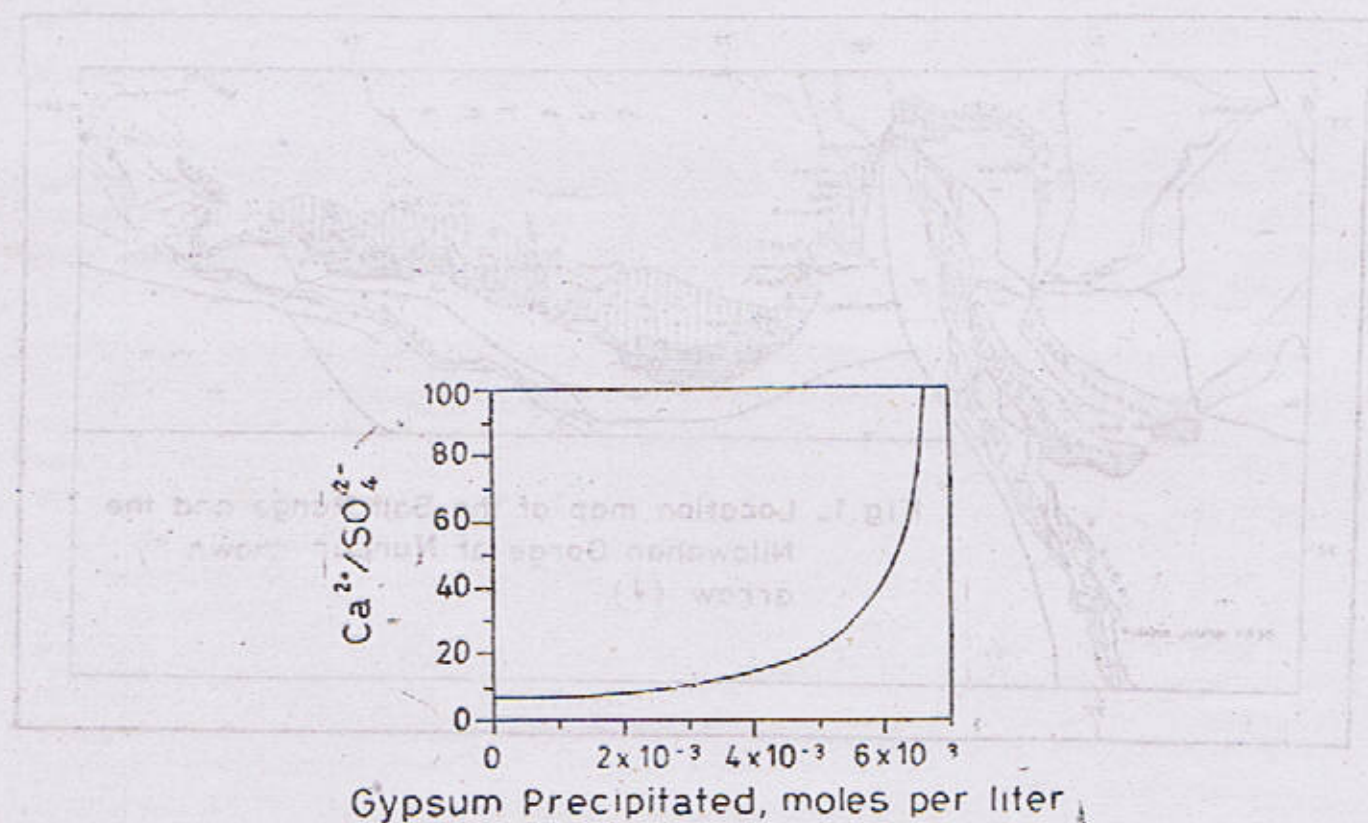


Fig. 3 Changes in the molar $\text{Ca}^{2+}/\text{SO}_4^{2-}$ ratio of a solution from which gypsum is precipitating (Faure, 1992)



Fig. 1 SECTION N 2 - S W ACROSS NILAWAHAN AT 0.8 KM FROM EXIT

URBAN GEOLOGY OF THE DERA GHAZI KHAN AREA, SOUTH PUNJAB PAKISTAN

By

SHEIKH MOHAMMAD IQBAL, MOHAMMAD AFAQ KHAN

Geological Survey of Pakistan, 16-G, Model Town, Lahore, Pakistan.

AND

SARFRAZ AHMED SHAFEEQ AHMAD

Institute of Geology, Punjab University, Lahore-54590, Pakistan.

Abstract :— A geological map of the Dera Ghazi Khan District (Survey of Pakistan sheet No. 39J/12) has been prepared on a scale of 1 : 2,50,000. All available information about the geological setting, economic deposits and groundwater studies are considered vital for the future urban development of the Dera Ghazi Khan City.

INTRODUCTION

The metropolitan area of Dera Ghazi Khan Quadrangle lies between longitude 70° 30' and 70° 45' E and latitude 30° 00' and 30° 15' N. It covers Dera Ghazi Khan District and its special areas in Punjab province, Pakistan. The city is well connected to all parts of the country by G.T. Road and Railway. The interiors parts of the mapped area is approachable through a network of metalled and unmetalled fair weather jeepable tracks.

The area has not arid zone with hot summers and moderate dry winters with average 15mm rainfall. May, June and July are the hottest months with mean maximum temperature 42° C. January and February are the coldest months with mean minimum temperature 71° C. Freezing temperature is rare in the area.

The northwestern part is a hilly terrain of the folded belt of the Sulaiman Range whereas the remaining portion is a part of the Lower Indus

Plain. The hilly terrain is composed of Chaudwan Formation of Pliocene and Sub-Recent Terrace gravel deposits. The part of the Lower Indus Plain is composed of silt, sand and gravel with eolian sand. Drainage of the area is controlled by Indus River. Chabbri Wah, Jhlu Nala, Rod Koli and Phullar are the main streams of the area forming a dendritic drainage pattern. The altitude generally increases from south to westward with local relief about 300 meters with minimum and maximum heights of 400 and 700 meters average mean sea level respectively.

PREVIOUS INVESTIGATIONS

Iqbal and Khan (1990) for the first time gave a detailed account of the Quaternary deposit for the study.

The present work is an attempt to describe the stratigraphy of the Quaternary surficial deposits in detail with reference to groundwater, economic deposits and engineering geological studies of the Dera Ghazi Khan Quadrangle. The nomenclature already in vogue has been followed.

QUATERNARY GEOLOGY

Terrace Gravel Deposits : These include gravel beds in the form of raised terraces, lying at the junction of alluvial fans with rock exposures. These have generally flat surfaces but at places dip upto 5° — 7° towards east. These are still in process of erosional degradation. It consists of an assemblages of gravel, stratified, semi consolidated and these are derived from older rocks. The gravel are sub angular to sub rounded and comprise mainly of limestone, quartz and sandstone.

Alluvial Fan Deposits : Consist of poorly sorted, sub angular to sub rounded boulders, cobbles of limestone, sandstone and quartz in unconsolidated silty matrix. The alluvial fan deposits are accumulated in front of Sulaiman Range where they form fan morphology.

Alluvial Plain Deposits : Comprise mainly clay, loamy clay, sand and minor gravel. The clay is earthy grey to light brownish grey and calcareous having kankers at places. Many sections have more clayey material indicating slow rate of deposition. The silt is interbedded with clay and kankers. The loamy clay beds are softer and badlands topography developed at eastern parts of Quadrangle. The estimated thickness of clay is 5-7m in the area. Major part of the unit has converted into farmland except other parts covered with the eolian sand, where wheat, sugar cane, rice and seasonal vegetables are grown. The alluvial plain deposits are cut by the tributaries of major nalas of the area. The clay is silty, calcareous and plastic at places and is used for making bricks and pottery.

Flood Plain Deposits : Consist of light brownish clay, silt and sand and occur only in the north eastern parts of the area. The younger flood plains are confined only at the course of the Indus River and consist of silty sand and clay with minor gravel. Some parts are developed as agriculture land and seasonal vegetables. Sugar cane and wheat are main crops of this unit.

Dune Sand Deposits : Occur in the form of low lying stabilized dunes of different sizes in the western and southern parts of area. The sand is composed of light brownish grey to light grey, medium to fine grained, sub rounded to sub angular grains. The sand has grains of quartz epidote, muscovite (very fine flanks) and minor heavy minerals. It is covered by gravel of older rocks at places. Wind blown ripple marks present at the surface of dunes show a regular pattern of parabolic dune.

Wild growth of green shrubs and small trees are the typical feature of this unit

Stream Channels Deposits : Occur in stream and river beds and comprise unconsolidated sand, silt and clay with boulders, cobbles of limestone, sandstone and quartzite.

ECONOMIC GEOLOGY

The most important minerals resources of Dera Ghazi Khan area are construction material including gravel for concrete and aggregate, sand for mortar and clay for bricks, tiles and pottery. All these stuff are quite abundant and have been used. Gravel for aggregate and construction purposes are obtained by digging alluvial gravel, terrace gravel and alluvial fan deposits. Sand is obtained from pits of Dune sand. Brick clay is dug from clay pits of alluvial plains deposits.

Huge reserves of important rocks and minerals material like gravel, sand and clay are present in the area.

Gravel : Holocene suitable for concrete and aggregate.

Sand : Holocene suitable for mortar and aggregate.

Clay : Holocene suitable for making bricks and Pottery.

GROUNDWATER RESOURCES AND QUALITY

Water resources are the basis for urbanization. Adequate good quality water supplies are of special concern of urban area. It is essential, therefore, that good quality groundwater supplies be identified and wisely managed.

The existence of groundwater in the form of freshwater in the Dera Ghazi Khan Basin is due to mainly presence of the Indus River. Besides this, there are three canals, coming from the Taunsa Barrage.

The D.G. Khan Canal is the main boundary between fresh water and saline water. The flow of groundwater is NE-SW from higher to lower altitude. The eastern part is combination of older and younger flood plains of the Indus River. These consist of sand, silt and clay. This part of flood plain has good freshwater reserves with scattered pockets of brackish or saline water. The western part is occupied by alluvial gravel with dune sand which has saline water with little pockets of fresh water. These pockets of water are along nalas which are coming from Sulaiman Range. The discharge of these streams is uncertain and depending upon the rainfall on catchment area.

The factors that substantially favour high salinity in groundwater, especially in western part of the D.G. Khan Quadrangle, is due to presence of evaporities, fast evaporation and less rainfall.

Field tests were carried out to measure quality of water. The results of dissolved solid concentration in water samples of different localities show variation from 234 m.g. l. to 3500.

Also abrupt changes in quality of water was also observed in western parts such as vidor and Kucha wadani localities.

The quality of groundwater in most parts of the D.G. Khan Basin varies from fresh to saline and this classification is recommended to U.S.

Geological Survey.

Class	Dissolved solid
Concentration :	(Milligram per liter)
Fresh :	0—1000 mgl
Slightly saline :	1000—1500 mgl
Moderately saline :	1500—3000 mgl
Very saline :	3000—10,000 mgl

The available analysis data from various field tests indicate that groundwater of the D.G. Khan city has saline contents of dissolved solids in the D.G. Khan Basin due to the presence of evaporite. On the basis of field data analysis the distribution of dissolved solids in the D.G. Khan Quadrangle (39 J/12) can be divided into three main divisions as shown in Fig. 2.

- (i) Excellent water : 0—500 mgl
- (ii) Fresh water : 500—1500 mgl
- (iii) Saline water : 1500—3000 mgl

It is concluded that fresh water and excellent water is available from active and abandoned flood plains of Indus River and along Shoria Link Canal and D.G. Khan Link Canal.

Following are main results of this study :—

1. Groundwater is good in quality and quantity with small pockets of saline water (eastern part). Most of the fresh water sources are along Shoria, D.G. Khan and Manka Canals.
2. Water supply to the urban area of the D.G. Khan city is provided from net work of tubewells at Gidarwala and Shoria link Canal, to be considered the best of quality with T.D.S. value 291 mgl.
3. The water resources in the western portion of the D.G. Khan Basin characterized by the peidmont plains, are meager and saline.

Development for further groundwater resources require extensive and detailed subsurface geological and hydrological studies to determine their capacity for development with increase of population. Water quality investigations to be conducted after every two years.

ENGINEERING GEOLOGY

Foundations failures are due to earthquake and subsidence but there is no foundation problem in D.G. Khan city excepting swelling soil. A number of cracks are developed in the buildings of city due to shrinkage of soil. Special tests to determine the engineering properties of the soil is recommended before the construction especially swelling and consolidation tests.

CONCLUSIONS

The quaternary geology with ground water resources, economic deposits and engineering geo-

logical studies provide a complete picture of urban geology of the Dera Ghazi Khan city and its new urban areas. All these informations are considered critical to city planners, engineers and municipal authority for solving their problems in collaboration with geologists. Data from these studies provide valuable guidelines to the city planners, engineers, financial advisers and designers for further development of the urban area with low cost and better management of water resources.

ACKNOWLEDGEMENT

Thanks are due to the Director General and Deputy Director General of the Geological Survey of Pakistan for technical support for this paper. Various agencies and individuals kindly allowed us to use their unpublished data. These include WAPDA and Irrigation department of D.G. Khan area.

REFERENCES

- Benneth, G. D. 1978. Groundwater, and undervalued resources. *U. S. Geol. Surv. Yearbook*, 2-10.
- Iqbal, S.M. and Khan M, A. Geology of Dera Ghazi Khan Area, Punjab, Pakistan (Unpublished Report). *Geol. Surv. Pakistan*
- John, E.C. 1981. Surficial Geology Building with the Earth. John Wiley and Sons, inc. New York, 145-176.
- Kamal, M. T. 1971. Geohydrology of the Dera Ghazi Khan District, West Pakistan. *WASID Bull.*, 18, 37-43.
- Nichods, R. D. 1975. Earth Sciences and the Urban Environment. *U.S. Geol. Surv. Annual Report*, 2-15.
- Sheikh, M. I. and Khan, M. A. 1992. Environmental Geology of Taunsa Area, Punjab, Pakistan. *Pak. Jour. Geol.* 1, 72-80.
- Valdiya, K. S. 1984. Environmental Geology. McGraw-Hill Publishing Company Limited New Dehli, 91-107.

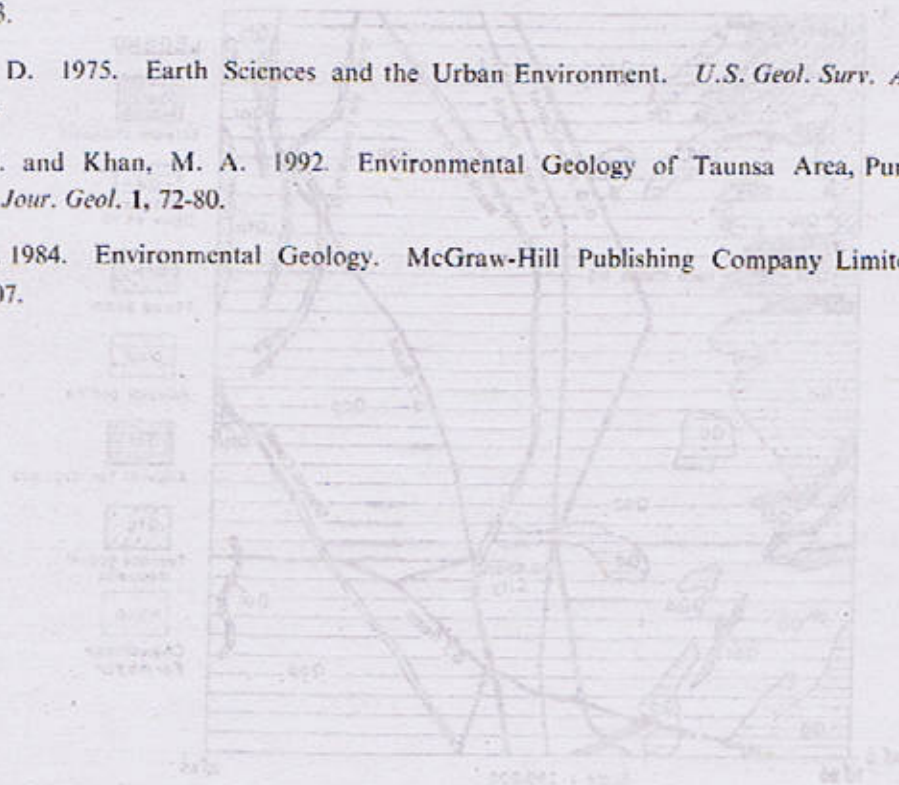


FIG. 1 GEOLOGICAL MAP OF DERA GHAZI KHAN

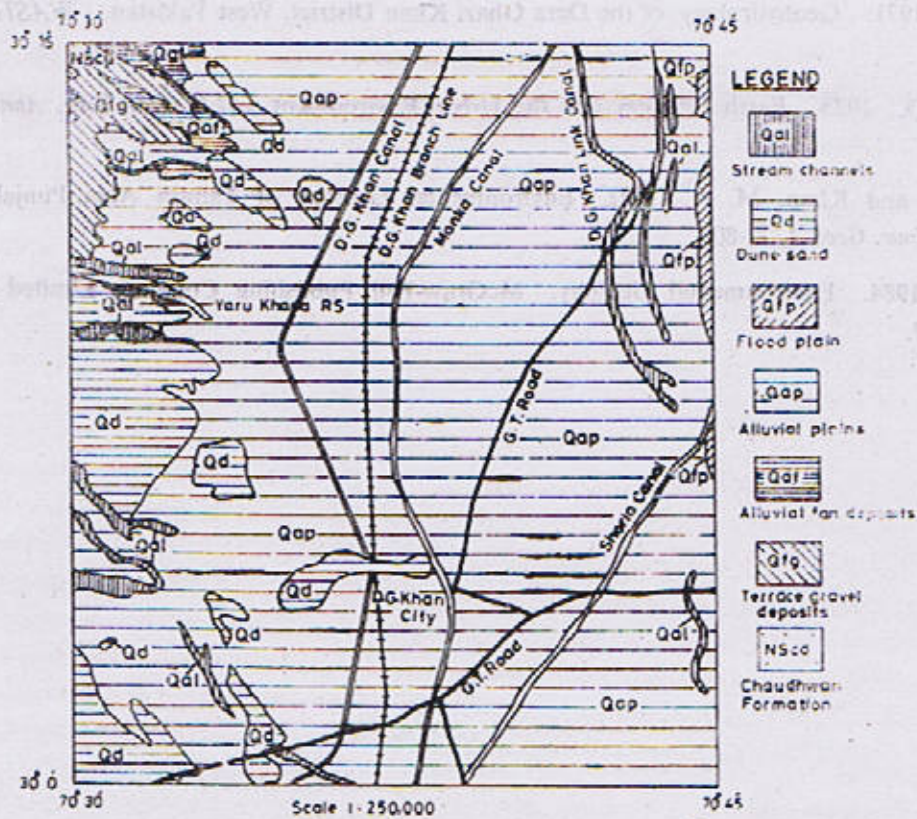


FIG.1 GEOLOGICAL MAP OF DERA GHAZI KHAN

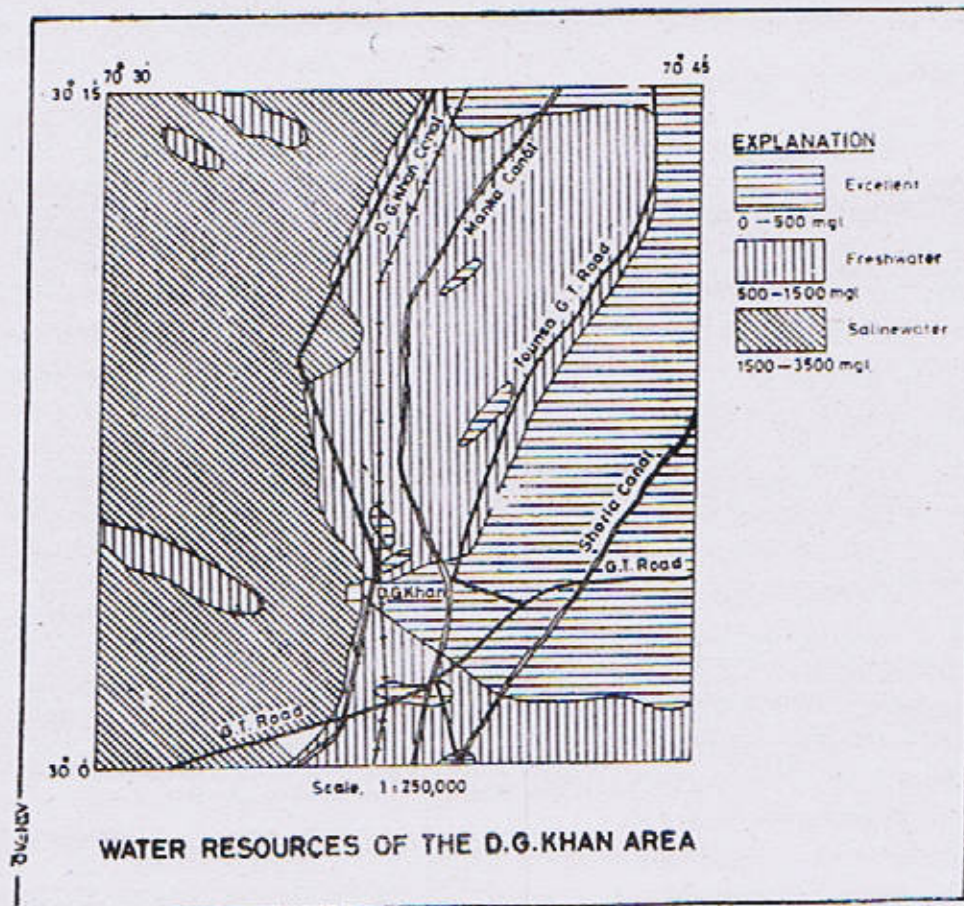


FIG. 2

A TURBIDIMETRIC TECHNIQUE FOR MEASURING THE SOIL STRUCTURAL STABILITY

BY

JAVED AKHTER, K. A. MALIK, M. H. NAQVI

Nuclear Institute for Agriculture and Biology, Faisalabad, Pakistan,

SHAFEEQ AHMAD

Institute of Geology, Punjab University, Lahore-54590, Pakistan.

AND

R. MURRAY

Department of Soil Science, Waite Agricultural Research Institute, Adelaide, South Australia.

Abstract : *There are many methods to test the stability of soil aggregates. Some of these are subjective and more or less empirical, while others do not provide reproducible data especially with saline soils. A new method for determination of soil aggregate stability for highly unstable soils was tried. The method involve continuous monitoring of turbidity in a fixed volume of water created by dispersion and slaking of aggregates with minimum energy input. The process is repeated after maximum dispersion of the aggregates. The stability index (SI) was established using initial and final turbidities extrapolated to zero time.*

Different soil weights (0.1-1 gm) comprising one aggregate or lots of aggregates of (1-2 mm) size, both dry and prewet were tried in reversed osmosis (RO) and irrigation water separately. Data indicate that the proposed method provides reproducible SI values with small standard error. The coefficient of variation (CV) increased with the increase in weight of aggregates both in RO and irrigation water. The method is less time consuming. It can be readily adapted to routine analysis with slight modifications according to the requirements after selection of proper combination of parameters for different soils.

INTRODUCTION

The ability of soil to maintain its particle arrangement (solid and void) despite external disruptive influences is described as soil structural stability. These disruptive influences arise from the action of water (swelling, dispersion and freezing) of mechanical disturbance (tillage, compaction) or a combination of both such as the impact of raindrops and sheet erosion. Soil strength di-

minishes with increasing water content and stability measurements are generally assessed from the break up of soil aggregates in water. Some soil aggregates slake abruptly when immersed in water. Slaking occurs mainly due to loss of cohesion, swelling of aggregates (Yoder, 1936) and release of entrapped air. The swelling may result from the repulsion of extensive diffuse layers as in sodium-saturated systems or from the limited swelling of calcium-saturated systems driven by hydration.

However, all these affects are exacerbated by rapid wetting.

The slaking of bigger aggregates into smaller aggregates in water creates new surfaces that enhances the release of particles which are able to disperse spontaneously. The dispersion of soil colloids is a pre-requisite for colloid mobility. This movement of soil colloids is responsible for structural degradation (crust formation, clay pans).

Soil aggregates of arid and semi-arid regions are generally unstable, especially the salt-affected soils slake and disperse spontaneously in rain or low electrolyte water and as a result loose soil structure. Several methods exist to determine the stability and many comparisons of different stability measurements have been made (William et al., 1966; Molohe et al., 1985; Matkin and Smart 1987; Pojasok and Kay 1989). These studies describe wet sieving, permeability, changes in soil moisture characteristics (Childs, 1940, slump test (Williams and Cook, 1961) and Emerson classification test (1967) for whole soil or soil aggregates.

Soil structural stability is determined for several purposes, one of which is to assess the effect of cropping on structural stability of soils which possess very weak structure. Matkin and Smart (1987) concluded that slump test provided better discrimination between soils which had low aggregate stability. At the scale of clay or silt size particles William et al., (1966) and Molohe et al. (1985) concluded that suspended clay (turbidimetry) was more sensitive to cropping history than other size fractions. Oades (1984) suggests that cropping history may affect stability differently depending upon the scale of measurement. Pojasok and Kay (1989) compared the method of wet aggregate stability and dispersible clay (turbidimetry) under conditions of similar energy input and concluded that dispersible clay was function of total clay content, organic matter and water content at the time of sampling.

The salt-affected soil, particularly sodium dominated slake and disperse spontaneously in rain or low electrolyte water and as a result loose soil structure. It is very difficult to evaluate structural stability and assess the effect of cropping history on the physical behaviour of these soils using available methods of determining soil structural stability. Stability measurement for such purposes should be reproducible and it should be free of the effect of pretreatment of samples. This is only possible by modifying the existing turbidimetry methods, keeping the energy input minimum at the stage of initial wetting when slaking and dispersion is allowed.

The objectives of this study were to establish a, rapid and reproducible laboratory method for determining stability from aggregates of highly unstable soils.

MATERIALS AND METHODS

Soils were taken from a biosaline research sub-station (BSRS) of Nuclear Institute for Agriculture and Biology situated at Lahore, in Pakistan. At BSRS, model plots have been established to demonstrate the economic utilization of salt-affected soils by growing salt tolerant crops using brackish irrigation water. This station will be used as a model for a long time in future.

Soil samples were taken from a highly saline sodic soil which were under kallar grass irrigated with brackish groundwater. Samples were collected randomly in triplicate from the horizon A (0-15 cm). Samples were air dried packed in tin containers and sterilized with gamma irradiation (50 kilograys) by quarantine before entry into Australia. Subsamples were analysed in the laboratory for soil physico-chemical properties using standard methods (USDA, 1954).

TURBIDIMETRY

Originally it was intended to assess the structural stability of these soils using the Emerson dispersion (Emerson, 1967) technique and slump test

(William and Cook, 1961). However, these methods did not produce reproducible data and results were erratic and there appeared to be poor agreement between visual and photometric measurements. The schematic diagram of design of experiment used in this study is shown in Fig. 1. We used peristaltic pump which pumped the solution with preselected flow rate through the photometric cell of the turbidimeter (Hach X/R Ratio) and computer recorded the turbidity after selected time intervals.

A glass beaker is filled up to the mark A (Fig. 1) so that water did not touch the base of the sieve, inlet and outlet tubes are adjusted at mark C and D respectively. The point C and D are selected so that flow of solution in and out of the container should add minimum energy into the system.

After adjusting the flow rate at 50 ml/s monitoring of initial water turbidity D_0 is started. The sieve holder and sieve are placed on the beaker. The aggregates are placed on the sieve and more water is poured in with long funnel to fill it up to mark B to make final volume 150 ml. The beaker is covered with polythene glad wrap to keep the dust out and minimize evaporation. The recording of turbidity (D_t) is continued after selected time intervals until it attains almost constant value.

The sieve and sieve holder were removed carefully by pouring all the sediments into the beaker. The supernatant is poured into other container. The settled sediments in 200 ml suspension are sonified for 60 seconds with an ultrasonic probe set at constant energy input. The sonification causes the maximum dispersion of all the soil particles. The sonified fraction is mixed in the removed suspension. The final turbidity (D_f) is recorded after mixing 200 ml soil suspension in 1500 ml water as described above but without sieve and sieve holder. The dilution is done to keep the turbidity of solution within the range of turbidimeter. The stability index (SI) was worked out as described in results

and discussion part.

PREPARATION OF SOIL AGGREGATES

To minimize the time of measurement soil samples of different weights (0.1-1 gm) comprising one aggregate and more aggregates of 1-2 mm size were used to establish the SI in reversed osmosis (RO) and irrigation water separately. The process was also repeated with prewet soil samples. The prewet aggregates were obtained by placing 5 gm (1-2 mm) aggregates on sintered glass funnels at 100 cm suction for a week. The irrigation water similar to the water used to grow kallar grass was prepared in bulk after a series of trial. The irrigation water was prepared by addition of required quantities of NaHCO_3 , CaO , MgO , HCl and H_2SO_4 and bubbling of CO_2 gas through the water to adjust required pH. This irrigation water was used in the experiments to follow.

The calibration of the turbidimeter was checked before using it for dispersion measurement of these soils. For this, 1% soil suspension was prepared one by gentle stirring and other by sonification with ultrasonic probe. The turbidity was monitored by stepwise increase of these soil suspensions in 1500ml RO water.

The SI of soils under study were established using following modification :--

- Air dried aggregates in RO water.
- Prewet aggregates in RO water.
- Air dried aggregates in irrigation water.
- Prewet aggregates in irrigation water.

RESULTS AND DISCUSSION

Results indicate that the relationship between turbidity and clay concentration is linear with r values of 0.9995 and 0.9999 before and after the sonification. The graph between turbidity and time is plotted for each case using example (Fig. 2) and values of D_i and D_f extrapolated for zero time are used to establish stability index (SI) as :—

$$SI = \text{Inv} (D_i - d_b) / (D_f - d_b)$$

Where D_i and D_f stand for extrapolated values of turbidity with minimum and maximum energy input respectively, and d_b is initial turbidity of water used.

It is clear that there is a sharp increase in initial turbidity as clay is released from the aggregate by slaking and dispersion (Fig. 2.) This initial process is rather erratic as plumes of dispersed clay are disposed somewhat randomly in the suspension and are taken into the turbidimeter. This is followed by a steady decrease in turbidity as mixing and sedimentation of some coarser particles occurs. Ultimately the turbidity approaches a value which is constant over the timescale (T) employed for these observations. Initial attempts were made to model this process and extrapolate the turbidity to a hypothetical situation at zero time in which mixing was complete but in which no sedimentation had occurred. This proved too difficult as the process is quite complex to allow this kind of treatment and requires a knowledge of the particle distribution created after slaking and dispersion.

The chemical composition of solution extracts of soil and irrigation water is given in Table 1. The soils have sandy clay loam texture. Major clay minerals are mica and kaolinite. The soils are highly saline sodic with Na concentration of 226, exchangeable sodium %age 72 and pH more than 10. The soils are very hard when dry and very soft when wet. The irrigation water used to grow kallar grass on these soils is brackish with RSC 9.61 and categorised as C_3S_2 USDA (1954) unfit for irrigation (chemical composition given in Table 1).

Tables 2-5 summarise the parameters investigated for optimum soil weight, aggregate size and medium to be used for establishing reproducible SI in a minimum time (T). Generally the T increased with the increase in weight of aggregate (both single and 1-2mm) in all the combinations (Tables

2-5). With the increase in weight of Aggregates the corresponding increase in T was more with prewetted than dry aggregates. Prewetted single aggregates in RO water consumed more T than all other combinations (Table 3)

The standard error (SE) and coefficient of variation (CV) in the SI values increased generally with the increase in aggregate weight (Tables 2-5). Minimum SE and CV was observed with 0.1g aggregates in all combinations. The SE and CV is more under prewet conditions with same Weight of single aggregates in RO and irrigation water (Tables 2, 4). In irrigation water 1-2mm prewetted aggregates showed more SE and CV in SI than dry aggregates (Table 5) and comparable SE and CV in SI determined in RO water (Table 3).

In general the SI values decreased slightly with the increase in the weight of soil sample under all combinations. (Tables 2-5). The SI values with prewetted single aggregates are lesser than dry aggregates in RO and irrigation water (Tables 2, 4). Both prewetted and dry 1-2mm aggregates produced comparable SI values in RO Water (Table 3) but in irrigation water with prewetted aggregates smaller SI were observed than dry aggregates (Table 5).

The reason for decrease in SI values, increase in SE and CV with the increase in soil sample weight is that more time is consumed in attaining constant D_i with bigger aggregates because of slow release and dispersion of clay. During this settling down of heavier particles continue which reduces the D_i slightly and consequently reduces SI value being D_f constant. The values of SI with prewet aggregates are generally lower in both RO and irrigation water which is contrary to the general observation. This may be due to removal of salts from extensive double layer and removal of cementing agents between the soil particles because of slow wetting. Both of these processes enhance slaking which creates more surface area and more dispersion which provides more D_i value, hence lower SI value.

We observed that air dried 0.1 gm (1-2mm) aggregate in irrigation water consumed reasonably less time with good reproducibility and these parameters were used to test the SI of these soils in the experiments to follow (not reported here). The method used to test stability seems to be quite useful and reproducible for soils of low stability. The method in general tests the stability index on a continuous scale with greater precision rather than classification tests. The proposed method is based on the turbidimetry with minimum energy input hence will be useful to all soil types without discrimination. The selection of optimum parameters

is a matter of convenience. The method is less time consuming. The proposed method can be readily adapted to the routine analysis with slight modifications in turbidimetric technique without further investment.

ACKNOWLEDGEMENT

We express our deep gratitude to Dr. W. Emerson from Division of Soils, CSIRO Adelaide, Australia, for his assistance in sample analysis. The financial support by the International Atomic Energy Agency is gratefully acknowledged.

Table 1. Chemical composition of saturated soil extracts and irrigation water.

	$(Ca + Mg)^{2+}$	Na^+	K^+	Cl^-	HCO_3^-	CO_3^{2-}	SO_4^{2-}	
	meqdm ⁻³							
Soil	3.0	226	0.4	72.4	103.4	14.2	39.4	
Water	3.65	10.5	0.2	0.7	12.86	0.4	0.1	
	pH	SAR	EC dSm ⁻¹	ESP	RSC	Clay %	Silt	Sand
Soil	10.4	180	22.0	72	—	22	23	55
Water	7.6	9.6	1.4	—	9.81	—	—	—

TABLE 2. S. I. Values and time consumed using one aggregate in reversed osmosis water with dry & prewet aggregates. C. V. stands for coefficient of variation.

Sample Weight (gms)	Dry			Prewet		
	Time (Min)	Stability Index	C.V. (%)	Time (Min)	Stability Index	C.V. %
0.1	25	2.010 \pm .096	4.77	50	1.828 \pm .133	7.3
0.2	35	2.005 \pm .087	4.84	60	1.830 \pm .145	7.92
0.3	40	2.000 \pm .132	6.60	75	1.800 \pm .148	8.22
0.4	60	1.999 \pm .139	6.95	100	1.795 \pm .151	8.14
0.5	90	1.995 \pm .143	7.16	502	1.791 \pm .155	8.55
0.6	100	1.990 \pm .156	7.48	1040	1.785 \pm .161	9.02
0.7	120	1.952 \pm .172	8.81	1859	1.774 \pm .176	9.92
0.8	125	1.901 \pm .189	9.94	2875	1.766 \pm .179	10.14
0.9	130	1.900 \pm .189	9.95	3463	1.740 \pm .185	10.62
1.0	135	1.899 \pm .195	10.26	85000	11.701 \pm 0.199	11.69

TABLE 3. S.I. Values and time consumed using 1-2mm size aggregates in Reversed Osmosis water with dry and prewet aggregates. C. V. stands for coefficient variation.

Sample Weight (gms)	Dry			Prewet		
	Time (Min)	Stability Index	C.Z. (%)	Time (Min)	Stability Index	C.Z. (%)
0.1	20	2.113 \pm .122	5.77	30	2.009 \pm .136	6.77
0.2	22	2.112 \pm .135	6.39	32	2.103 \pm .121	5.75
0.3	25	2.105 \pm .136	6.46	35	2.003 \pm .125	6.24
0.4	26	2.100 \pm .139	6.62	40	2.054 \pm .129	6.28
0.5	30	2.101 \pm .141	6.71	45	2.051 \pm .145	7.06
0.6	35	2.092 \pm .155	7.39	50	2.063 \pm .157	7.61
0.7	40	2.091 \pm .167	7.98	52	2.058 \pm .147	7.14
0.8	42	2.043 \pm .179	8.76	50	2.040 \pm .141	6.91
0.9	43	2.000 \pm .186	9.3	60	2.010 \pm .168	8.35
1.0	45	2.051 \pm .199	9.7	62	2.001 \pm .171	8.45

TABLE 4 S.I. Values and time consumed using one aggregate in irrigation water with dry and prewet aggregates. C. V. stands for coefficient of variation.

Sample Weight (gms)	Dry			Prewet		
	Time (Min)	Stability Index	C.V. (%)	Time (Min)	Stability Index	C.V. (%)
0.1	25	1.870 ± .123	6.5	50	1.785 ± .162	9.07
0.2	35	1.880 ± .113	6.01	60	1.780 ± .153	8.59
0.3	60	1.863 ± .119	6.38	88	1.770 ± .166	9.37
0.4	75	1.865 ± .125	6.70	150	1.775 ± .145	8.17
0.5	101	1.855 ± .131	7.06	160	1.763 ± .183	10.38
0.6	130	1.893 ± .143	7.55	170	1.752 ± .165	9.42
0.7	142	1.885 ± .139	7.37	172	1.749 ± .181	10.35
0.8	151	1.879 ± .148	7.87	175	1.746 ± .162	9.27
0.9	160	1.874 ± .145	7.73	179	1.735 ± .199	11.43
1.0	171	1.832 ± .148	8.07	212	1.719 ± .156	9.07

TABLE 5 S.T. Values and time consumed using 1-2 mm size aggregates in irrigation water with dry and prewet aggregates. C. V. stands for coefficient of variation.

Sample Weight (gms)	Dry			Prewet		
	Time (Min)	Stability Index	C.Z. (%)	(Min) Time	Index Index	C.Z. (%)
0.1	17	1.96 ± .015	0.76	35	1.761 ± .134	7.6
0.2	21	1.93 ± .031	1.6	37	1.723 ± .125	7.25
0.3	22	1.92 ± .023	1.19	40	1.704 ± .153	8.52
0.4	30	1.95 ± .033	1.69	43	1.621 ± .163	10.06
0.5	32	1.893 ± .011	0.58	50	1.595 ± .168	10.53
0.6	31	1.899 ± .036	1.86	55	1.668 ± .169	10.13
0.7	33	1.912 ± .044	2.3	56	1.756 ± .178	10.13
0.8	31	1.924 ± .063	3.27	58	1.745 ± .181	10.37
0.9	30	1.918 ± .067	3.49	60	1.631 ± .181	11.09
1.0	31	1.991 ± .079	3.96	63	1.699 ± .173	10.18

REFERENCES

- Child, E.C. 1940. The use of soil moisture characteristics in soil studies. *Soil Sci.* 50, 239-252.
- Emerson., W.W. 1967. A classification of soil aggregates based on their coherence in water. *Aust. Jour. Soil. Res.* 5, 47-27.
- Matkin, E.A., and Smrt. P. 1987. A comparison of tests of soil structural stability. *Jour. Soil. Sci.* 38, 123-125.
- Molope, M.B., Page E.R. and Grieve. I.C. 1985. A comparison of soil aggregate stability tests using soils with contrasting cultivation histories. *Soil. Sci. Plant. Anal.* 16, (3)315-322.
- Oades, J.M. 1984. Soil organic matter and structural stability. Mechanisms and implications for management. *Plant Soil.* 76, 319-333.
- Pojasok, T., and Kay. B.D. (1989). Assessment of a combination of wet sieving and turbidimetry to characterize the structural stability of moist aggregates. *Canad. Jour. Soil Sci.* 70, 33-42.
- William, B. G. Greenland. D. J., Lindstron. E. R. and Quirk. J. F. 1966. Techniques for determination of the stability of soil aggregates. *Soil Sci.* 101, 157-163.
- U.S. Salinity Laboratory 1954. Diagnosis and improvement of saline and alkali soils. *USDA Handbook* 60. US Government Printing Office Washington DC.
- Williams, R.J.B. and Cooke, G.W. 1961. Some effects of farmyard manure and of grass residues on soil structure. *Soil Sci.* 92, 30-33.
- Yoder, R.E. 1936 A direct method of aggregate analysis and a study of the physical nature of erosion losses. *Amer. Jour. Sci. Agron.* 28, 337-357.

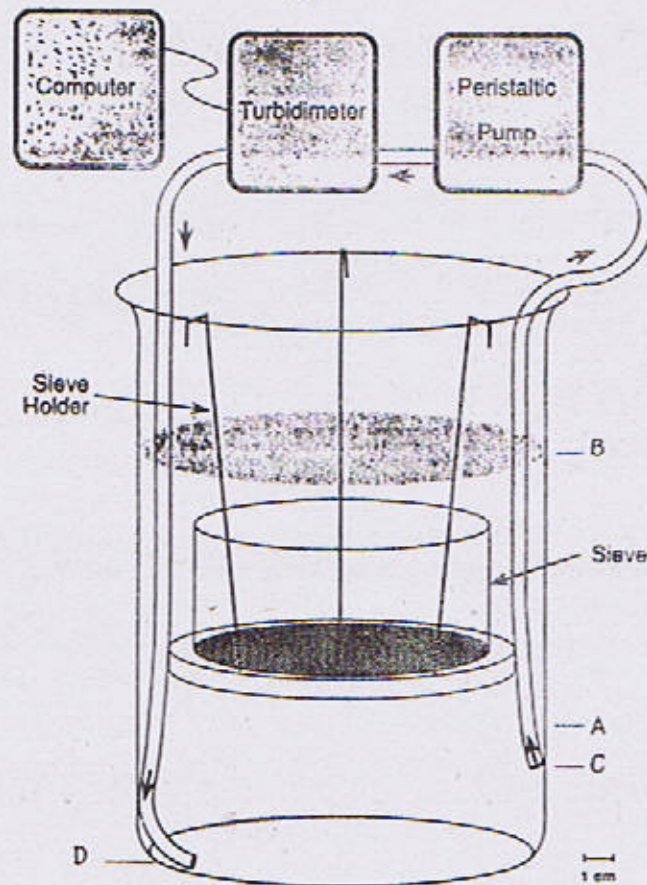


Fig 1. Schematic diagram of set of equipment and sample container used in the studies.

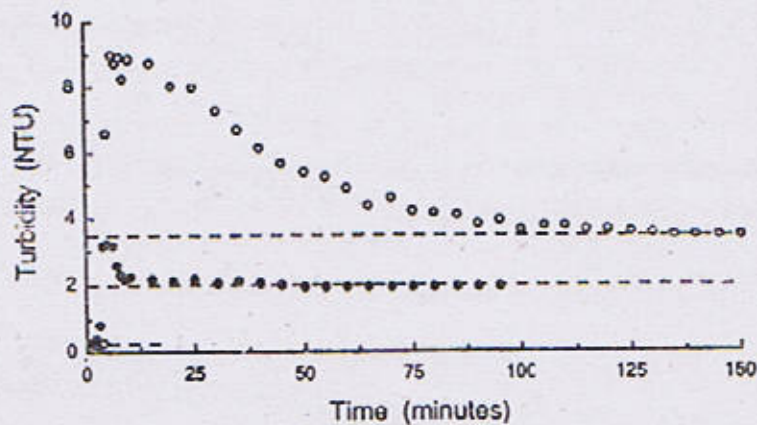


Fig 2. Behaviour of turbidity with time and calculation of stability index (SI)

$$D_i = 3.5, D_f = 2 \text{ db} \pm 0.25$$

$$SI = \text{Inv.} \frac{(3.5 - 2.5)}{(2.0 - 2.5)75}$$

$$SI = 40.38$$

AGGREGATE STABILITY OF A SALINE SODIC SOIL UNDER IRRIGATED KALLAR GRASS FAISALABAD, PAKISTAN

BY

JAVED AKHTER, K.A. MALIK, M.H. NAQVI

Nuclear Institute for Agriculture and Biology, Faisalabad, Pakistan.

SHAFEEQ AHMAD

Institute of Geology, Punjab University, Lahore-54590, Pakistan

AND

R. MURRAY

Department of Soil Science Waite Agricultural Research, Adelaide, South Australia.

Abstract : A field study was conducted to find out the effect of cropping kallar grass on soil physical properties of a highly unstable saline sodic soil irrigated with brackish ground water under the scheme of biological amelioration of salt-affected soils. Soil samples were collected at the end of each growth year of kallar grass from three pre-selected depths for five years and were analysed for stability index (SI), water retention, Kfs, pH, Ec and carbon contents. Five years cropping of kallar grass resulted an increase in SI, Kfs, and water retention. Both SI and Kfs, were improved significantly at depth A compared to fallow soil. The SI increased at depth B and C after one year and decreased with further growth of grass, but the Kfs improved at A and B depth compared to fallow soil. The soil organic carbon show significant increase with years of cropping and its interaction with SI is also highly significant. The soil organic matter seems to increase aggregate stability, Kfs, and water retention, which may be due to air encapsulation that prevent, slaking of aggregates. Furthermore, the drying and wetting events may have enhanced the aggregate stability and related parameters. We conclude that salt-affected soils can be utilized effectively by cropping kallar grass irrigated with brackish water along with improvement in soil physical conditions.

INTRODUCTION

The soil aggregate stability is important to maintain the agricultural productivity of soils. Poor aggregate stability causes clay dispersion and decrease infiltration rate in the soils of arid region, having high exchangeable sodium. Adverse effects of increase in pH on soil dispersion has been reported by Lebron and Suarez, (1992), when SAR of soil was high enough to break the illite domains.

Several investigators have demonstrated that high sodium levels decrease the soil hydraulic conductivity (Quirk and Schofield 1955 ; McNeal and Coleman, 1966 ; Millar and Baharruddin, 1986 ; Miller et al., 1990). The degree of dispersion and the factors which causes it have been recognized by many researchers (McNeal and Coleman, 1966 ; El-Sway et al., 1970 ; Frankel et al., 1978 ; Shainberg et al., 1981 ; Rangasamy et al., 1984).

The hazards of using poor quality water on soil properties and plant growth have been indicated by many workers. The most important among these include clay dispersion and clogging of pores within the soil which reduces infiltration rates. Even at low ESP and high water salinity, Agassi et al., (1985) showed that crust formation is mainly due to soil aggregate disintegration. However, at ESP more than 2.5 and low water salinity, chemical dispersion plays an important role in determining the infiltration rate (IR) of soils.

Based on the observations that increase in solute concentration increases the soil stability, some recommendations regarding the stability have been laid by many scientists (Rhoades, 1982; Ayres and Westcott, 1985). Increase or persistency in IR has also been reported by Hades and Frankel (1982) and Gupta (1986) after long term use of saline sodic water. Kay and Dexter (1990) suggests that response of structural stability of soils to a change in water content depends upon the cropping history. They observed that long term growth of grasses have diminished the sensitivity of soil structural stability to changes in water content. Cropping treatment have been shown to strongly influence the structural stability, particularly the proportions of water stable aggregates (Tisdall and Oades, 1980b; Ried and Goss, 1981). Baldock and Kay (1987) showed that in the field the size and stability of aggregates increased with cropping bromegrass.

The objectives of the study were to determine the influence of continuous growth of kallar grass on soil physical properties such as structural stability, field saturated hydraulic conductivity (K_f), water retention, soil carbon, EC and pH of a highly saline sodic soil irrigated with brackish underground water.

MATERIALS AND METHODS

The study was conducted at biosaline research substation (BSRS) of Nuclear Institute for Agriculture and Biology situated at Lahore, Pakistan.

The station is located at longitude $74^{\circ}7'$ and latitude $31^{\circ}6'$. Average annual rainfall is about 500mm. At BSRS, model plots have been established to demonstrate the economic utilization of salt-affected soils by growing salt tolerant crops using brackish irrigation water. This station will be used as a model for a long time in future.

Kallar grass was planted on 3 plots ($100 \times 100 \text{ m}^2$), a plot of same size was kept as a fallow/control and was preserved without any vegetation. Kallar grass was irrigated after 15 days with flood irrigation of about 7.5cm depth. Kallar grass being perennial crop was continuously grown upto 5 years and was harvested from the field in 5-7 cuttings per year. The green matter yield was about 50 tons $\text{ha}^{-1} \text{ year}^{-1}$ (Malik et al., 1986). Soil samples were collected from the fields at the end of every growth year of grass (November) upto 5 years. Virgin soil was obtained from the field that has not been cultivated and kept as control. Samples were collected randomly in triplicate from the horizon A (0-15 cm), B (40-60 cm) and C (90-100 cm) to determine aggregate stability. Samples were air packed dried, in tin containers and sterilized with gamma irradiation (50 kilo greys) by quarantine before entry into Australia.

The natural soil aggregates were sieved through 2mm sieve and bigger aggregates were broken by pressing with hand. The powder soil $< 1 \text{ mm}$ was sieved away and aggregates between 1-2mm were separated for further use. The aggregate stability was measured by turbidimetric method (Akhter et al., 1994) modified from Pojasok and Kay (1989) and Molope et al., (1985) on natural dry and pre-wet aggregates of 1-2mm size. Turbidities were continuously monitored in a fixed volume of irrigation water with minimum energy input and after sonification of solution with ultrasonic probe for a time until it attained a constant value. The turbidity values extrapolated to zero time were used to determine stability indices. Pre-wet aggregates were prepared by placing the aggregates on sintered glass

funnels at 100cm suction for a week. The stability was determined in irrigation water. The irrigation water similar to the water used to grow Kallar grass was prepared in bulk after a series of trial. The water was prepared by addition of required quantities of NaHCO_3 , K_2CO_3 , CaO , MgO , HCl and H_2SO_4 and bubbling of CO_2 gas through the water to adjust required pH.

Subsamples composited from the pre-selected depths, were air dried, ground and passed through a 2mm sieve for textural and chemical analyses. The total carbon (Ct) was determined by dry combustion method using a LECO carbon analyser (LECO Instruments, Canada). The inorganic carbon (Ci) was determined with volumetric calcimetric method (Collins, 1906 modified) in which soil was treated with 4N HCl in the presence of FeCl_2 in a closed system and volume of CO_2 released was determined. The organic carbon (Co) was determined by difference. Soil texture was determined by the pipette method (Gee and Bauder, 1986). Saturated soil paste extracts and irrigation water were analysed chemically using standard methods (USDA, 1954). The pH and EC of saturated soil paste were determined with Corning pH meter 130 and WTW Conductivity meter LF 530 respectively.

The Kfs was measured with Guelph permeameter (Model 2800KI, Soil Moisture Equipment CORP. USA) method described by Reynold and Eirick (1985). Measurements of Kfs were carried out at A and B horizons at 10 sites randomly selected in the fields including control soil at the end of each cropping year. The amount of water retained by the soils was determined by pressure plate extractor (Soil Moisture Equipment Corporation USA). The soil samples placed in extractor were saturated and equilibrated for a week at .003, .01, .03, .1, .2, .5, and 1.5 MPa pressures. Soil moisture content of these samples was determined gravimetrically.

The data was analysed statistically in two factor-factorial experiment in randomised complete block design. The data was subjected to analyses of variance followed by least significant difference (LSD) test using MSTAT programme on a microcomputer. Linear correlations were determined between stability indices and soil pH, EC at horizons A, B, and C and total inorganic and organic carbon at horizon A.

RESULTS AND DISCUSSION

The chemical composition of solution extracts of soil and irrigation water is given in Table 1. The soils have sandy clay loam texture. Major clay minerals are mica and kaolinite. The soils are highly saline sodic with Na concentration of 226meL^{-1} , exchangeable sodium percentage 72 and pH more than 10. The soils are very hard when dry and very soft when wet. The irrigation water used to grow kallar grass on these soils is brackish with RSC 9.61, adjusted SAR 12.7 and categorised as C3S2 (USDA 1954), unfit for irrigation (chemical composition given in Table 1).

The influence of cropping kallar grass on SI is illustrated (Fig. 1). Generally, kallar grass produced aggregates which were more water stable. The original soils showed more stability index at B and C horizons than surface horizon. Analysis of variance of data indicated that variation among the fields was non significant. The effect of cropping years on soil horizons and interactions between them differed significantly.

Both SI and Kfs were significantly influenced at depth A with years of cropping of kallar grass (Figs. 1-2, Table 2). The Kfs improved at A horizon upto four years linearly and increased sharply after five years (Figs. 1). The SI increased at B and C horizon after a year and decreased with further growth of grass (Fig. 1) so trend at B and C was non significant. The Kfs increased quite substantially at A and B depths with cropping years (Table 2, Fig. 2). The effect of cropping on Kfs

was significantly more at depth B which was non-significant on SI at same depth. The Kfs showed strong relationship with SI (Table 2) which is highly significant. This is in accordance with findings of Horn (1990) that structured soils have more Kfs which persists even under unsaturated conditions.

The soils have a very low carbon content generally, so the data of only A horizon soil is presented here (Fig. 3). The total carbon content increased with the cropping of KG. The inorganic carbon increased sharply after one year but declined after two years and showed nonsignificant trend with further growth of grass (Table 2). The change in C_t is due to change in C_o ; therefore C_o will be included in further discussion. The soil organic carbon showed significant relationship with years of cropping KG and its interaction with SI is also highly significant (Table 2). The amount of organic carbon seems to be responsible to a larger extent for increase in stability index. It has already been suggested that increase in soil organic matter stabilizes aggregates through cementing mechanism (Russell, 1973; Quirk, 1978; Tisdall and Oades 1982; Elliott, 1986). Similar result has been reported by Bruce et al. (1992) which describes an increase in soil stability and infiltration rates with increase in soil carbon content.

Generally, the soil water content increased (Table 3) with the cropping years at three horizons on all the applied matric pressures but the increase in retention is more at B and C horizons with the growth of grass. The capacity of soil to retain water at matric pressure 0.03 MPa and difference between water contents at 1.5 MPa is available water for plant use and is considered as a standard value. (U.S. Salinity Laboratory 1954). Therefore, the available water can be used as a parameter which improves the soil physical conditions consequently improving soil structural stability. The available water increased with the growth of KG at three depths under study. (Table 3).

It has been suggested by some researchers that organic matter increases water stable aggregation by slowing water entry into the aggregates (Emerson, 1954; Coughlan et al., 1973). However, Sullivan (1990) suggests that organic matter can increase the air encapsulation which reduces water uptake rates which in turn prevents slaking of aggregates. The other parameters pH and EC were found to be correlated with SI nonsignificantly (Table 2). As the soils were irrigated after about fifteen days interval which provided extensive wetting and then followed by a drying cycle of about 10 days throughout the year. This drying and wetting cycle may have enhanced the aggregate stability. It has already been suggested that aggregate strength depends upon intensity, number and time of swelling and drying events in addition to other factors and such aggregates are more dense and stable.

CONCLUSION

The study showed that 5 year growth of Kallar grass resulted an increase in structural stability, saturated hydraulic conductivity and water retention of a highly unstable saline sodic soil irrigated with brackish water. The above results indicate that improvement in some physical properties may be due to increase in soil organic matter, enhanced biological activity and/or drying and wetting cycles which continued throughout the years. The effect of growth was not significant at B and C horizons but all the parameters persisted during growth of KG. So areas where good quality water is scarce, soils are salt-affected and underlain by brackish water, a lot of biomass can be produced and soils can be effectively utilized without amendments. Improvement in soil properties and their persistence for longer times is considered a by product of this scheme of biological amelioration of salt-affected soils.

ACKNOWLEDGEMENTS

We express our deep gratitude to Dr. J. M. Oades, Chairman Department of soil science, Waite Agricultural Research Institution Adelaide,

Australia for his cooperation in providing facilities and guidance in analytical work. The financial support by the International Atomic Energy Agency is gratefully acknowledged.

TABLE 1

Chemical composition of saturated soil extracts and irrigation water

	$(Ca+Mg)^{2+}$	Na^{+}	K^{+}	Cl^{-}	HCO_3^{-}	CO_3^{2-}	SO_4^{2-}		
	meqdm ⁻³								
Soil	3.0	226	0.4	72.4	103.4	14.2	39.4		
Water	3.65	10.5	0.2	0.7	12.86	0.4	0.1		
	pH	SAR	SARadj	EC	ESP	RSC	Clay	Silt	Sand
				dSm ⁻¹			%		
Soil	10.4	180	—	22.0	72	—	22	23	55
Water	7.6	9.6	12.7	1.4	—	9.81	—	—	—

TABLE 2

Characteristics of regression equation relating years of cropping of Kallar Grass with SI and SI with pH, EC and soil carbon at depth A

Parameters		Intercept	slope	r
Years * SI	..	-28.70	41.125	0.850*
Years * Ct	..	0.36	0.052	0.861*
Years * Ci	..	0.24	-0.004	-0.06NS
Years * Co	..	0.22	0.036	0.995**
pH * SI	..	6120.20	-52.650	0.343NS
EC * SI	..	121.60	-5.790	-0.505NS
Ct * SI	..	-254.60	664.28	0.828*
Ci * SI	..	67.47	29.400	0.045NS
Co * SI	..	276.90	1141.500	0.862*
Kfs * SI	..	-8.65	-0.338	0.980**

**,* Significant at $P=0.01$ and 0.05 , respectively

Ct : Total Ci : Inorganic Co : Organic carbon respectively

NS : Non significant

TABLE 3

Water retained by soils at different matric pressures at depths A, B and C as a function of growth of KG.

		Water Content (g/g)						
		1.5	.5	.2	.1	.03	.01	.003
YEARS		MPa						
0	A	.0525	.0725	.1000	.1338	.2074	.2407	.2827
	B	.0596	.0834	.1103	.1334	.2142	.2596	.2955
	C	.0530	.0791	.1150	.1605	.2035	.2441	.2890
1	A	.0917	.1204	.1516	.1803	.2442	.2737	.3204
	B	.1235	.1612	.2015	.2247	.2686	.3073	.3871
	C	.1067	.1447	.1696	.1885	.2429	.3109	.4016
2	A	.0660	.0868	.1105	.1311	.1771	.2418	.3142
	B	.0919	.1215	.1496	.1706	.2160	.2671	.3878
	C	.0894	.1061	.1406	.1591	.2143	.2712	.3777
3	A	.0890	.1042	.1289	.1482	.2151	.2716	.3594
	B	.0870	.1237	.1402	.1767	.2382	.3057	.4089
	C	.0737	.0998	.1333	.1623	.2298	.2742	.3629
4	A	.0569	.0741	.0961	.1293	.2054	.2518	.3490
	B	.0750	.0963	.1235	.1510	.2117	.2594	.3872
	C	.0609	.0820	.1136	.1427	.2243	.2637	.3872
5	A	.0791	.1035	.1269	.1293	.2264	.2870	.3490
	B	.1173	.1445	.1748	.2020	.2601	.2996	.4075
	C	.1131	.1423	.1777	.2181	.2695	.3211	.3872

REFERENCES

- Agassi, M., Morin J. and Shainberg I., 1985. Effect of rain drop impact energy and water salinity on infiltration rates of sodic soil. *Amer. Jour. Soil Sci. Soc.* **49**, 186-190.
- Ayers, R.S., and Westcot D.W., 1985. Water quality for agriculture. *Irrig. Drain. Paper 29*, FAO, Rome.
- Akhter, J. Shaheen R., and Naqvi M.H., 1994. A turbidimetric technique for measuring the soil structural stability. *Fifth Nat. Congr. Soil Sc.* Peshawar, Pakistan.
- Baldock, J.A. and Kay B.D., 1987. Influence of cropping history and chemical treatment on the water stable aggregation of a silt loam soil. *Canad. Jour. Soil Sci.* **67**, 501-511.
- Bruce, R.R., Langdale G.W., West L.T., and Miller W.P., 1992. Soil surface modification by biomass inputs affecting rainfall infiltration. *Amer. Jour. Soil Sci. Soc.* **56**, 1614-1620.
- Coughlan, K.J., Fox, W.E., and Hughes, J.D. 1973. A study of the mechanism of aggregation in Krasnozern soil. *Aust. Jour. Soil Res.* **11**, 65-73.
- Elliot, E.T., 1986. Aggregate structure and carbon, Nitrogen and phosphorus in native and cultivated soils. *Amer. Jour. Soil Sci. Soc.* **50**, 627-33.
- El-Swaify, S.A., Ahmed, S., and Swindale L.D., 1970. Effects of adsorbed cations on physical properties of tropical red and tropical black earths. ii. Liquid Limit, degree of dispersion, and moisture retention. *Jour. Soil Sci.* **21**, 188-198.
- Emerson, W.W. 1954. The determination of the stability of soil crumbs. *Jour. Soil Sci.* **5**, 233-43.
- Frenkel, H., J.O. Goertzen and J.D. Rhoades. 1978. Effect of clay type and content, exchangeable sodium percentage and electrolyte concentration on clay dispersion and soil hydraulic conductivity. *Amer. Jour. Soil Sci. Soc.* **42**, 32-39.
- Gee, G.W., and Bauder J.W., 1986. Particle size analysis. P. 383-412. In A. Klute (Ed.) Methods of soil analysis. Part 1. 2nd ed. Agron. Monogr. 9, ASA and SSSA, Madison, WI.
- Gupta, S.K., 1986. Physico-chemical characteristics of saline soils under reclamation. *Jour. Agri. Eng. ISAE*, **23**, (1)
- Hades, A., and Frankel, H., 1982. Infiltration as affected by long term use of sodic-saline water for irrigation, *Amer. Jour. Soil Sci. Soc.* **42**, 32-39.
- Horn, R., 1990. Aggregate characterization as compared to soil bulk properties. *Soil and Tillage Res.* **17**, 265-289.
- Kay, B.D., and Dexter A.R., 1990. Influence of aggregate diameter, surface area antecedant moisture content on the dispersibility of clay. *Canad. Jour Soil Sci.* **70**, 655-667

- Lebron, I. and D.L. Suarez, 1992. Variation in soil stability within and among soil types. *Amer. Jour. Soil Sci. Soc.* **56**, 1412-1421.
- Malik, K.A., Aslam Z., and Naqvi, M., 1986. Kallar grass. A Plant for Saline Land. Ghulam Ali Printers, Lahore, Pakistan, pp. 93.
- McNeal, B.L., and N.T. Coleman, 1966. Effect of solution composition on soil hydraulic enductivity. *Proc. Amer. Soil Sci. Soc.* **30**, 308-312.
- Miller, W.P. and M. K. Baharuddine, 1986. Relationship of soil dispersibility to infiltration and erosion of south eastren soils. *Soil Sci.* **142**, 235-240.
- Miller, W.P., Frenkel H., and D. Newman K., 1990. Flocculation concentration and sodium/calcium exchange of Kaolinitic soil clays. *Amer. Jour. Soil Sci. Soc.* **54**, 346-351.
- Molope, M.B., Page, E.R., and Griever, I.C., 1985. A comparison of soil aggregate stability tests using soils with contrasting cultiation histories. *Soil. Sci. Plant Anal.* **16** (3), 315-322.
- Pojasok, T., and Kay. B.D., 1989. Assessment of a combination of wet sieving and turbidimetry to characterize the structural stability of moist aggregates. *Canad. Jour. Soil Sci.* **70**, 33-42.
- Quirk, J.P., 1978. Some physico-chemical aspects of soil structural stability. A Review. 3-16 In modification of soil structure W.W. Emerson, R.D. Bond and A.R. Dexter (Eds) John Wiley. & Sons London.
- Quirk, J.P., and Schofield R.K. 1955. The effect of electrolyte concentration on soil permeability *Jour. Soil Sci.* **6**, 163-178.
- Rengasamy, P.R., S.B. Greene, G.W. Ford and A.H. Mehanni, 1984. Identification of dispersive behaviour in the management of red-brown earths. *Aust. Jour. Soil Res.* **22**, 413-422
- Ried, J.B., and Goss, M.J., 1981. Effect of living roots of different plant species on the aggregate stability of two arable soils. *Jour. Soil Sci.* **32**, 521-641.
- Reynolds, W.D., and Elrick D.E., 1985. A method for simultaneous in situ measurement in the vadose zone of field-saturated hydraulic conductivity, sorptivity and the conductivity-pressure head relationship *Ground Water Monitoring Review*.
- Rhoades, J.D., 1982. Reclamation and management of salt-affected soils after drainage. p. 123-197. Proc. Annu. Western Provincial Conf. on rationalization of water and soil research and management 1st, Lethbridge, Alberta, Canada. 27 Nov. - 2 Dec. 1982. Saskatchewan Water Corp., Saskatoon.
- Russell, E.GW., 1973. Soil conditions and plant growth. (10th Ed.) Longmans, London.
- Shainberg, I., D. Rhoads J., L. Suarez D., and J. Prather R., 1981 a. Effect of mineral weathering on clay dispersion and hydraulic conductivity of sodic soils. *Amer. Jour. Soil Sci. Soc.* **45**, 287-291.

- Shainberg, I., Rhoads J.D., Suarez D.L., and J. Prather R. 1981 b. Effect of mineral weathering on clay dispersion and hydraulic conductivity of sodic soils. *Amer. Jour. Soil Soc. Sci.* **45**, 273-277.
- Sullivan, L.A. 1990. Soil organic matter, air encapsulation and water-stable aggregation. *Jour. Soil Sci.* **41**, 529-534.
- Tisdall, J.M. and Oades, J.M. 1982. Organic matter and water stable aggregates in soils. *Jour. Soil Sci.* **33**, : 141-163.
- Tisdall, J.M. and Oades, J.M. 1980 b. The effect of crop rotation on aggregation in a red-brow earth. *Soil Res.* **18**, 423-433.
- U.S. Salinity Laboratory. 1954. Diagnosis and improvement of saline and alkali soils. *USDA Hand book 60*. US Government Printing Office Washington, DC.

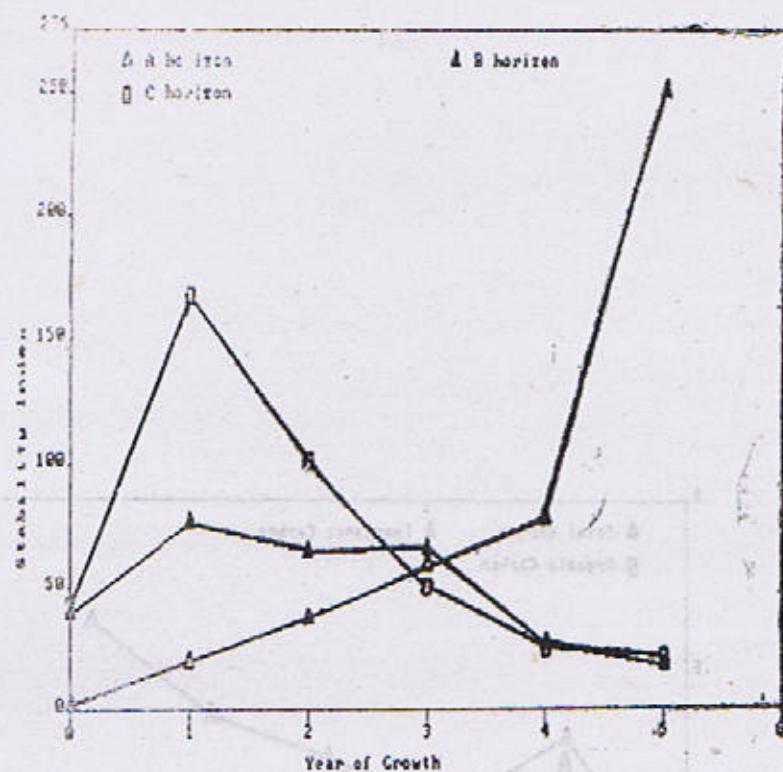


Fig. 1. Aggregate Stability as a function of Kallar Grass growth.
L.S.D. for 5 %

Years of growth	..	1.487
Soil Depth	..	1.95
Growth years x Depth	..	3.612
Over all	..	2.575

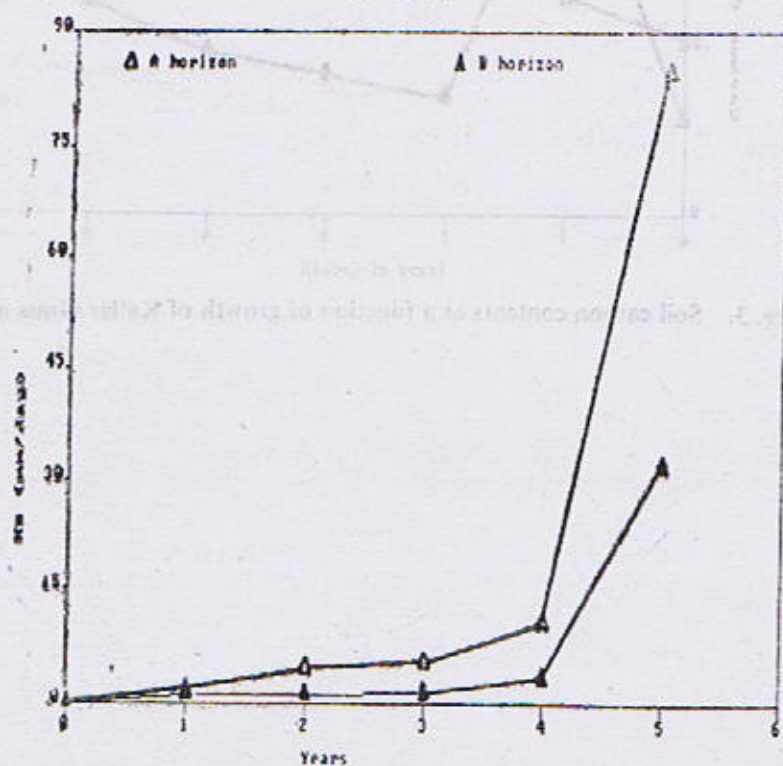


Fig. 2. Saturated hydraulic conductivity of the soil as a function of growth of Kallar Grass at depth A and B.

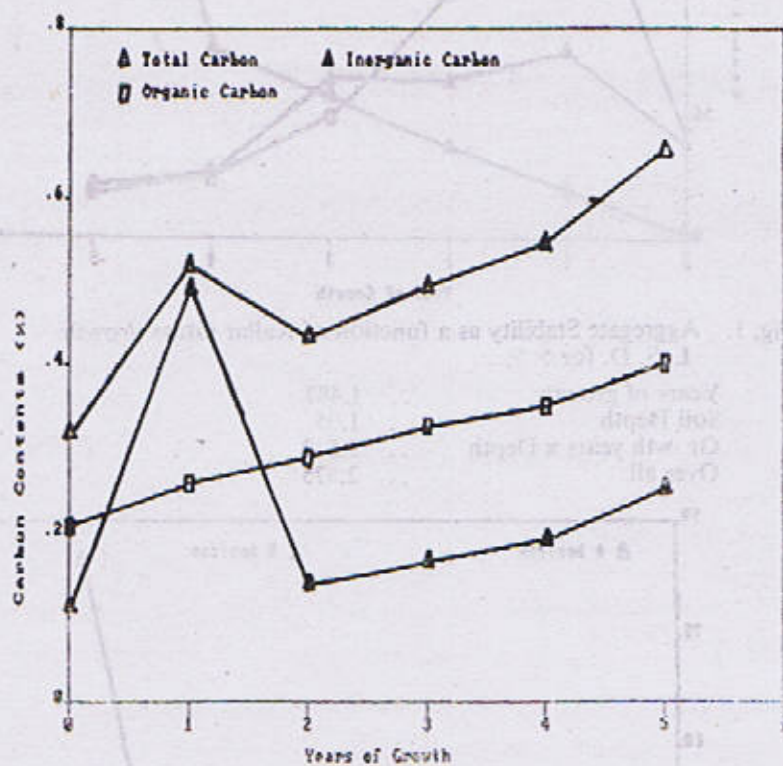


Fig. 3. Soil carbon contents as a function of growth of Kallar Grass at depth A.

CLAYS—A SOURCE OF ENVIRONMENTAL DEGRADATIONS AND A REMEDY FOR ENVIRONMENTAL POLLUTION

BY

AKHTAR ALI SALEEMI AND SHAFEEQ AHMAD

Institute of Geology, Punjab University, Lahore-54590, Pakistan.

Abstract : *Clays because of their certain typical physical characteristics, are both as a source of pollution and as absorbent of elements hazardous to human life. A detailed study of certain clay deposits from Pakistan indicates that some of the clay deposits can be utilized as an effective adsorbent for contaminants from coal mine drainage and industrial effluents.*

INTRODUCTION :

Clays, natural earthy, fine grained material largely composed of hydrous aluminium silicate minerals, are derived from alteration of a many types of rocks. Clays vary widely in chemical composition and have well characteristic physical properties, that make them useful as industrial mineral. These are broadly divided into three categories i.e. Kaolin group, smectite group and the illite group. The minerals constituting smectite group are finely divided clays having strong adsorption characteristics.

A number of clay deposits have been reported from various localities, the most important being :

bentonite and fullers earth from Azad Kashmir, Hyderabad Division, Peshawar Division, Rawalpindi Division, Kaolin and China clay from Hyderabad Division, Peshawar Division, Fire clay from Dera Ismail Khan Division, Hyderabad Division, Multan Division, Rawalpindi Division and Sargodha Division (Fig. 1) (Ahmed, and Siddiqui 1992).

ENVIRONMENTAL IMPACTS OF ELEMENTS

On the basis of behaviour of certain elements on health and diseases in animals, humans and plants, Larry (1993) classified the useful elements into four groups (Table 1).

TABLE 1

Classification of elements with respect to their usefulness

Essential for all elements and plants.	Essential for several classes of animals and plants	Essential for wide variety of species in one class	Essential for one or two species only.
H, C, N, O, Na, Mg, P, S, Cl, K, Ca, Mn, Fe, Cu, Zn,	Si, V, Co, Mo, I	B, F, Cr, Br	Li, Al, Ni, Sr, Ba

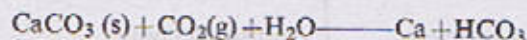
Certain diseases have been reported due to the deficiency of about twenty elements in animals and humans and to the deficiency of about thirteen elements in plants. However the presence of these elements in excess of a certain limit in an environment become toxic and such an environment is considered to be hazardous (e.g. Se upto 0.4 ppm is required in the diet of cattle, but it becomes toxic when its concentration is greater than about 4 ppm.)

These elements have been classified into essential elements, required for the survival of animals and plants; while the elements that are not required are non essential. The elements such as fluorine, copper, selenium, molybdenum etc.; which are trace essential elements can be hazardous if present at high levels. The toxic limit of non essential heavy elements such as arsenic, lead, chromium cadmium is at a much lower value as compared to the trace essential elements.

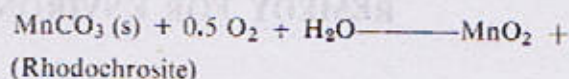
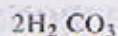
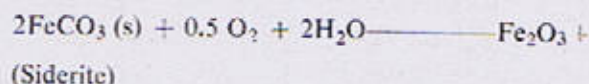
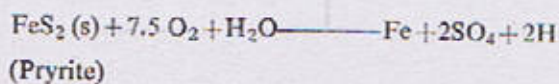
The majority of our environmental problems are associated with the pollution of surface and ground water, due to the natural and human processes. Natural water flowing through rocks, soils dissolve some of the soluble minerals and organic substances. Water containing high concentration of minerals deposit them to the waterways (Swamps and marshes often produce acidic and coloured waters).

RELEASE OF CONTAMINANTS :

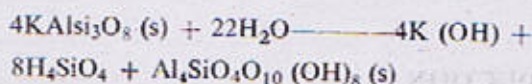
Eversince the creation of the earth, major role is being played by chemical weathering processes within the earth crust. Water acts as conveyor of the dissolved constituents and of such weathering agents as CO_2 and O_2 . The weathering agents like CO_2 dissociate the carbonates to bicarbonates;



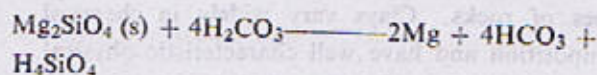
The oxidative reactions of various rocks and minerals give rise to acidic solutions :



The chemical weathering of silicates is the predominant reaction in nature and is the major source of many dissolved constituents, e.g.



These reactions are very slow processes and may require several years for their completion. Frequently, silicates may undergo an acidic reaction



This reaction suggests the attack of carbonic acid on forsterite and similar silicates may be a source of bicarbonate alkalinity.

The natural sources of toxic substances are the rocks, volcanoes, sediments and soils. For example, water flowing through sedimentary rocks in central Oklahoma is contaminated with arsenic, chromium, selenium and uranium. Cooling magma beneath lake Nyos in Cameroon produced carbon dioxide that bubbled up and suffocated 2000 people in 1986. Under specific chemical environment, elements present in mineral deposits rocks, or soils get mobilised into water.

The mobilisation of hazardous elements into water depends upon the geochemistry of the elements, and it increases manifold as a result of mining activities, chemical reactions taking place due to acidic mine drainage waters or as industrial

effluents. The natural processes and man made activities mobilise the elements that find their ways into surface and ground water and aquatic life. Human activities, such as smelting, refining, chemical industries, use of fertilisers and waste disposals add toxic substances to the environment. In most of the cases there are no political or geographical boundaries to the distribution of harmful elements and compounds. Polar ice and snow has recorded numerous elements, due to human activity in the form of industrial revolution and global circulation of metal contaminants and synthetic compounds.

In an industrial state, 20 Km from Lahore, chemical industries discharge effluents in a nearby storm water channel. The use of water from this channel for irrigation purposes is likely to have deleterious effects on soils. Similarly coal mining in Punjab is effecting the adjacent areas and downstream areas; due to release of mining waste and acid mine drainage. With the enhancement of human activities, its impact on the environment is on the increase.

CLAYS AND ENVIRONMENT

The extent of degradation depends upon the chemical and mechanical stability of rocks. The clay minerals, due to their absorptive behaviour expand their lattice and contribute significantly towards deterioration of rocks.

It is well established by clay mineralogists that there are hundreds of clay minerals and no two clay minerals are identical even if they have similar mineralogical and chemical composition, and no artificial mixture can exactly have the diagnostic physical and chemical properties of a specific clay.

Clays due to their extraordinary properties, play an important role in the environment. The ease of hydration and liquefaction causes landslides and submarine slumping on the one hand, while on the other hand, the absorptive properties of clays make them useful in waste management.

Due to certain specific physical characteristics, certain clay minerals causes catastrophic impact on the environment. These effects may be avalanches, landslides and submarine sediment slumping. These phenomenon are mostly caused by the presence of Smectite or poorly crystalline clays.

The environmental impact of clay minerals depends on the following factors;

1. Ease of hydration
2. Ease of liquefaction
3. Neoformation of the clays
4. The binding forces between the ions and the clays.

Ease of Hydration

The waste absorption behaviour of clays cause loosening of bonds between clay particles. This results into a change in the clay consistency. Clays due to their absorption and adsorption properties can accumulate certain hazardous elements such as heavy metals, sulphur, fluorine and boron etc. As soon as the state of equilibrium of these elements and clays is disturbed, the hazardous elements are introduced to the environment. The degree of release of these hazardous elements depend upon the water absorption behaviour of clays.

Ease of Liquefaction

Liquefaction in clays is introduced by the absorption of water resulting into loosening of bonds between clay particles. A small disturbance in the clay containing materials causes a flow, particularly on unstable slopes.

The ease of hydration and liquefaction of clays are greatly influenced by the area of clays and to amount of water and period to which these clays are exposed.

Neoformation of Clay Minerals

The neoformation of clay minerals in the construction material and decorative and monumental stone depends upon the intensity of alteration during interactions with physical and chemical

agents from atmosphere, hydrosphere and biosphere.

The binding forces between the ions and the clays

The release of elements to the environment is also dependent on their binding force with clays. The weaker the bond, the greater are the chances of their release to the environment.

CLAYS AND WASTE MANAGEMENT

Clays find application in the control of environment due to their following characteristic properties

1. Absorption :

The absorption property of clays is due to the fact that the basal oxygen layers of the clays which have a charge of less than 0.6 but greater than 0.2 per $O_{10}(OH)_2$ are negatively charged. The absorption characteristics are well exhibited by the swelling clays and Sepiolite-Palygorskites. The interactions of clays-organic molecules make them useful as an absorbent of hazardous element from effluents of a number of chemicals industries.

In hydrated clay complex, containing inter-layer cations surrounded with water molecules ; the cations satisfy the negative charge on the clay surface through hydrogens of the co-ordinated water molecules. Water and organic material compete for the interlayer site., when organic material is placed in an aqueous solution and ; this depends upon their proportion (Velde, 1992).

2. Adsorption :

In adsorption, only the clay surface is involved and depends upon the pH or exchange cations concentrations. The swelling property of clays is not required for the adsorption process. Kaolinite, due to its chemically inertness and stability

in different pH and oxidation potential environment can be used for adsorption.

The impermeability characteristics of certain clays make them suitable to act as insulators in many waste disposals and can also be used as liners for radioactive wastes, hazardous chemical wastes, etc. (Pusch, 1992 ; Meunier, 1992).

Clays are also expected to be useful in large waste depositories to contain effectively the potential contamination due to municipal waste and fly ashes (Kuhnel 1993). Highly adsorbing clays, when blended with wastes can effectively scavenge many contaminants, released due to the reaction in the waste. Kuhnel (1993) suggested four major operations for the removal of contaminants from soils/clays etc.

1. Immobilization
2. Isolation
3. Dispersion (dilution) by scattering
4. Cleaning by treatment

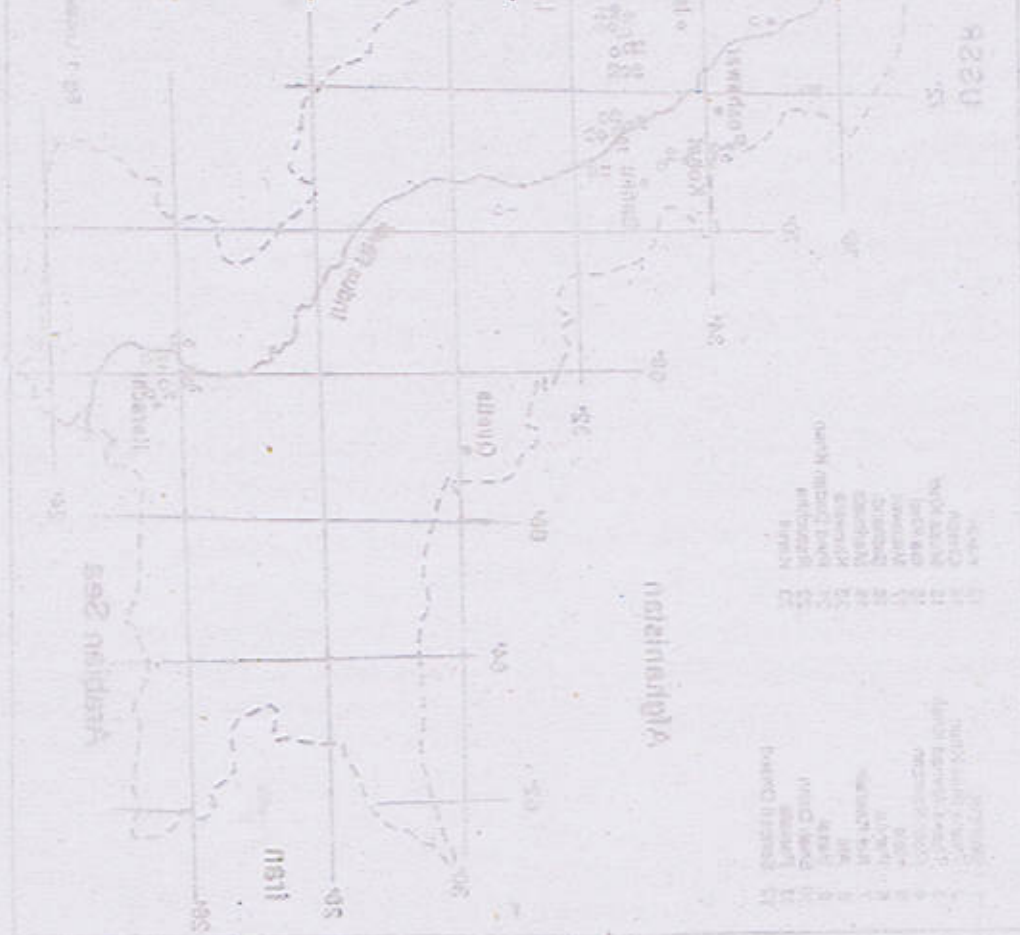
Due to these, dispersion is the cheapest operation and is frequently used, resulting into contamination of soils, sediments, rivers and oceans. However recently various technologies are being developed to remove the contaminants from the soils/clays by chemical treatment to make them reusable.

CONCLUSIONS

Chemical weathering of clays, add hazardous elements to the environment. Clays, due to their certain characteristics physical properties, after activation can be used to remove hazardous elements from mine drainage/wastes and effluents from chemical industries.

REFERENCES

- Ahmed, Z. and, Siddiqui, R.A. 1993. Minerals and Rocks for Industry. *Geol. Surv. Pakistan*, 1, 203-239.
- Kohnel, R.A.I., 1992. Clays and clay minerals in environmental research. *Acta, Min. Pet.* 35, 1-11.
- Larry, P. 1993. Understanding our Fragile Environment. *U.S. Geol. Surv. Circular*, 11-05.
- Meunier, E. 1992. Clays and Hydrosilicate gels in nuclear fields. *Appl. Clay Sci. Special Issue*, 7 (1-3).
- Pusch, R. 1992. Uses of bentonite for isolation of radioactive waste products. *Clay Minerals*, 7, 253-361.
- Velde, B. 1992. Introduction to Clay Minerals. Chapman and Hall, London. 164-195.



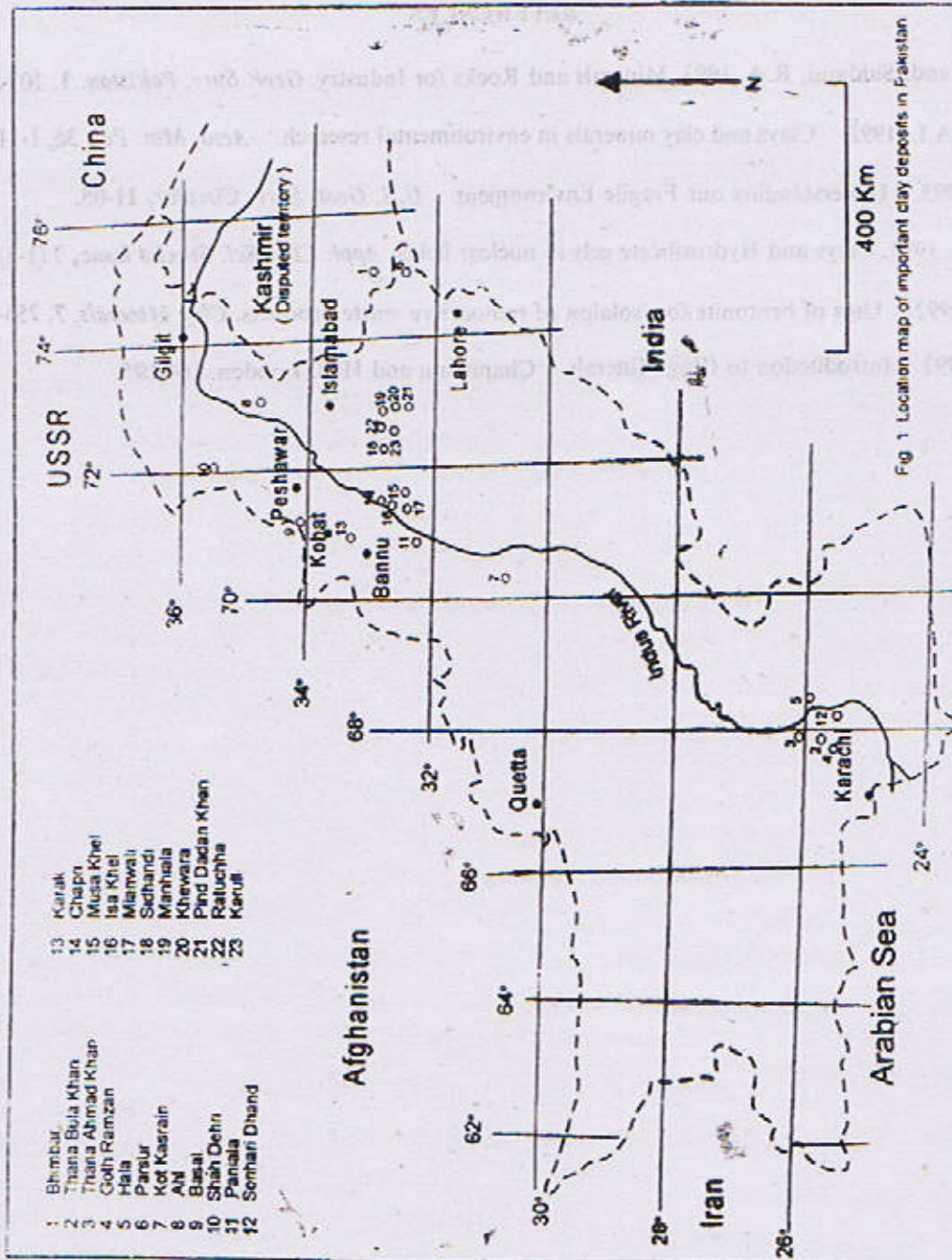


Fig. 1 Location map of important clay deposits in Pakistan

GEOLOGY AND STRUCTURE OF THE MAIN MANTLE THRUST (RAIKOT-NARAN SEGMENT), SOUTH EASTERN KOHISTAN NORTHERN PAKISTAN

By

M. ASIF KHAN, M. AHMED KHAN, M. SUFIAN QAZI AND M. QASIM JAN

National Centre of Excellence in Geology, University of Peshawar, Pakistan

Abstract : *The Main Mantle Thrust (MMT) marks the suture zone between the Indian Plate and the Kohistan Terrane. This study records observations on the geology and structure of its Raikot-Naran segment. At Raikot, the MMT is spatially superimposed by the active Raikot Fault at the western margin of the Nanga Parbat Syntaxis. Westwards, however, the two bifurcate; the MMT marks the interface between the lithologies of the Indian Plate and those of the Kohistan Terrane, while the Raikot Fault, either dies down of Raikot or remains restricted to the Indian Plate. For much of its length, in the studied area, the MMT is a sharp fault structure defined by a Greenschist-Facies Mylonite Zone extending several tens of meters on the either side of the interface between the lithologies of the two interacting plates. There is a clear evidence of south ward-directed upthrust movement at the Babusar Pass, which superimposes a north-dipping fabric (F2) on south-dipping (F1) fabric in the footwall metapelites. In the Sapat area, however, sheath folds and crenulations in the mylonites associated with the MMT record a SSE reverse movement. The trace of the MMT is folded into horizontal, southward closing open recumbent folds. With respect to the magneto-stratigraphic set up of the Kohistan Terrane, the MMT is observed to laterally ramp successively upsection from Jijal in the west to Raikot in the east. Finally, we have observed staurolite-grade metapelites retrogressed when involved in the shear zone associated with the MMT, suggesting that peak metamorphism in the higher Himalayas may not necessarily be later than the initiation of the MMT as is believed commonly.*

INTRODUCTION

Soon after the advent of the theory of plate tectonics, it became obvious that the gigantic Himalayan mountain range of south-central Asia formed in response to collision between continental plates previously separated by oceans (Dewey and Bird, 1970). Several faults of regional lateral extent were already known from within the Himalayas. Gansser (1964) recognised that one of these faults which he referred to as the Indus Suture, was in fact a tectonic boundary

between the Indian Plate in the south and the Eurasian Plate in the north. The western extension of this fault, in Pakistan part of the subcontinent, remained unknown until early seventies. Martin et al. (1962) noted that the Upper Swat Hornblende Group (later on identified as the assemblage constituting the Kohistan Arc) may have a thrust contact with Lower Swat-Buner Schistose Group. Subsequently, Jan and Tahirkheli (1969) showed that the thrust extends NE into the lower Indus Valley and Jan (1977) proposed that the thrust may well be the western

extension of the Indus Suture. Further studies have substantiated this view. Tahirkheli et al. (1976, 1979) proposed the name Main Mantle Thrust (MMT) and established its significance as a plate boundary between the Indian Plate and the Kohistan Arc Terrane.

At the time of publication of the first geological map of Kohistan (Tahirkheli and Jan, 1979), the location of the MMT in SE Kohistan was only known at Jijal and Babusar Pass. Since then, the MMT has been mapped at several locations between these two points (Chaudhry and Ghazanfar, 1987; Greco et al., 1989; Ghazanfar et al., 1991; Chamberlain et al., 1991; Jan et al., 1993; Spencer, 1993; Smith et al., 1992; Hubard et al., in press). We initiated a field study of the lower crust of the Kohistan Island Arc exposed at, and to the north of the drainage divide between SE Kohistan and Kaghan. During the course of this study, we had a chance to map a segment of the MMT exposed between Naran in the Kaghan Valley and Raikot in the Indus Valley. In this paper we present an account of our observations regarding the geology and structure of the MMT together with a geological map.

MAIN MANTLE THRUST

A Working Definition

The Main Mantle Thrust, as observed in its better studied segments, i.e., Swat and Indus Valleys, is either a knife-edge sharp fault or a broad fault zone. In either case, the tectonic interaction is between the Kohistan Terrane in the hangingwall and the Indian Plate in the footwall. In the first case, the MMT emplaces the lithologies of the Kohistan Terrane directly on to those of the Indian Plate. The type example of such a relationship is exposed at Jijal in the Indus Valley where the ultramafic rocks at the base of the Kohistan Sequence tectonically overlie the basement gneisses of the Indian Plate. In contrast at several places, e.g., Shamoza, Mingora,

Shangla Pass, Allai and Mohamand-Malakand, the Kohistan lithologies are separated from those of the Indian Plate by a broad fault zone reaching several kilometers in thickness. This fault zone, called MMT melange, comprises essentially an assemblage which belonged to the Tethyan ocean-crust closed at the site of the MMT with some elements of the arc and the Indian Plate. It consists of ophiolite ultramafic rocks transformed to serpentinites and talc-carbonate schists, altered gabbros and plagiogranites, metavolcanics transformed into greenschists and blueschists, and pelagic sediments comprising shales, cherts and Mn nodules some of which have been transformed to schists with piemontite or glaucophane. A tectonic imbrication between the crusts of the two interacting plates is reported from Babusar (Chamberlain et al., 1991) and is suspected from Bajaur (Badshah, 1979), but is not common elsewhere.

A succession of graphitic pelites occurs in close association with the MMT in many parts of northern Pakistan. These rocks are known as Saidu Formation in the Swat area (Kazmi et al., 1984; Lawrence et al., 1988; DiPietro et al., 1993), Banna Formation in the Allai Kohistan area NW of Besham (Treloar et al., 1989), and graphitic schists (Smith et al., 1992; Greco et al., 1989), Babusar mylonites (Chaudhry and Ghazanfar, 1987; Ghazanfar et al., 1991) or Parla Sapat unit (Khan et al., submitted) in the upper Kaghan area. Apart from a variable grade of metamorphism, which ranges from chlorite to staurolite, these rocks retain a restricted pelitic composition with minor graphitic content. Lensoid bodies of marbles, talc-carbonate schists and greenschists occur in the upper part of this stratigraphic succession. This has led some workers to suggest, especially in the Kaghan area, that the graphitic pelites represent part of the MMT melange (Ghazanfar et al., 1991; Smith et al., 1992). But in Allai Kohistan and Swat (where both the graphitic metapelites and the MMT melange, *sensu stricto*, occur),

the graphitic pelites are not involved in the MMT melange. Therefore, we prefer to exclude the Kaghan graphitic pelites from the MMT melange; rather we consider them an olistostrome possibly formed prior to the creation of the MMT. In summary, our definition of the MMT, at least in the presently studied segment, is the tectonic interface between the lithologies of Kohistan and those of the Indian Plate including graphitic metapelites. This is irrespective of the shearing and transformation into mylonites on either side of this tectonic contact.

Location

The trace of MMT was accessed at several points in its Naran-Raikot segment during the course of this work (Fig. 1). From west to east, these include Kinari Valley, Sapat Gali (western), Noor Jamal the Baihk (downstream from the eastern Sapat Gali), Bamgatta Gali, Buto Gali, Shutta Pass, Babusar Pass, Niat Gah, Halala in the Bunar Gah and Raikot (Indus Valley). The MMT in the Raikot area is spatially overlapped by the active fault zone called the Raikot Fault (Lawrence and Ghauri, 1983) or the Liacher Thrust (Butler and Prior, 1988). From Raikot westward, the MMT follows a more westerly course compared to the south-westerly course of the Raikot Fault. We observed a small brittle fault within an alluvial fan in the lower reaches of the Bunar Valley. The fault does not appear to be laterally continuous and, although it may be related to the Raikot event, we do not consider it to be an offshoot of the Raikot Fault.

The MMT in the Bunar Valley follows a south westerly course at the eastern slopes of the valley, passes just to the east of the Diamer-Bunar confluence and crosses the Bunar Valley at the Village Halala. It may be noted that our mapped location of the MMT in the Bunar Gah is far to the south of the location marked by Ghazanfar et al. (1991). In the Niat Gah, too, the presently marked

location of the MMT is too southerly compared to that marked by Ghazanfar et al. (1991). However, in the area between the Babusar Pass and Bamgatta Gali, we find close match in the location of MMT observed by us and that marked by Ghazanfar et al. (1991), Ghazanfar and Chaudhry (1987) and Spencer (1993). In the upper reaches of the Sapat Valley, Chaudhry and Ghazanfar (1987) and Ghazanfar et al. (1991) mark the location of the MMT at Domel, whereas our observed location is way up-stream, north of the Parla Sapat Village just to the south of the pass at western Sapat Gali. In this area, we find a close match in our marked location of the MMT and that mapped by Smith et al. (1992).

Hangingwall Geology (The Kohistan Terrane)

The hangingwall of the MMT is ubiquitously occupied by the Kohistan Terrane. Our geological mapping in SE Kohistan has resulted in the recognition of four lithological units in this part of the Kohistan Terrane (Fig. 1), which, from south to north, include 1) Sapat mafic-ultramafic Complex, 2) Niat Metavolcanic Unit, 3) Jal Amphibolite Unit (= Kamila Amphibolite), and 4) Chilas mafic ultramafic Complex. Presently, all these units have tectonic contacts with each other, though we believe that originally some of these contacts were magmatic intrusive.

Between Naran and Babusar Pass, the hangingwall of the MMT is occupied by the Sapat Complex (Jan et al., 1993). The Sapat complex comprises three units; ultramafic cumulates at the base, layered gabbros in the middle and isotropic gabbros at the upper stratigraphic levels. Lenticular ultramafic bodies, however, do occur in the higher-level gabbroic units of the Complex. The basal ultramafics of the Sapat Complex are best exposed between the western Sapat Gali and Bamgatta Gali, occupying the immediate hangingwall of the MMT. Both to the east and west, the basal ultramafics have been scrapped off, resulting in the occurrence of intermediate or higher

level gabbroic rocks along the MMT. The ultramafic bodies and associated amphibolites at the Babusar Pass (Ahmed and Chaudhry, 1976; Khan and Thirlwall, 1988) and the pyroxenite body in the upper reaches of the Kinari and Neeli Nadi Valleys (Ghazanfar et al., 1991) are parts of the higher-level ultramafic cumulates in the Sapat Complex (Khan et al., submitted). The basal part of the ultramafic cumulates, directly above the MMT, is strongly sheared and transformed into serpentine mylonites. Likewise, the gabbroic rocks, where occupying the hangingwall of the MMT, are transformed into mafic schists and gneisses (mylonites) through ductile shearing.

The exposed width of the Sapat Complex does not represent its true thickness. The complex is folded through at least two phases of open folding. The first phase is characterised by open, horizontal folds with upright or inclined axial surfaces, verging to the south near the MMT and to the north away from the MMT (Fig. 2 a, b, c). The second phase of folding is again characterised by horizontal fold axes but, unlike the upright or inclined first-phase folds, these folds are open recumbent. Unlike the phase-I folds, the phase-II folds do affect both the Kohistan as well as the underlying Indian Plate lithologies. The restored thickness of the Sapat complex, after removing the effect of folding and thrusting, approximates two kilometres.

Somewhere between the Babusar Pass and Niat Gah, the Sapat Complex gives way to the Niat Metavolcanic Unit in the hangingwall of the MMT. Between Niat Gah and Bunar Gah, once again, there is a change in the hangingwall lithology where the MMT comes to rest at the base of the Jal amphibolites. From here eastwards, it follows the base of the Jal Amphibolites (Fig. 1).

Footwall Geology (The Indian Plate Crust)

The Indian Plate rocks, forming the footwall of the MMT in the studied area, belong to Higher

Himalayas of Upper Kaghan (Greco et al., 1989; Ghazanfar and Chaudhry, 1987; Spencer, 1993). The lithology which commonly occupies the immediate footwall of the MMT in this region is a graphitic metapelite, which we refer to as the Parla Sapat Metapelite Unit. Locally, the Parla Sapat Unit pinches out and the MMT is directly emplaced onto a sheet of granitic gneisses (Fig. 1). The Parla Sapat Metapelite Unit has been previously mapped by Ghazanfar et al. (1991) under the name of Babusar Mylonites and the rocks were identified as garnetiferous-graphitic schists. Greco et al. (1989), too, showed this unit on their regional map of the Upper Kaghan Valley as graphitic schist. Smith et al. (1992) mapped this unit as "grey phyllites with marble" and considered it to be a thrust sheet of the MMT zone.

This unit occupies the upper reaches of the Kinari and Sapat Valleys in a NE-SW regional trend, preferentially located along and to the south of, the MMT. Westward, the unit swings first to an E-W trend and then to a WNW-ESE trend in the upper reaches of the Nili Nadi Valley. Eastwards, the unit squeezes between the ultramafic mylonites of the Kohistan Plate and the Indian-Plate granitic gneisses and pinches out before reaching the northern slopes of the Eastern Sapat Gali (pass). Further northeast, the unit is missing for about 12 kilometers, and the ultramafic mylonites of the Kohistan Plate directly overlie granitic gneisses. The Parla Sapat Metapelites reappear at the ridge to the northeast of the Bamgatta Gali. Our observations in the upper reaches of the Lūhyalul Nar at the Shutta and the Babusar Passes confirm regional north-easterly distribution of this unit along and to the south of the MMT.

The Parla Sapat Metapelites in the upper reaches of the Sapat Valley, north of Domel, are grossly homogeneous but strongly foliated. They are black in appearance and contain minor graphite. Other minerals include quartz, biotite and muscovite. The rock may thus broadly be named as graphitic schist or, more precisely, graphitic

quartz-mica schist. The unit is heterogeneously sheared; the areas which escaped the shearing have retained higher grade minerals such as garnet and staurolite (garnet staurolite schists or garnet mica schists), while the sheared ones are retrogressed in greenschist-facies conditions and are devoid of garnet or staurolite. Even immediately below the ultramafic mylonites, garnetiferous and non-garnetiferous rocks are found in close association, suggesting a partial lack of penetrative deformation. Nonetheless, the unit is extensively sheared and application of the terms mylonites or blastomylonites is not inappropriate (Gazanfar et al., 1991). In the vicinity of the contact with the ultramafic mylonites of the Kohistan Plate, the metapelites are extensively crenulated with a strong E-W lineation plunging steeply towards west.

The Parla Sapat Metapelites in the Kinari Valley are divisible into a southern schistose unit and a northern phyllite unit. The schistose unit is a typical garnet-quartz-mica schist with a strong foliation, whilst the phyllite subunit is devoid of garnet. As noted in the Sapat Valley, the phyllites are probably derived from the garnetiferous schists (\pm staurolite) through greenschist-facies ductile-brittle shearing and retrograde metamorphism. Locally, we noted the presence of greenschists and talc-carbonate schists intercalated with the graphitic phyllites. These rocks were probably derived from ultramafic or volcanic precursors, as is the case in the Shangla Melange (Jan et al., 1981; Kazmi et al., 1984). We interpret this relationship to be olistostromal in nature rather than being a product of tectonic mixing as the enclosing phyllites are laterally continuous around these lensoid bodies.

Minor amounts of marble bands are present in the Parla Sapat Unit both in the Kinari Valley as well as to the west in the Nili Nadi Valley (Smith et al., 1992). Marbles and calcareous garnet-mica schists are also observed in the Parla Sapat Unit in the Upper reaches of the Lohyalul Valley (at the Kulwan confluence) and short of

the Babusar Pass. A notable absence is that of the Panjal-type basic igneous rocks which are very common in all the other lithologies of the region.

As mentioned above, the ultramafic (serpentine) mylonites are in direct contact with the Indian Plate granitic gneisses in the area between Noor Jamal the Baihk and Bamgatta Gali. These gneisses are typically fine-medium grained and strongly foliated with well-developed millimeter-scale gneissic banding. The granitic gneisses appear to be originally fine-medium grained with no signs of megacrysts or augens. Compositionally, the rocks are rich in micas, particularly muscovite. Observations in the Bamgatta Valley suggest that the granitic gneisses themselves are composite, comprising alternating sheets of very felsic and felsic compositions. The less felsic variety contains greater proportions of biotite and muscovite. In the same area, two to ten meter thick sheets of granitic gneiss alternate with sheets of similar sizes comprising garnetiferous greyish-black slates, schists and paragneisses. The metasediments are internally banded with alternating quartzofeldspathic and micaceous bands both of which contain abundant garnet. The granitic gneisses do contain sheets of garnetiferous amphibolites, both in the Noor Jamal Di Baihk area as well as to the north of the Bamgatta Gali.

Structure

The serpentinite mylonites along the MMT are strongly foliated but lack lineations. The quartz-mica phyllites (belonging to the Parla Sapat Metapelite Unit), directly below the MMT, are strongly banded and comprise bands of ribbon quartz alternating with bands rich in muscovite and biotite. These phyllites are extensively crenulated at a microscopic to mesoscopic scale (an area of 10 cm² contains several dozen crenulations). Considering that these crenulations are restricted to the vicinity of the MMT, we interpret them to be sheath folds in nature rather than being parasitic to a major fold. The attitude of fold axes, i.e.

E-W and 50-60°W plunge, suggests an ESE direction of thrusting for MMT in the Sapat area.

The trace of the MMT at the Sapat drainage divide is clearly folded. The folding is typically open recumbent type with subhorizontal fold axes. The trace of the MMT, as shown on the map, dips towards the north in the lower reaches of the valleys (Fig. 2a, c), but towards the south at the high-altitude ridges (Fig. 1, 2b), forming a southwards-closing recumbent fold. This phase of folding is observed to affect both the Kohistan and the Indian Plate rocks equally. In the deep-cut valley just to the west of the Parla Sapat, there are indications that the Parla Sapat unit is folded into a northward closing open, recumbent fold, complementary to the southward-closing open recumbent fold at the higher altitude ridges.

It is interesting to note that a northward-closing open recumbent fold is also observed at the Babusar Pass within the quartz-mica schists (= Parla Sapat Unit) (Fig. 2d), which, at least superficially, resembles with those west of the Parla Sapat Village (though with a closure to the north). The structure at the Babusar Pass, however, is controlled by ductile shearing associated with the southward thrusting of the MMT rather than with a post-MMT folding event. The garnet-mica schists of the Parla Sapat Unit approaching the Babusar Pass are characterised by a strong F1 fabric with an attitude of EW/50°S. At the pass, however, the predominant fabric is EW/30°N. A closer observation suggests that this N-dipping fabric transposes the S-dipping foliation into spectacular meso and microscopic crenulations. This superimposition of the two fabrics is observed at a scale of several tens of meters, with a net effect such that the MMT (which marks a south-verging shear zone) causes a spectacular transposition of the south-dipping quartz-mica schists into north-dipping mylonites forming a northward-closing open recumbent fold.

DISCUSSION

In SE Kohistan, the MMT is defined by a sharp interface between the lithological elements belonging to the Kohistan terrane in the hanging wall and those of the Indian Plate crust in the footwall. However, the rocks are ductilely sheared and transformed into mylonites over tens of meters on both sides of the tectonic contact. The deformation operated under greenschist-facies conditions. In the hangingwall, dunites and peridotites are transformed into serpentinite mylonites and gabbroic rocks into greenschists. In the footwall, the amphibolite-facies garnet-staurolite schists are retrogressed to phyllites. The sense of movement is oblique-reverse in a direction of ESE (i.e., Kohistan overthrusts the Indian Plate in an ESE direction), at least in the Sapat area. We do not conceive the idea of development of a wide melange zone in association with the MMT. The Parla Sapat Metapelite Unit, which occurs directly below the MMT, contains local lenses of greenstone, talc-carbonate schists and marbles which are probably olistostromal in nature rather than representing a tectonic melange. The MMT, at least in the Sapat Gali area, is clearly folded through a phase of open recumbent folding.

The ESE directed reverse sense of movement associated with the MMT, noticed in this study, conforms to that previously documented by Greco et al. (1989) from the upper Kaghan area. But it may be noted that in the area between Babusar and Toshe Gali (upper reaches of Bunar Gah), Hubbard et al. (in press) found no evidence of a SE directed movement associated with the MMT. Their study area lies to the east and south of the presently studied area, so we cannot comment on their observations. However, right at the Babusar Pass, the interface between Kohistan terrane and the Indian-plate cover is marked by a south-verging ductile shear zone, which clearly transforms the south-dipping F1 fabric in the Indian-plate metapelites along N-dipping shear fabric F2.

As mentioned above, we have noticed that the Parla Sapat Metapelite Unit has suffered a retrogressive metamorphism from staurolite grade to chlorite grade, when involved in the deformation associated with MMT. This would imply that the staurolite-grade of metamorphism in the Parla Sapat unit took place prior to the activity related with the MMT. Three possibilities arise:

1) it is pre-Himalayan, i.e., Late Precambrian or earlier (Baig and Lawrence, 1987; Williams et al., 1988).

2) it is related with the subduction of the Indian Plate beneath Kohistan prior to the final movement between the two plates at the site of the MMT.

3) the MMT was reworked following its initial emplacement and accompanied regional metamorphism.

It is possible that the regional metamorphism of the Indian Plate has started during its subduction stage prior to its actual contact with the Kohistan Terrane and creation of the MMT. This may also apply that the widely publicised high-pressure (eclogite-facies) metamorphism reported from upper Kaghan (Tonarini et al., 1993; Spencer, 1993) might have been accomplished prior to the final emplacement of the MMT. We are awaiting radiometric age data for the Parla Sapat Metapelites to evaluate the validity of our interpretation. But there is also the possibility that the regional prograde metamorphism was related to emplacement of the Kohistan Terrane onto India, followed by extensional tectonics and retrograde metamorphism in the MMT zone. Treloar (1991) have, indeed, suggested post-metamorphic extension in the neighbourhood of MMT.

Finally, an aspect of the MMT which we wish to bring into notice is the lateral variation in its level of propagation with respect to its position in the magmatic stratigraphy of the Kohistan Terrane.

The MMT at Jijal in the Indus Valley carries garnetiferous mafic and ultramafic rocks at its hanging-wall which represents the petrological Moho (Tahirkheli et al., 1979; Miller et al., 1991). In the Sapat area, at the Kohistan-Kaghan Drainage Divide, the MMT runs through the basal ultramafics of the Sapat Complex, which we consider a relatively higher level magnato-stratigraphic unit in the Kohistan Crust. Further to the east, in the area between the Noor Jamal the Baihk and the Bamgatta Gali, the MMT climbs upsection laterally and carries the layered to isotropic gabbroic rocks of the Sapat Complex. Eastward, towards the Babusar Pass, the MMT apparently follows this stratigraphic level. However, before reaching the Niat Gah, it once again climbs upsection, and rests along the contact between the Sapat Complex and the overlying metavolcanic basement (unpublished data; Ahmed Khan). Finally, near Halala (Buner Gah), the MMT once again cuts upsection and rests along the base of the Kamila Amphibolite Unit, from where onward towards Gilgit it retains this stratigraphic level. A similar, lateral staircase geometry is followed by the MMT to the west of the Indus Valley in the Swat and Dir Valleys.

In summary, the Naran-Raikot segment of the MMT defines it as a ductile shear zone, which, with respect to the magmato-stratigraphy of the Kohistan Terrane, has a staircase lateral geometry. The MMT retrogresses staurolite-grade metapelites, suggesting that either the MMT formed later than the peak Himalayan metamorphism or was reactivated later than its initial emplacement. Treloar et al. (1991) suggest Miocene extension in the MMT zone.

ACKNOWLEDGEMENT

This study was financed by an NSRDB GRANT No. E. Sc. 24. We are grateful to Yaqoob Shah and Ashfaq Sajjad of Pakistan Mineral Development Corporation for drawing our attention towards the magnificent geology of the Sapat Gali area.

REFERENCES

- Ahmed, Z. and Chaudhry, M.N. 1978. Geology of the Babusar area, Diamir district, Gilgit, Pakistan. *Geol. Bull. Punjab Univ.*, **12**, 67-78.
- Badshah, M.S. 1979. Geology of Bajaur and norther parts of Mohmand. *Geol. Bull. Peshawar Univ.*, **11**, 163-179.
- Baig, M. S., Lawrence, R. W. and Snee, L. W. 1988. Evidence for Late Precambrian to Early Cambrian orogeny in Northwest Himalaya, Pakistan. *Geol. Mag.*, **125**, 83-86.
- Butler, R. W. and Prior, D. J. 1988. Tectonic control on the uplift of Nanga Parbat, Pakistan Himalaya. *Nature*, **333**, 247-250.
- Chamberlain, C. P., Zeitler, P. K. and Erikson, E. 1991. Constraints on the tectonic evolution of the north-western Himalaya from geochronological and petrological studies of Babusar Pass, Pakistan. *Jour. Geol.*, **99**, 829-849.
- Chaudhry, M. N. and Ghazanfar, M. 1987. Geology, structure and geomorphology of Upper Kaghan valley, NW Himalaya, Pakistan. *Geol. Bull. Punjab Univ.*, **22**, 13-57.
- Dewey, J. F. and Bird, J. M. 1970. Mountain belts and the new global tectonics. *Jour. Geophys. Res.*, **75**, 2625-2647.
- DiPietro, J. A., Pogue, K. R., Lawrence, R. D., Baig, M. S., Hussain, A. and Ahmad, I., 1993. Stratigraphy south of the Main Mantle Thrust, Lower Swat, Pakistan. *Geol. Soc. London, Spec. Publ.* **74**, 207-220.
- Gansser, A. 1964. Geology of the Himalayas. *Wiley Intersci., London*, 289 p.
- Ghazanfar, M., Chaudhry, M. N. and Hussain, M. 1991. Geology and petrotectonics of southeast Kohistan, northwest Himalaya, Pakistan. *Kashmir Jour. Geol.*, **8**, 9, 67-9.
- Greco, A., Martinotti, G., Papritz, K., Ramsay, J. G. and Rey, 1989. The crystalline rocks of the Kaghan valley (NE Pakistan). *Eclog. Geol. Helvet.*, **82**, 629-653.
- Hubard, M. S., Spencer, D. A. and West, D. P. 1993. Tectonic exhumation of the Nanga Parbat Mssif northern Pakistan. *Earth Planet. Sec. Sci. Lett.* (in press).
- Jan, M. Q., Kamal, M. and Khan, M. I. 1981. Tectonic control over emerald mineralization in Swat. *Geol. Bull. Peshawar Univ.*, **14**, 101-109.
- Jan, M. Q. and Tahirkheli, R. A. K. 1969. The geology of the lower part of Indus Kohistan, Swat. *Geol. Bull. Peshawar Univ.*, **4**, 1-131.
- Jan, M.Q., Khan, M.A. and Qazi, M.S. 1993. The Sapat mafic-ultramafic complex, Kohistan arc, North Pakistan. In: Treloar P. J. & M. P. Searle, (eds.). *Himalayan Tectonics Geol. Soc. London, Spec. Publ.* **74**, 113-121.
- Kazmi, A. H., Lawrence, R. D., Dawood, H., Snee, L. W. and Hussain, S. 1984. Geology of the Indus suture zone in the Mingora-Shangla area of Swat, N. Pakistan. *Geol. Bull. Peshawar Univ.*, **17**, 127-144.

- Khan, M. A. and Thirwall, M. F. 1988. Babusar amphibolites : Arc tholeiites from the southern Kohistan arc, N. Pakistan. *Geol. Bull. Peshawar Univ.*, **21**, 147-158.
- Khan, M. A. Jan, M. Q., Qazi, M. S., Khan, M. A., Shah, Y., and Sajjad, A. (in Press) Geology of the drainage divide between Kohistan and Kaghan, N. Pakistan. *Geol. Bull. Peshawar Univ.*, (in press)
- Lawrence, R. D. and Ghauri, A. A. K. 1983. Evidence of active faulting in Chilas District, Northern Pakistan. *Geol. Bull. Peshawar Univ.*, **16**, 1-10.
- Lawrence, R. D., Kazmi, A. H. and Snee, L. W. 1989. Geological setting of the emerald deposits. In : Kazmi, A. H. and Snee, L. W. (Eds.) Emeralds of Pakistan. *Van Nostrand Reinhold, New York*, 13-38.
- Martin, N. R., Siddiqui, S. F. A. and King, B. H. 1962. A geological reconnaissance of the region between the lower Swat and Indus Rivers of Pakistan. *Geol. Bull. Punjab Univ.*, **2**, 1-14.
- Miller, D. J., Loucks, R. R. and Ashraf, M. 1991. Platinum group elements mineralization in the Jijal layered mafic-ultramafic complex, Pakistani Himalayas. *Econ. Geol.*, **86**, 1093-1102.
- Smith, H. A., Chamberlain, C. P. and Zeitler, P. K. 1992. Evidence for Late Eocene anatexis within the Indian Plate as a result of Eocene Himalayan orogeny. *7th Himalayan-Karakoram-Tibet Workshop. Oxford*, p. 84.
- Spencer, D. A. 1993. Tectonics of the Higher and Tethyan Himalaya, Upper Kaghan Valley, NW Himalaya Pakistan : Implications of an early collision, high pressure (eclogite facies) metamorphism to the Himalayan belt. *Ph.D. dissertation, Swiss Federal Institute of Technology, Zurich*
- Tahirkheli, R. A. K. and Jan, M. Q., 1979. Geology of Kohistan, Karakoram, Himalaya, Northern Pakistan. *Geol. Bull. Peshawar Univ.*, **11**, Spec. Issue.
- Tahirkheli, R. A. K., Mattauer, M., Proust, F. and Tapponnier, P. 1976. Some new data on the India-Eurasia convergence in the Pakistan Himalaya. *Colloq. Internat. C. N. R. S.* **286**. *Ecologie Del' Himalaya*, 209-211.
- Tahirkheli, R. A. K., Mattauer, M., Proust, F. and Tapponnier, P. 1979. The India-Eurasia suture zone in northern Pakistan : synthesis and interpretation of data at plate scale. In : Farah, A. and DeJong, K. A. (Eds.) Geodynamics of Pakistan. *Geol. Surv. Pakistan, Quetta*, 125-130.
- Tonarini, S., Villa, I. M., Oberli, F., Meier, M., Spencer, D. A., Pognante, U. and Ramsay, J. G. 1993. Eocene age of eclogite metamorphism in Pakistan Himalaya : Implications for India-Eurasia collision. *Terra Nova*, **5**, 13-20.
- Treloar, P. J., Rex, D. C. & Williams, M. P., 1991. The role of erosion and extension in unroofing the Indian Plate thrust stack, Pakistan Himalaya, *Geol. Mag.*, **128** 465-478.
- Treloar, P. J., Williams, M. P. and Coward, M. P. 1989. Metamorphism and crustal stacking in the north Indian plate, north Pakistan. *Tectonophysics*, **165**, 167-184.
- Williams, M. P., Treloar, P. J. and Coward, M. P. 1988. More evidence of pre-Himalayan orogenesis in Northern Pakistan. *Geol. Mag.*, **125**, 651-652.

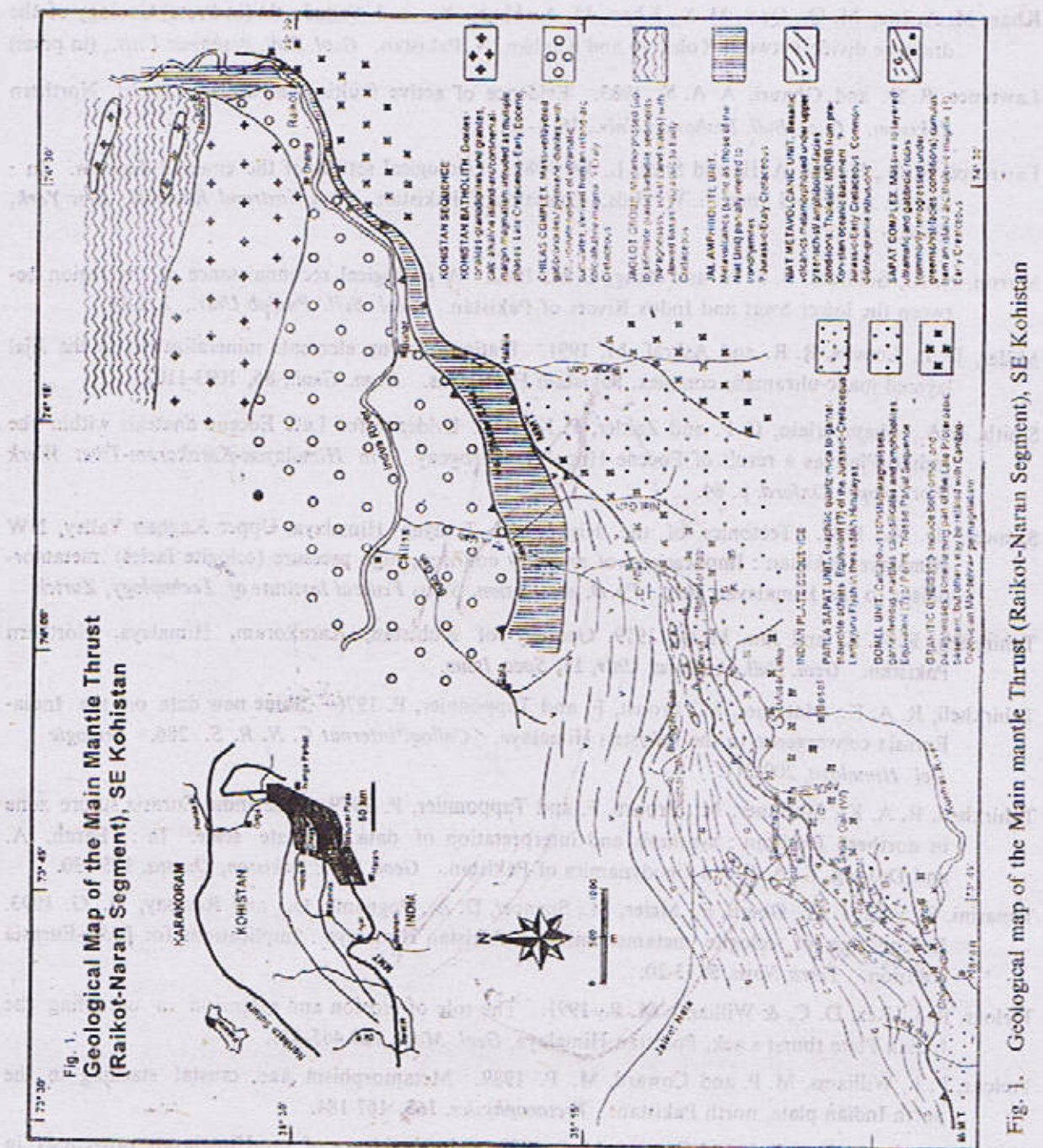


Fig. 1. Geological map of the Main mantle Thrust (Raikot-Naran Segment), SE Kohistan

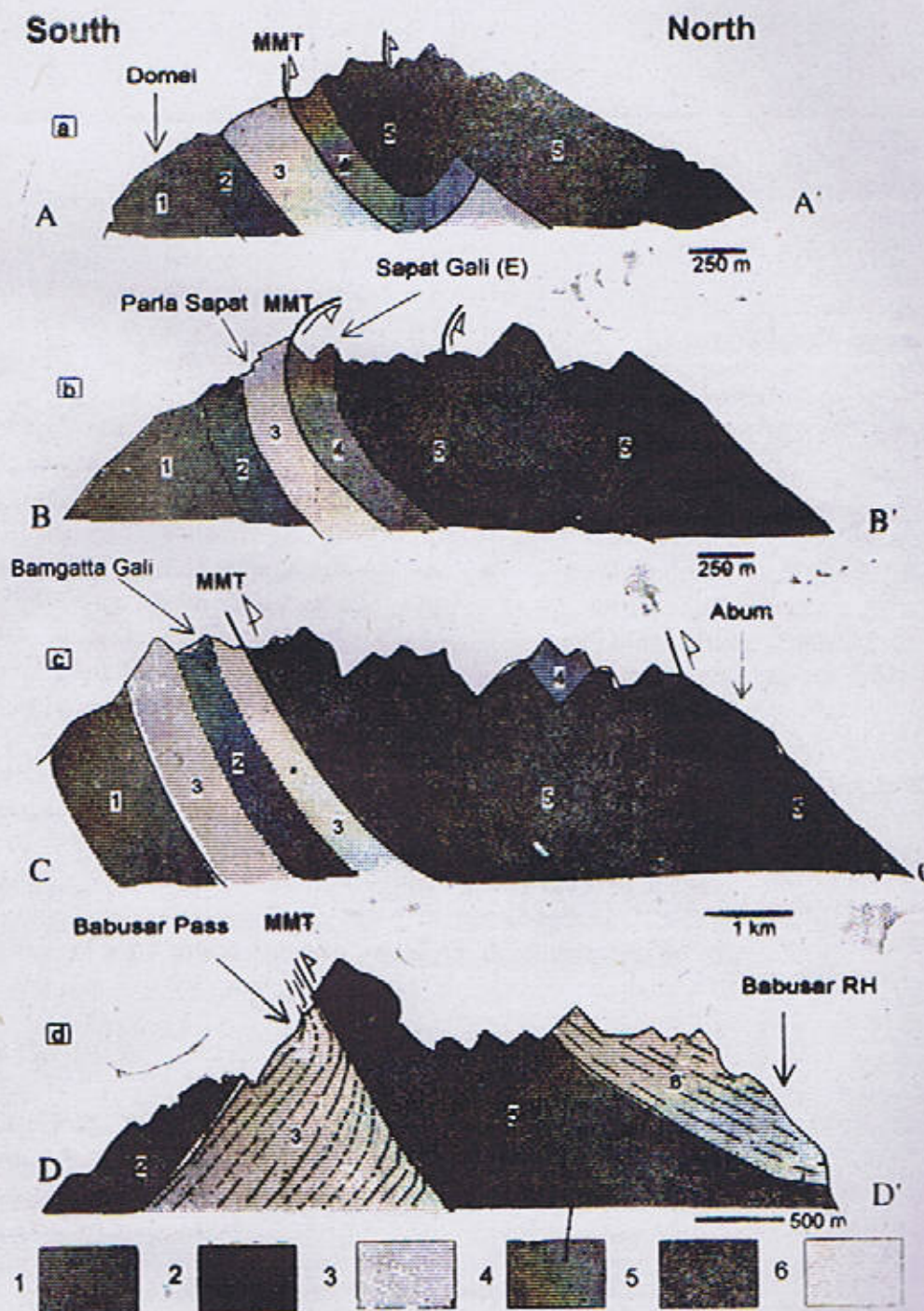


Fig. 2. Selected sections across the Main Mantle Thrust (Raikot-Naran Segment).